ISBN 978-82-575-1004-6
ISSN 1503-1667

Norwegian University of Life Sciences
NO–1432 Ås, Norway
Phone +47 64 96 50 00
www.umb.no, e-mail: postmottak@umb.no

Anne Line Norberg

Norwegian University of Life Sciences • Universitetet for miljø- og biovitenskap
Department of Chemistry, Biotechnology and Food Science
Philosophiae Doctor (PhD) Thesis 2011:41

A detailed study of substrate positioning in family 18 chitinases

En detaljert studie i substrat posisjonering i familie 18 kitinaser

Anne Line Norberg

Philosophiae Doctor (PhD) Thesis 2011:41

A detailed study of substrate positioning in family 18 chitinases

En detaljert studie i substrat posisjonering i familie 18 kitinaser

Philosophiae Doctor (PhD) Thesis

Anne Line Norberg

Institute of Chemistry, Biotechnology and Food Science
Norwegian University of Life Sciences

Ås 2011

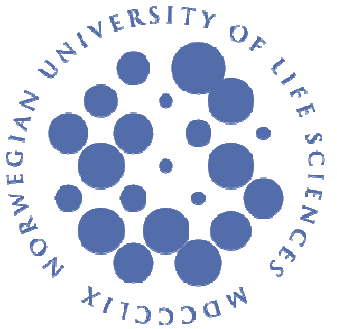

Thesis number 2011:41
ISSN 1503-1667
ISBN 978-82-575-1004-6

Table of Contents

ACKNOWLEDGEMENTS

The work presented in this thesis was carried out during the period 2007-2011, in the Institute of Chemistry, Biotechnology and Food Science (IKBM) at the Norwegian University for Life Sciences (UMB). It was co-funded by the Norwegian research council and IKBM.

I would like to thank my supervisor Morten Sørlie and co-supervisor Vincent G. H. Eijsink for giving me the opportunity to be a PhD student in their labs and for all their help and support along the way. I am very grateful for having such skillful and enthusiastic supervisors. Special thank**s** to Morten, for some reason you never stop believing in me!

I would also like to thank Kjell Morten Vårum of the Norwegian University of Science and Technology for sharing the secrets of chitosan with me. Jasna Peter-Katalinić, Michael Mormann and Klaus Dreisewerd of the University of Münster, Department of Medical Physics and Biophysics, thank you for letting me stay in your lab and teaching me valuable knowledge in the field of mass spectrometry.

Fellow PhD students contributing to this work deserve special mention; Kristine Bistrup Eide, Ellinor B. Heggseth, Henrik Zakariassen and Anette I. Dybvik, and former masters student Anne Rita Lindbom. Also thanks to Øyvind, for being my personal "Mr fix-it" in the lab and to Simen, for the great lunch deal and good friendship.

To all my past and present colleagues in the chemistry group, thanks for all the good times and fun discussions, of both scientific and personal topics. I have really enjoyed being a part of this group! A special thanks to Yngve Stenstrøm, Anne Marie Langseter and Marius Aursnes for saving me when I decided to become a "real chemist".

Thanks to all the people in the PEP group for all their kind help and technical assistance, especially Anne Cath for having a practical solution to everything and for meaningless but joyful girl-talk.

I am very grateful to my family and friends who are always supportive, despite my *ad hoc* life and sometimes deep "chemistry coma", you deserve a salute! Lastly, I am indebted to Bård-Anders for being my best friend and for not being a scientist!

LIST OF PUBLICATIONS

Paper I: Determination of substrate binding energies in individual subsites of a family 18 chitinase

A. L. Norberg, V. Karlsen, I. A. Hoell, I. Bakke, V. G. H. Eijsink, M. Sørlie, *FEBS Lett.* 2010

Paper II: Dissecting factors that contribute to ligand-binding energetic for family 18 chitinases

A. L. Norberg, V. G. H Eijsink, M. Sørlie, *Thermochim. Acta* 2010

Paper III: Substrate positioning in chitinase A, a processive chito-biohydrolase from *Serratia marcescens*

A. L. Norberg, A. I. Dybvik, H. Zakariassen, M. Mormann, J. Peter-Katalinić, V. G. H. Eijsink, M. Sørlie, *FEBS Lett.* 2011

Paper IV: The action of the human chitotriosidase on chitosan

K. B. Eide, A. L. Norberg, E. B. Heggset, A. R. Lindbom, K. M. Vårum, V. G. H. Eijsink, M. Sørlie**, s**ubmitted to *Carbohyd. Polym.* 2011

Paper VI: Analysis of productive binding modes reveals differences between human chitinases

A. L. Norberg, K. B. Eide, A. R. Lindbom, V. G. H. Eijsink, M. Sørlie, *manuscript in preparation*

Paper V: Analysis of noncovalent chitinase-chitooligosaccharide complexes by infrared matrix-assisted laser desorption/ionization and nano-electrospray ionization mass spectrometry

A. I. Dybvik, A. L. Norberg, V. Schute, J. Soltwisch, J. Peter-Katalinić, K. M. Vårum, V. G. H. Eijsink, K. Dreisewerd, M. Mormann, M. Sørlie, *Anal. Chem.* 2011

Papers not included in the thesis:

Production of chitooligosaccharides and their potential applications in medicine

B. B. Aam, E. B. Heggset, A. L. Norberg, M. Sørlie, K. M. Vårum, V. G. H. Eijsink, *Marine Drugs* 2010

Degradation of chitosans with a family 46 chitosanase from *Streptomyces coelicolor* A3(2)

E. B. Heggset, A. I. Dybvik, I. A. Hoell, A. L. Norberg, M. Sørlie, V. G. H. Eijsink, K. M. Vårum, *Biomacromol.* 2010

Comparative studies of chitinases A, B and C from *Serratia marcescens*

S. J. Horn, M. Sørlie, G. Vaaje-Kolstad, A. L. Norberg, B. Synstad, K. M. Vårum, V. G. H. Eijsink, *Biocatal. Biotransfor.* 2006

ABSTRACT

Chitin is a linear polymer consisting of β-1,4-linked *N*-acetyl-glucosamine (GlcNAc; A) units tightly packed in a crystalline structure. It is produced by living organisms in large quantities per year and is a structural component of fungi, insects and crustaceans. A soluble derivative of chitin, chitosan, is obtained by deacetylation of the chitin polymer, resulting in a hetero-polymer consisting of *N*-acetyl-glucosamine and glucosamine (GlcN; D) units. Despite, the large amounts of chitin produced, it does not accumulate in nature because it is broken down efficiently by a group of enzymes known as chitinases. Chitin turnover is of considerable economic interest, and inhibition of chitinases is a desirable target in the development of fungicides, pesticides and therapeutics. The primary goal of the work described in this thesis was to study the binding of chitin, fragments of chitin (chitooligosaccharides), and chitosan to different chitinases to gain an insight into the mechanisms behind chitin degradation.

Papers I and II describe a detailed thermodynamic characterization of binding of *N*-acetylated chitooligosaccharides and the pseudosaccharide allosamidin to ChitinaseB (ChiB) from *Serratia marcescens*, providing new insights into the contributory factors of ligand-binding. Remarkably, binding of chitooligosaccharides was found to be driven exclusively by entropy despite several conserved stacking interactions between the ligand and the active site. Paper III describes a study of the role of the conserved tryptophan in subsite −3 and a putative "+3" binding site by comparing how ChitinaseA (ChiA) from *Serratia marcescens* and its −3 subsite mutant ChiA-W167A interact with chitooligosaccharides and chitosan. The results reported in this paper highlight the importance of Trp^{167} for ligand binding and suggest there are important interactions between the enzyme and the ligand which have not been studied previously.

Humans possess two active and highly conserved family 18 chitinases, acidic mammalian chitinase (AMCase) and chitotriosidase (HCHT), which are believed to

be a part of the human immune system. Papers IV and V deal with the productive and non-productive binding of HCHT, and compare preferences of substrate positioning for HCHT and AMCase. The results help to elucidate the mechanisms of ligand binding to human chitinases and have important implications for the future design of AMCase inhibitors. Inhibitor development requires efficient and fast screening methods to identify strongly binding molecules. Paper VI describes a novel method using infrared matrix-assisted laser desorption/ionization mass spectrometry (IR-MALDI MS) for rapid and robust detection of noncovalent complexes, which is a promising tool in the search for efficient chitinase inhibitors.

SAMMENDRAG

Kitin er en lineær polymer bestående av β-1,4-linkede *N*-acetyl-glukosamin (GlcNAc; A) enheter tett pakket i en krystallinsk struktur. Kitin er en viktig strukturell komponent i sopp, insekter og skalldyr og blir produsert i enorme mengder årlig. Kitosan er et vannløslig derivat av kitin som fremstilles ved deacetylering av kitin polymeren til en hetro-polymer bestående av *N*-acetyl-glukosamin og glukosamin (GlcN; D) enheter. Til tross for de enorme mengdene kitin som produseres årlig akkumulerer ikke kitin i naturen. Dette skyldes en mengde proteiner som effektivt bryter ned kitin, kjent som kitinaser. Nedbrytning av kitin er av stor økonomisk interesse og inhibering av kitinaser er ønskelig for utvikling av nye fungicider, persticider og medisiner. Målet med dette prosjektet har vært å studere bindingen av kitin, kitin fragmenter (kitooligosakkarider) og kitosan til forskjellige kitinaser for og beder å forstå mekanismene bak nedbrytningen av kitin.

Artikkel I og II gir en detaljert termodynamisk karakterisering av bindingen av *N*-acetylerte kitooligosakkarider og pseudosakkaridet allosamidin til KitinaseB (ChiB) fra *Serratia marcescens*, noe som gir et nytt innblikk i hvilke faktorer som bidrar til ligand binding. Det ble observert at binding av kitooligosakkarider i all hovedsak ble drevet av entropi, til tross for at flere konserverte interaksjoner mellom liganden og enzymet i det aktive setet. I artikkel III blir betydningen av den konserverte tryptofan i subsete −3 og det antatte "+3" bindingsetet studert ved å sammenlikne hvordan KitinaseA (ChiA) fra *Serratia marcescens* og dens subsete −3 mutant ChiA-W167A binder til kitosan og kitooligosakkarider. Resultatene fra dette studiet understreker betydningen til Trp^{167} når det kommer til binding av ligander og retter ny oppmerksomhet mot interaksjoner mellom enzymet og liganden utenfor det definerte aktive setet.

Mennesker har to aktive, svært konserverte familie 18 kitinaser, acidic mammalian chitinase (AMCase) and chitotriosidase (HCHT), som antas å være en del av det humane immun systemet. I artikkel IV og V har vi studert både produktive og ikke-

produktive bindinger til HCHT og preferanser for substratbinding er sammenliknet med den for AMCase. Dette gir en ny innsikt i bindings mekanismer hos humane kitinaser og gir verdifull informasjon for videre design av AMCase inhibitorer. Utviklingen av nye inhibitorer krever effektive og raske metoder for screening av molekyler som binder strekt til enzymet. Artikkel VI beskriver en ny metode for rask og robust deteksjon av ikke-kovalente komplekser ved hjelp av infrarød matrix assisert laser desorption ioniserings masse spektrometri (IR-MALDI-MS). Denne metoden har et stort potensial i jakten på effektive kitinase inhibitorer.

1. INTRODUCTION

Carbohydrates exist in numerous forms and account for about two-thirds of the carbon in the biosphere, with cellulose being the most abundant biopolymer [1]. Traditionally, carbohydrates were considered to function only as structural components and energy sources. In the past decades, they have earned new attention as crucial molecules for life participating in signaling and cellular communication [2]. Moreover, there is a growing economic interest in developing efficient methods to convert recalcitrant biopolymers to easily fermentable compounds, such as glucose. Studying and exploiting polysaccharides is not straightforward due to the inherent structural complexity of sugars and the extreme stability of the glycosidic linkage connecting sugar units, which has a half-life of approximately 5 million years [3]. Despite the high stability of the glycosidic linkage and the large amounts of carbohydrates produced per annum, they do not accumulate in the biosphere. Nature has evolved efficient catalytic systems for the degradation of carbohydrates through enzymatic hydrolysis. Enzymes that cleave and build glycosidic linkages are known as carbohydrate-active enzymes (CAZymes) [4]. To understand how these enzymes work, it is important to study the interactions between the carbohydrate and the protein. This thesis describes an extensive investigation of the enzymatic hydrolysis of the polysaccharide chitin, chitooligosaccharides, and its soluble analogue chitosan using calorimetric, mass spectrometric, and chromatographic techniques.

1.2 Chitin and chitosan

Chitin is a linear polysaccharide that consists of β-1,4 linked *N*-acetyl glucosamine units (GlcNAc; A) which are rotated 180° to each other (Figure 1) [5].

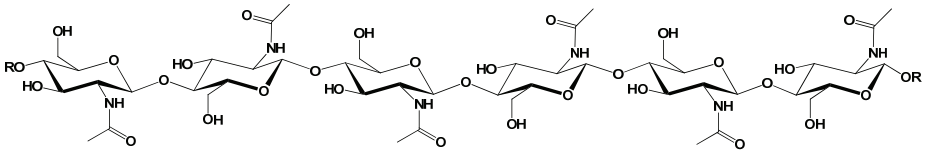

Figure 1: The structure of chitin comprising β-1,4 linked *N*-acetyl-glucosamine units rotated 180° to each other.

Chitin is widespread in nature and is produced by a number of organisms, including lower plants and animals. It is a structural component of the cell wall of fungi, including yeast**,** and the exoskeleton of arthropods [6]. It is produced in large quantities per annum and is considered to be the second most abundant biopolymer in nature after its analogue cellulose. Polymers of chitin are tightly packed with two main forms of crystallization; α-chitin consists of anti-parallel strands of GlcNAc polymers, whereas in β-chitin the strands are orientated in a parallel direction. The less common γ-chitin consists of two parallel and one anti parallel strands and is described as a variant of α-chitin [6, 7]. In both crystalline forms, the polymeric strands are tightly held together by hydrogen bonds, mainly the strong C-O···HN bond. The anti-parallel orientation of α-chitin allows a larger number of hydrogen bonds to be formed than in β-chitin, resulting in tight packing of the polymeric strands and high stability of the crystalline structure. Thus, α-chitin is endowed with a high degree of strength and stability, and hence is the most common form of crystallization. In contrast, β-chitin is not as common in nature and possesses fewer inter-molecular hydrogen bonds between the polymeric strands. As a consequence, more alcohol or acetyl groups interact with surrounding water molecules in β- than α-chitin, leading to a more flexible structure [8].

Due to its crystalline nature, chitin is not soluble in water, and thus accessibility is often a major problem for its study and degradation [9]. Deacetylation of chitin generates the analogue chitosan (Figure 2). Removal of the acetyl group in the C-2 position of the repeating GlcNAc unit leaves a free NH_2-group that can act as a proton acceptor in acidic solutions. Partial deacetylation converts the polysaccharide into a polyelectrolyte that is soluble in aqueous, acidic solution [6]. Having a soluble analogue opens new doors when it comes to applications and modifications of the polymer. Properties of chitosan are described by the fraction of acetylation (F_A), the pattern of acetylation (P_A), degree of polymerization (DP_n) and molecular weight distribution [10].

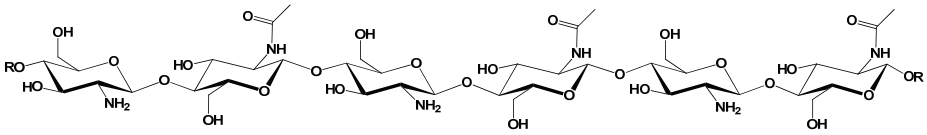

Figure 2: The structure of chitosan comprising randomly distributed β-1,4 linked *N*-acetyl-glucosamine and glucosamine units rotated 180° to each other.

Chitin and chitosan exhibit interesting biological properties, including antibacterial and antifungal activities, and therapeutic properties [6, 10, 11]. Because they are non-toxic, bio-compatible and biodegradable, chitin and chitosan are desirable components for use in medicine [12-14], agriculture [15], and the food and feed industries [16]. Hydrolysis of chitosan generates hetero chitooligosaccharides (CHOS) consisting of GlcNAc and D-glucosamine (GlcN; D) of random sequence and size. These oligomers are characterized by DP_n, F_A, P_A [17] and have been shown to have several interesting medicinal properties, e.g., tumor growth inhibition [18], wound healing effects [19] and malaria prevention [20]. The short chain CHOS are water soluble and possess higher permeability than chitosan.

1.3 Enzymes that catalyze hydrolysis of polysaccharides – glycosyl hydrolases

Enzymes that break down polysaccharides are called glycosyl hydrolases (GH) or glycosidases in general. Traditionally, glycosidases were classified according to the IUB Enzyme Nomenclature based on substrate specificity and the type of reaction that the enzyme catalyses. This classification system does not consider the structure of the enzyme and can be problematic when it comes to promiscuous enzymes that hydrolyze more than one substrate. Motivated by the desire for a more informative classification system, Henrissat and coworkers developed a system where glycosidases are classified into different families based on sequence similarities [4]. Updated information about these families is available on the CAZY web site (http://www.cazy.org/).

Generally, the 3D-structure of an enzyme is more highly conserved than the amino acid sequence, and therefore high sequence similarity within a family indicates similar folding [21]. This enables sequence information obtained from the CAZY classification system to be used to predict protein structure based on similarities within a GH family. Although glycosidases from disparate families fold differently, the overall topology of the active site can be divided into three general classes; (i) pocket, (ii) cleft and (iii) tunnel [22], which have evolved to hydrolyze the natural substrates of the enzymes. Glycosidases harboring a wide active-site pocket specialize in hydrolyzing substrates with a large number of reducing ends, whereas the active-site cleft is usually found in endo-acting enzymes hydrolyzing polymeric substrates. The active-site tunnel surrounds the substrate and is typical for enzymes acting in an exo-manner. Traditionally, the active-site tunnel was thought to be essential in processive hydrolysis, where the enzyme performs multiple cuts on the bound substrate. In a number of enzymes, binding of the substrate also depends on interactions with subsites distant from where the glycosidic bond is actually cleaved. These defined subsites are denoted $-n$ where the non-reducing end of the polymer binds and $+n$ where the reducing end of the polymer binds. Cleavage of the

glycosidic bond takes place between subsites −1 and +1 [23]. The subsites where the polymer binds are termed glycon subsites, whereas the subsites binding the product are termed aglycon subsites [24].

1.3.1 Mechanism of hydrolysis

Enzymatic hydrolysis of the glyosidic bond takes place via a general acid catalysis, requiring two conserved catalytic acids in the active site of the glycosidase: one acts as a proton donor and the second acts as a nucleophile. Regardless of family, glycosidases can be divided into two major groups based on the mechanism utilized for hydrolyzing the glycoside linkage, involving either retention or inversion of the anomeric configuration [1, 25]. Both mechanisms involve an oxocarbenium-ion-like transition state [26]. The inverting glycosidases hydrolyse the glycosidic linkage via a direct displacement of the sugar moiety in the positive subsites (aglycon subsites) (Figure 3), leading to a change in anomeric configuration.

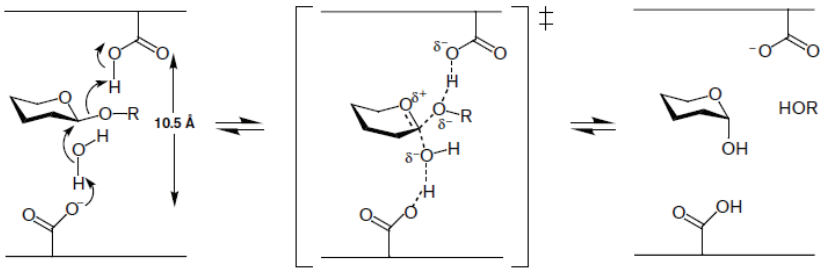

Figure 3: General mechanism of inverting glycosyl hydrolase**s**, resulting in newly formed reducing ends possessing α-anomeric configuration [26].

The two carboxylic acids involved in the inverting mechanism are separated by approximately 10 Å, which allows a water molecule to insert between the base and the sugar required for hydrolysis. The carboxylic acid acting as a nucleophile attacks the incoming water molecule, forming a hydroxyl group. The activated water then reacts with the anomeric carbon of the pyranose ring, to form the oxocarbenium-ion-like transition state, while the other carboxylic acid acts as a general acid by donating a proton to the negative glycosidic oxygen that becomes the leaving group to complete the hydrolysis (Figure 3) [1, 2, 26].

Retaining glycosidases hydrolyse the O-glycosidic bond via a double displacement reaction, leading to retention of the anomeric configuration (Figure 4).

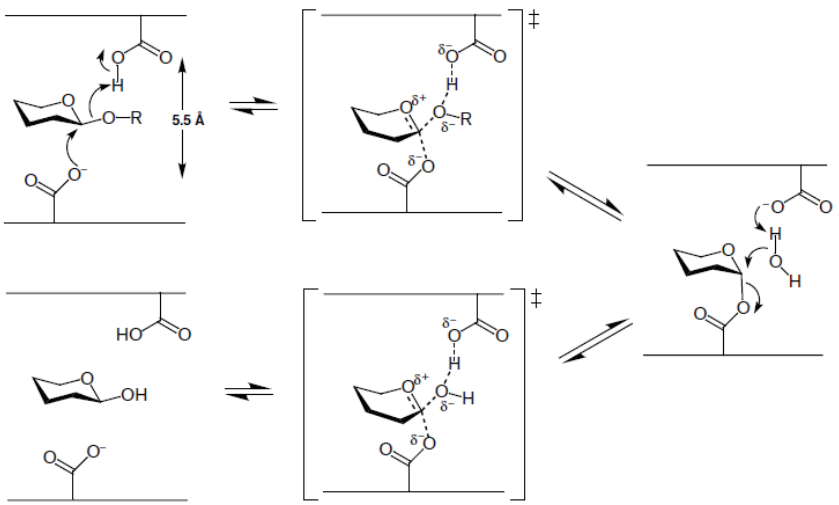

Figure 4: General mechanism of retaining glycosyl hydrolases, resulting in newly formed reducing ends with β-anomeric configuration [26].

Retaining enzymes have the two carboxylic acids distanced about 5 Å apart, which interact directly with the sugar moiety. The catalytic nucleophile attacks the anomeric carbon of the sugar moiety creating a net negative charge of the glycosidic oxygen. The catalytic nucleophile attacks the anomeric carbon of the sugar moiety, creating a net negative charge on the glycosidic oxygen, which then receives a proton from the general acid and forms the leaving group. A covalent glycosyl-enzyme intermediate is formed referred to as the oxocabenium intermediate.

Cleavage of the O-glycosidic bond occurs via activation of an incoming water molecule by the catalytic acid, now acting as a base, forming a hydroxyl ion that reacts with the anomeric carbon of the glycon moiety generating a β-anomeric transition state, which collapses to form the new reducing end (Figure 4) [2, 22, 26].

1.3.2 Chitinolytic enzymes

In nature, the degradation of chitin is catalyzed by chitinases. Depending on their amino acid sequence, chitinases are divided into the two GH families, 18 and 19 [27]. Family 19 chitinases are mostly found in higher plants, and are thought to play a part in defense mechanisms against fungal pathogens [28]. Family 18 chitinases are much more widespread across species and are found within several organisms, including bacteria, fungi, nematodes, insects and mammals. The function of family 18 chitinases differs between organisms. For example, bacteria hydrolyse chitin as an energy source, whereas in humans, chitinases are involved in the immune system [29]. Even though both family 18 and 19 chitinases hydrolyse chitin, there are no similarities in sequence or structure [30]. The catalytic domains of family 19 chitinases consist of several α-helices [31], and the enzymes exhibit a catalytic mechanism whereby the anomeric configuration is inverted [32]. In contrast, the catalytic domain of family 18 chitinases consists of a TIM-barrel ($(\alpha/\beta)_8$ barrel) fold with the highly conserved DXXDXDXE sequence motif at the fourth β-strand of the barrel and the catalytic Glu in an equivalent position at the C-terminal end [33-36].

In addition to the TIM-barrel domain, family 18 chitinases often contain a small (α+β) domain and a β-strand-rich domain that is involved in substrate binding, i.e., the chitin binding domain.

1.3.3 Family 18 chitinases from *Serratia marcescens*

Species that depend on efficient chitin turnover usually produce a set of chitinases to effect breakdown. The extensively studied Gram negative soil bacterium *Serratia marcescens* has well-developed chitinolytic machinery consisting of three active chitinases, ChiA, ChiB, and ChiC (Figure 5), in addition to a chitin binding protein, CBP21, and a hexosaminidase [37-39].

The three active chitinases have different roles in chitin hydrolysis for efficient breakdown of the substrate. ChiA and ChiB both have deep active-site clefts covered with a path of aromatic residues that continues over the surface of the chitin-binding domain (Figure 5) [33, 40]. The active-site cleft of ChiA contains six defined subsites from –4 to +2 [33, 41] with an N-terminal chitin binding domain extending the substrate-binding cleft where the non-reducing end of the substrate binds, implying that ChiA hydrolyses chitin towards the non-reducing end [40]. ChiB exhibits an active-site cleft with defined subsites from –3 to "+3" [40]. In contrast to ChiA, ChiB contains a C-terminal chitin binding domain extending the active-site cleft where the reducing end of the polymer binds, indicating hydrolysis takes place towards the reducing end of the substrate [42].

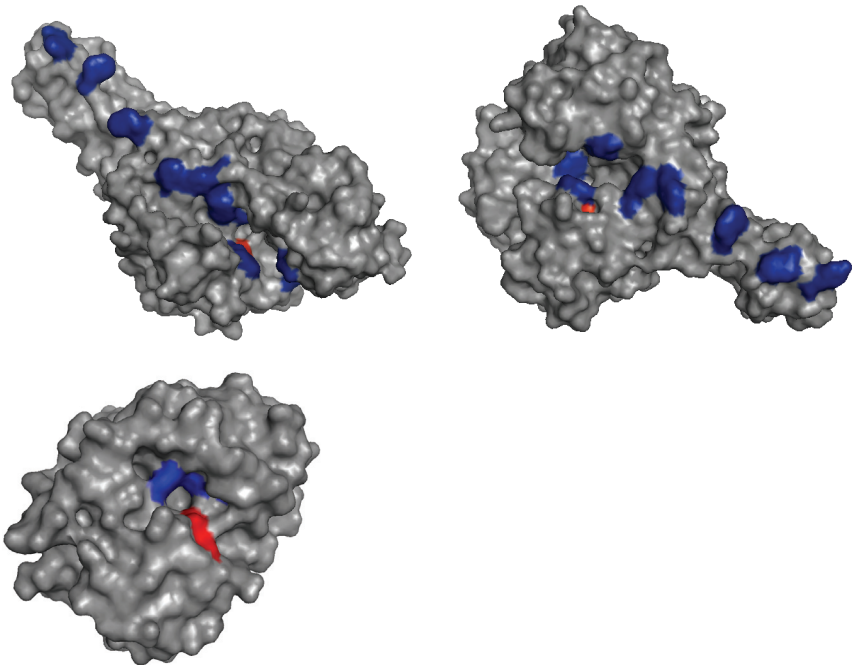

Figure 5: Structure of the two exo-chitinases ChiA (upper left (1CTN)) and ChiB (upper right (1E15)) from *S. marcescens*, and the endo-chitinase hevamine that resembles ChiC (lower (2HVM)) from *Hevea brasiliensis*. Conserved aromatic residues important for substrate binding are marked in blue, while the catalytic acid is marked in red.

ChiA and ChiB both hydrolyze insoluble chitin from the chain ends i.e., in an exo-manner [42, 43], even though it has been shown that they work on soluble chitosan in an endo-manner [44]. They also work in a synergetic fashion with opposite directionality in hydrolyzing the polymeric substrate, leading to accumulation of $(GlcNAc)_2$ [42, 45]. Despite being an exo-chitinase, ChiA has been shown to possess some endo-activity with insoluble substrates [45]. By comparing the structure of the two exo-chitinases, it is clear that in ChiB partial closure of the roof over the active-site cleft occurs upon substrate binding, and hence it possesses a more tunnel-like catalytic cleft. The active-site cleft of ChiA is more open even after

binding a ligand, which is a typical characteristic of endo-acting enzymes [40, 44, 46].

The structure of the third active chitinase from *S. marcescens*, ChiC, has not been resolved, but sequence alignments with exo-chitinases indicate that ChiC lacks the α/β-domain forming the walls of the substrate binding cleft in ChiA and ChiB. This could indicate that ChiC possesses a more open and shallow active-site cleft, resembling the plant endo-chitinase hevamine from *Hevea brasiliensis* (Figure 5) [35, 47]. Endo-activity of ChiC is suggested by the fact that long chitooligosaccharides are produced upon chitin degradation as well as its high activity towards complex polymeric substrates (i.e., substrates that are likely to be the primary target of an endo-acting member of the chitinolytic enzyme machinery), and low activity towards oligomeric substrates compared to processive exo-chitinases [38, 44, 47]. In the chitinolytic machinery of *S. marcescens*, the endo-chitinase ChiC enhances the accessibility of crystalline chitin for exo-chitinases and works synergistically with the exo-chitinase ChiA, resulting in complete conversion of β-chitin [44]. ChiB only appears to work in a synergetic manner with ChiA and not with ChiC.

The chitin binding protein CBP21 is cooperatively regulated with the three active chitinases. Recently, it has been observed that CBP21acts as a helper protein by catalyzing cleavage of glycosidic bonds in crystalline chitin through an oxidative mechanism, making the inherently inaccessible substrate more accessible to chitinases [48].

1.3.4 Human chitinases

Although humans do not possess chitin, two active mammalian chitinases have been identified; Acidic Mammalian Chitinase (AMCase) [49] and Human Chitotriosidase (HCHT) [50]. HCHT was first discovered in elevated amounts in the plasma of humans suffering from the lysosomal storage disorder Gaucher's disease [51] and

appears in human macrophages. AMCase is mainly found in the stomach and in lesser amounts in the lungs, nasal polyps and tears [52-54]. Both HCHT and AMCase are family 18 chitinases showing high sequence homology with chitinases from lower organisms [50, 55]. The structures of AMCase and HCHT are highly conserved; the active site is an open cleft covered with a path of aromatic residues (Figure 6).

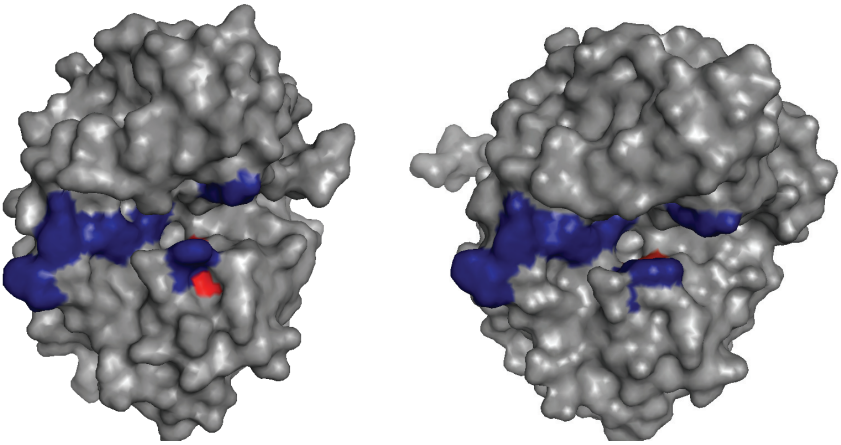

Figure 6: Aligned crystal structures of HCHT (left [50], 1GUV) and AMCase, (right [56], 3FXY). Conserved aromatic residues important for substrate binding are marked in blue, and the catalytic acids are marked in red.

The active site is divided into defined subsites stretching from −3 in the glycon sites to +2 in the aglycon sites, suggesting hydrolysis of the substrate occurs from the reducing end [50, 56]. Both human chitinases are synthesized as 50 kDa proteins containing a 39 kDa N-terminal catalytic domain and a C-terminal chitin-binding domain [54]. The 39 kDa form without the chitin binding domain is not able to bind to chitin [57]. HCHT is processed to an extent in lysosomes, where it loses its chitin

binding domain and appears as a 39 kDa enzyme [58]. An important structural difference between the two enzymes is that three polar residues in the active site of AMCase (His^{208}, His^{269} and Arg^{145}) are instead Asn^{208}, Arg^{269}, and Gln^{145} in HCHT. These three residues are thought to be responsible for the low pH-optimum of AMCase required for tolerating the extreme environment of the gastrointestinal tract [54, 56].

AMCase is associated with asthma and chronic inflammatory disorders, which affect millions of people worldwide [59]. Asthma and inflammatory diseases are believed to be a consequence of an exaggerated Th-2 response elicited independently of parasitic infection [29]. It is assumed that Th-2 inflammation originally evolved as a defense mechanism to protect the host against parasites [60]. It has been proposed that this mechanism is poorly controlled allowing elicitation of Th-2 responses independent of parasitic infections, and thus triggering asthma and allergy [60, 61]. AMCase is up-regulated in response to Th-2 mediated inflammation and has been found in elevated amounts in lung macrophage cells of allergen-challenged asthma patients. Inhibition of the over-expressed AMCase has been shown to decrease asthmatic symptoms [49]. Consequently, inhibition of AMCase is a target for therapeutic purposes. However, inhibition of AMCase should be carefully considered in light of the properties discovered for HCHT. Studies have shown that HCHT inhibits hyphal growth of chitin-containing fungi, such as *Aspergillus* and *Candida* species [62, 63] and it is thought to play a role in the human defense mechanism against chitin-containing pathogens. Hence, inhibition of human chitinases needs to be AMCase specific in order to avoid the elimination of important anti-pathogenic activities as a consequence of total chitinase inhibition.

1.3.5 Hydrolytic strategies of family 18 chitinases

Across the catalytic cleft and chitin binding domain of family 18 exo-chitinases, there is a series of conserved aromatic residues that interact with the substrate through hydrophobic stacking interactions with the pyranose rings [33, 40, 64]. In ChiA, aromatic residues located on the chitin binding domain and on the glycon side (substrate binding subsites) of the active site are crucial for binding crystalline chitin [65-68]. In contrast, aromatic residues on the aglycon (product release subsites) side of the active site are assumed to play an important role in product release and/or pulling the crystalline substrate through the active site for the next catalytic cycle [24, 66, 68]. This is reflected by the activation parameters upon chitosan hydrolysis, which show the enthalpic penalty diminishes to a larger extent when glycon aromatic residues are removed compared to aglycon residues [69]. In ChiB, which has the opposite directionality of ChiA, the aglycon subsites are responsible for substrate-binding, while the glycon subsites are involved in product-release [24, 68, 70]. Mutational studies on the aromatic residues throughout the active site and catalytic domain of family 18 chitinases have confirmed the important role of these residues [66, 68].

It has been shown that substrate association is the rate-limiting step in the hydrolysis of crystalline chitin, whereas product release is the rate-limiting step in the hydrolysis of a soluble substrate [66, 70]. Chitinases have developed a processive mechanism, whereby the enzyme remains closely associated with the substrate for several catalytic cycles [70, 71]. This ensures efficient chitin degradation by allowing many hydrolytic events to occur, once the barrier of substrate association for an insoluble crystalline substrate has been overcome. By sliding the substrate through the active site between catalytic cycles instead of releasing it, the enzyme does not need to search for new substrate and the efficiency of the hydrolysis reaction is enhanced [71, 72]. A common feature of processive enzymes is a tunnel-like topology of the active site, which is thought to embrace the substrate and prevent it from dissociating [71, 72]. None of the three active chitinases from *S.*

marcescens exhibit a clear tunnel-shaped active site.; only ChiB shows a partial closure of the active-site roof upon binding a substrate, which is caused by Asp^{316} rotating towards Trp^{97} and forming a hydrogen bond [73]. Despite the lack of a defined active-site tunnel, both ChiA and ChiB have been shown to hydrolyze chitin in an exo-processive mode of action [44, 46]. The lack of an active-site tunnel in the structure of the processive chitinases indicates that other factors must contribute to keep the substrate closely associated with the enzyme. Aromatic residues covering the active site and the chitin-binding domains interact with the substrate through hydrophobic stacking interactions, providing a strong but "fluid" binding and sliding of the substrate [74, 75]. Mutational studies have shown that these aromatic residues are responsible for the sliding and steering of the polymer through the active site during processive hydrolysis [43, 66, 68, 70]. ChiC does not possess the same path of conserved aromatic residues as ChiA or ChiB, and does not appear to hydrolyze chitin in a processive manner [44].

1.3.6 Hydrolytic mechanism of family 18 chitinases

Chitin consists of β-1,4-linked *N*-acetyl glucosamine units that are rotated 180° to each other. Thus, total conversion of chitin by GH family 18 chitinases gives the product $(GlcNAc)_2$ with retention of the anomeric configuration of the newly formed reducing end [34]. It has been observed that GH family 18 chitinases hydrolyze chitin by a substrate-assisted mechanism rather than using two catalytic acids like several retaining glycosidases [33, 35, 40]. An oxazolinium ion intermediate is formed, which interacts with the catalytic base, as expected for a double-displacement mechanism [34, 35, 73, 76]. The substrate-assisted mechanism involves several structural rearrangements in the active site of the enzyme. For ChiB from *S. marcescens*, the mechanism has been investigated extensively by crystallographic studies [73]. In the apo-enzyme, a water molecule is located within hydrogen bond distance from the catalytic acid Glu^{144} and is eliminated when the substrate enters the active site, leaving Glu^{144} deprotonated. Upon binding of the

substrate to ChiB, the sugar located in subsite −1 interacts with Tyr^{214} and Asp^{215} through hydrogen bonds, and stacks with Trp^{403}, making hydrophobic contacts. These interactions force the pyranose ring of the GlcNAc unit in subsite −1 to distort from the relaxed $^{4}C_{1}$ chair conformation to the skewed $^{1,4}B$ boat conformation (Figure 7) [77]. This distortion of the sugar ring has been shown to be energetically unfavorable for the substrate, raising the free energy by about 8 kcal/mol [78]. The conformational changes that occur upon substrate distortion help to place the glycosidic oxygen near the catalytic residue Glu^{144} and position the leaving saccharide in a pseudo axial position, facilitating nucleophilic attack on the anomeric carbon [77, 78].

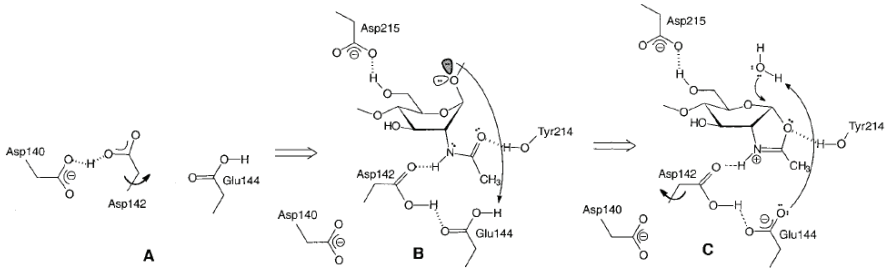

Figure 7: Proposed mechanism of substrate-assisted hydrolysis by family 18 chitinases. (A) Enzyme active site before substrate binding. (B) Substrate enters the active site and is distorted into a skew-boat conformation at the −1 subsite. Asp^{142} rotates towards Glu^{144} donating a proton, which is followed by protonation of the O-glycosidic bond by Glu^{144}. (C) The resulting oxazolinium ion is attacked by an activated water molecule from the β-direction, generating the active-site leaving group [73].

To reduce the pK_a of Glu^{144} so that it can act as a proton donor, Asp^{142} rotates away from Asp^{140} towards Glu^{144}, forming a hydrogen bond between the acid and the N-H bond of the N-acetyl group, which helps to stabilize the positively charged oxazolinium intermediate. The catalytic acid donates a single proton to the oxygen atom of the glycosidic linkage, which is followed by nucleophilic attack on the C1 carbon of the pyranose ring by the carbonyl oxygen of the C-2 acetoamide group from the α-direction, generating the oxazolinium intermediate [73, 79, 80] (Figure 7). Finally, a deprotonated water molecule attacks the C1 of the intermediate from the β-direction, resulting in hydrolysis and formation of a new reducing end with retained β-configuration.

1.3.7 Transglycosylation activity

Glycosidases have also been shown to catalyze transglycosylation reactions, which result in formation of new glycosidic bonds between a donor and an acceptor saccharide [81]. Even though family 18 chitinases are believed to be hydrolytic enzymes, there are reports that some chitinases produce longer CHOS during hydrolysis [68, 82-84]. As described above, GH family 18 chitinases perform hydrolysis via a substrate-assisted mechanism, resulting in net retention of the anomeric configuration. Under hydrolytic conditions, a water molecule reacts with the oxazolinium ion intermediate to form the new reducing end. If instead the oxazolinium ion intermediate reacts with a hydroxyl group in a carbohydrate, transglycosylation occurs. Transglycosylation is a kinetically controlled process. Mutational studies on several types of chitinases have shown that strong binding of incoming carbohydrate molecules in aglycon subsites and prevention of the correct positioning of the water molecule involved in hydrolysis are the most important factors for determining whether the transglycosylation reaction proceeds in high yield [84-86].

1.4 Thermodynamics of ligand-protein interactions

In general, interactions between a protein and a ligand**,** such as chitinase and chitin, are noncovalent. The most important parameter in the thermodynamic description of binding is the Gibbs free energy change (ΔG_r °), which can be related to the binding affinity of a ligand to an enzyme. The free energy change can be expressed in terms of the equilibrium constant of the binding reaction (K_a) and can be divided into an enthalpic (ΔH_r°) and entropic (ΔS_r°) part (Equation 1).

$$\Delta G_r\,^\circ = -RT\ln K_a = \Delta H_r^\circ - T\Delta S^\circ_r \qquad (1)$$

where R is the gas constant and T is temperature.

The enthalpy change of a binding reaction reflects changes in the weak interactions between the ligand and the enzyme compared to their interaction with the solvent. The entropic change is normally divided into three separate terms; the loss of translational entropy when two entities are combined (ΔS_{mix}), the change in the entropy of solvation upon ligand binding (ΔS_{solv}), and the change in entropy due to conformational changes in both the ligand and enzyme upon binding (ΔS_{conf}) (Equation 2):

$$\Delta S^\circ_r = \Delta S_{solv} + \Delta S_{mix} + \Delta S_{conf} \qquad (2)$$

Individual enthalpic and entropic contributions upon binding can vary, but often in a compensatory manner, resulting in only small variations in the free energy that ultimately determines the thermodynamic stability of the process. This phenomenon is known as the enthalpy-entropy compensation and is often observed in aqueous systems where noncovalent interactions dominate [87, 88].

The solvatization entropy, ΔS_{solv}, is directly linked to the heat capacity (ΔC_p) of a protein and can be derived from ΔC_p by assuming that ΔS_{solv} is close to zero for proteins near 385 K [89]. Equation 3 gives ΔS_{solv} at 20 °C.

$$\Delta S_{solv} = \Delta C_p \ln (T_{293K} / T_{385K}) \qquad (3)$$

The change in the entropy of mixing of the solvent and solute molecules, ΔS_{mix}, can be calculated as a statistical correction that accounts for the entropy change due to changes in translational/rotational degrees of freedom [90]. For a bimolecular binding reaction this can be given as:

$$\Delta S_{mix} = R \ln (1 / 55.5) \quad (4)$$

where R is the gas constant. ΔS_{conf} can then be calculated from ΔS_r by substituting the calculated values for ΔS_{mix} and ΔS_{solv} into Equation 2.

A typical strategy to enhance binding is the use of rigid ligands to reduce the loss in ΔS_{conf} upon binding [91]. However, in terms of medical applications, drugs where the binding has been enthalpically optimized have so far performed better than drugs which have been entropically optimized [92]. Therefore, to develop good inhibitors, it is important to have detailed thermodynamic data for the binding reaction.

Changes in heat capacity (ΔC_p) of protein-ligand interactions can provide information on the mechanism of ligand binding [93]. The heat capacity reflects the capacity of any given substance to absorb heat energy without changing the temperature [93]. Substances in the liquid phase have translational and rotational degrees of freedom, and hence can absorb thermal energy to a greater extent than solid substances. Negative ΔC_p values have typically been associated with hydration of hydrophobic residues [94, 95], but recently it have been shown that a negative ΔC_p value can also indicate cooperative disorder of hydrogen bond networks [93]. Even though changes in enthalpy and entropy have traditionally been used to indicate changes in the conformation and interactions upon binding, both the magnitude and sign of ΔC_p can reflect physical changes within the protein behind the mechanism of protein-ligand interaction [96, 97].

1.5 Studying ligand-protein interactions

Several techniques have been used to study interactions between proteins and ligands. Traditionally, ultracentrifugation was widely used to determine the molecular mass and binding affinity of interactions with K_d of 10^{-9} to 10^{-20} M [98]. In the past few decades, several biophysical techniques have been developed that allow protein-ligand interactions to be directly monitored. X-ray crystallography and nuclear magnetic resonance (NMR) are now well-established techniques which provide structural information on the ligand-binding sites in a protein, whereas mass spectrometry (MS), isothermal titration calorimetry (ITC), and surface plasmon resonance (SPR) are popular techniques for characterizing the thermodynamics and kinetics of binding.

ITC is a robust technique that is commonly used to analyze interactions in biological systems. It allows measurement of the equilibrium constant and enthalpy change of ligand-binding by measuring the change in heat evolved when a ligand is added stepwise to a protein solution until the protein is saturated [99, 100]. These experiments enable direct determination of K_a and ΔH_r from a single experiment, which is a major advantage of ITC compared to other titration techniques. Binding analysis using ITC is performed in solution, with proteins in their native form without requiring chemical modification, labeling, immobilization or limits on the size of interacting species. Thermodynamic values obtained by ITC measurements include contributions from all equilibria occurring during the change in the molecule from a free to a bound state, including solvent interactions. The thermodynamic data are therefore considered as observed rather than absolute values [98].

Using SPR, the protein of interest is immobilized to a surface and a solution of the ligand is passed over. The ligand-protein interaction is monitored by measuring the change in refractive index of the surface as a result of complex formation [98, 101, 102]. SPR allows determination of kinetic parameters, such as association and dissociation rate constants as well as dissociation equilibrium constants (K_D).

MS is a versatile tool that has several advantages for studying molecular interactions, including specificity, sensitivity and speed. Using MS, the binding between a ligand and an enzyme can be monitored and specificity, binding strength and dissociation kinetics can be determined in the same experiment [103, 104]. However, it should be mentioned that interactions observed in the gaseous phase do not necessarily reflect those occurring in the condensed phase.

1.5.1 Ionization of noncovalent complexes

Binding of a ligand to an enzyme involves noncovalent interactions, which are solvent-dependent. In conventional ionization techniques, such as electronic ionization (EI) and chemical ionization (CI), these interactions are not preserved in the gas phase, and hence are not suitable for studying ligand binding. The development of soft ionization techniques, e.g., matrix assisted laser desorption ionization (MALDI) [105, 106] and electrospray ionization (ESI) [107], has allowed noncovalent biomolecular interactions complexes to be studied by MS. In 1991, Ganem *et al.* were the first to report the use of MS to study a noncovalent complex by detecting an enzyme-substrate interaction using ESI MS [108]. ESI MS has since been applied to numerous noncovalent complexes, including protein-protein, protein-ligand, protein-DNA and DNA-DNA complexes [109, 110], and is the most widely used technique because it involves ionizing analytes directly from the liquid phase, thus reflecting the natural environment of the biomolecule [109].

Although ESI is by far the most frequently employed technique for detecting noncovalent complexes, MALDI MS has also been used successfully to detect such complexes [111-113]. MALDI offers advantages over ESI, e.g., it is less sample consuming, faster, and more tolerant to salts and detergents than ESI. Ultraviolet (UV) lasers are commonly used to perform ionization in MALDI. However, the solid state of most UV matrices will generally disrupt weak noncovalent interactions. Therefore, in UV-MALDI, complexes are usually only detected after

the first laser pulse, i.e., the “first shot phenomenon” [114]. This phenomenon arises due to the high energy of the laser irradiation deposited in the matrix dissociating the noncovalent complex. By using a liquid matrix under near physiological conditions during MALDI ionization, several of the limitations associated with solid matrixes are overcome.

When transferring a complex from a solvent to a gaseous phase, the change in environment is likely to affect intramolecular interactions within the complex. The hydrophobic effect that drives interactions between apolar groups plays an important role in binding a ligand to an enzyme. These interactions depend on the presence of water, and so are lost in the gaseous phase. Electrostatic interactions in a complex are usually strengthened when the solvent is removed, resulting in new and potentially stronger interactions compared to those present in the liquid phase. It is therefore important to bear in mind, when searching for ligands that bind strongly to a protein using MS, that complexes may dissociate upon ionization and non-specific complexes can be formed in the gas-phase, which do not reflect the nature of the complexes in the condensed phase [115].

1.6 Inhibition of family 18 chitinases

Chitin metabolism is essential for fungi and arthropods, and hence the ability to control chitin turnover is of great interest in developing new fungicides [116], pesticides [8] and medicines [17]. Family 18 chitinases are particularly interesting because they are essential for several pathogenic and pest organisms, and are associated with asthma and inflammatory diseases in humans. The majority of known chitinase inhibitors are competitive inhibitors, which block the substrate from entering the binding sites. These molecules can be divided into two general groups based on whether they (1) interact with the aromatic residues in the active site in a similar fashion to chitin, i.e., by stacking interactions [117] or (2) mimic the oxazolinium ion reaction intermediate of family 18 chitinases [118]. The most

extensively studied inhibitor of family 18 chitinases is the pseudosaccharide allosamidin isolated from *Streptomyces sp.* [119]. Allosamidin binds to the subsites from −3 to −1 in the active site of family 18 chitinases. The allozamizoline moiety binds to the −1 subsite and resembles the oxazolinium intermediate of substrate-assisted catalysis [73, 120, 121], with binding affinities in the sub- to low-micromolar range [24, 122, 123]. Detailed thermodynamic characterization of allosamidin binding to ChiA, ChiB and ChiC of *S. marcescens* has been performed and revealed large differences in the entropic and enthalpic contributions to binding between the three enzymes, which depend on their hydrolytic character [24].

Recently, peptides that mimic carbohydrates have attracted attention as chitinase inhibitors [124]. The cyclic pentapeptides argadin [125] and argifin [126] isolated from fungi are particularly interesting because they inhibit family 18 chitinases with affinities in the nanomolar to micromolar range [127]. Both argadin and argifin interact with the conserved aromatic residues in subsites −1 to +2 in a similar fashion to the stacking interactions with chitin, albeit with different orientation and location [128]. They can both be synthesized using standard peptide chemistry, and hence are more accessible synthetically than allosamidin. The medical potential of peptide inhibitors is somewhat limited due to their high molecular weight and the large number of potential hydrogen bond donors/acceptors, which according to the Lipinski rule [129] exceeds the optimum required for solubility and permeability of a drug candidate.

Since family 18 chitinases operate by substrate-assisted catalysis, the hydrolysis reaction depends upon positioning a GlcNAc moiety in subsite −1 [34, 73]. It has been shown that in crude mixtures of different CHOS isomers with the same F_A and DP_n but different sequences, some isomers will act as substrates for the enzyme, while other isomers will bind unproductively, and hence act as inhibitors [122, 130]. In order to bind non-productively, oligomeric substrates must be positioned with a GlcN unit in the −1 subsite of the active site [122, 130, 131]. Several subsites in both ChiA and ChiB have been shown to exhibit clear preferences for GlcNAc and

are involved in positioning the substrate in a non-productive manner [44, 73]. In addition, it is believed that the energetically unfavorable transformation of the pyranose ring from the relaxed $^{4}C_{1}$ chair conformation to the skewed $^{1,4}B$ boat conformation does not take place, or at least does not take place completely, when a GlcN is bound in subsite −1, and hence binding of the substrate to the enzyme is more favorable.

2. AIMS OF THIS STUDY

An important long-term goal of the work described in this thesis was to provide a detailed understanding of how substrates and inhibitors bind to chitinases. This is important for developing approaches to control biological processes such as defense mechanisms in plants and mammals, and to exploit the enormous amounts of biopolymers readily accessible in nature.

The main objective of the work described in this thesis was to investigate interactions between the enzyme and the substrate at a molecular level. This was achieved using different calorimetric, chromatographic and mass spectrometric methods.

The work involved the following aims:

- Undertake a detailed thermodynamic characterization of the enthalpic and entropic contribution of the defined subsites which participate in the interaction between CHOS and ChiB from *Serratia marcescens*, in order to improve understanding of the binding thermodynamics to assist the development of chitinase inhibitors.
- Investigate the involvement of the –3 subsite and a putative "+3" subsite in positioning the substrate in the active site of ChiA from *Serratia marcescens*, compare how ChiA and its –3 subsite mutant W167A interact with soluble polymeric substrates and investigate interactions beyond the aglycon subsites, which could potentially be important for processivity and endo-activity.
- Study the human macrophage chitinase HCHT with respect to endo-/exo-activity, processivity and binding preferences to provide insights into the enzymatic mechanism and reveal differences between HCHT and the other known human chitinase, AMCase.

- Develop a fast, simple and sensitive screening method to search for noncovalent binding between enzymes and ligands using mass spectrometric techniques.

3. RESULTS IN BRIEF

Paper I: Determination of substrate binding energies in individual subsites of a family 18 chitinase

Thermodynamic parameters for binding of *N*-acetylglucosamine oligomers to the individual subsites of ChiB from *S. marcescens* were determined using ITC. We observed that $(GlcNAc)_6$ and $(GlcNAc)_5$ bound with a K_d of 0.13 ± 0.009 μM and 0.67 ± 0.02 μM, respectively. Binding of both oligomers was clearly driven by the change in entropy with $-T\Delta S_r°$ of −10.9 ± 0.4 kcal/mol and – 9.1 kcal/mol, respectively, and an enthalpic penalty of $\Delta H_r°$ = 1.7 ± 0.3 kcal/mol and 0.8 ± 0.2 kcal/mol, respectively. $(GlcNAc)_4$ binds with a K_d of 2.7 ± 0.19 μM, and was also shown to be entropically driven ($-T\Delta S_r°$ of –6.5 ± 0.2 kcal/mol) with a small favorable enthalpic contribution ($\Delta H_r°$ = –1.0 ± 0.1 kcal/mol). In contrast, when $(GlcNAc)_3$ bound (K_d = 377 ± 22 μM), we observed that the reaction was driven by the change in enthalpy ($\Delta H_r°$ = −4.9 ± 0.9 kcal/mol) with a small entropic penalty of $-T\Delta S_r°$ = 0.2 ± 0.2 kcal/mol. ChiB has six subsites spanning from –3 to "+3" [40], and previous studies have shown the binding preferences of $(GlcNAc)_n$, where n = 3-6 [41]. Therefore, the thermodynamic signature of single subsites could be calculated from the results obtained.

Paper II: Dissecting factors that contribute to ligand-binding energetic for family 18 chitinases

We studied the binding of a hexameric *N*-acetylglucosamine, $(GlcNAc)_6$, to an inactive mutant of ChiB (ChiB-E144Q) from *S. marcescens* using ITC and compared the results with binding of allosamidin to ChiA and ChiB from *S. marcescens*. Binding of $(GlcNAc)_6$ was measured at pH 6.0 and temperatures

ranging from 15 °C to 37 °C. The change in reaction heat capacity was $\Delta C_{p,r} = -158 \pm 5$ kcal/K mol. At 20 °C, $(GlcNAc)_6$ was found to bind with a $\Delta G_r°$ of −9.1 ± 0.3 kcal/mol and binding was clearly driven by entropy ($-T\Delta S°_r = -10.3 \pm 0.4$ kcal/mol), and had an enthalpic penalty of $\Delta H_r° = 1.2 \pm 0.3$ kcal/mol. To investigate the effect of pH on $(GlcNAc)_6$ binding, additional measurements were performed at pH 7.0 and 8.0, but only minor changes in the thermodynamic parameters were observed. Parameterization of $-T\Delta S_r°$ showed that binding of $(GlcNAc)_6$ to ChiB-E144Q was driven by the value of $-T\Delta S°_{solv}$, which was −12.5 ± 0.4 kcal/mol. Interestingly, binding of allosamidin to ChiA or ChiB was driven by different factors; For ChiA, binding was driven by the change in conformational entropy ($-T\Delta S°_{conf} = -10.8 \pm 0.5$ kcal/mol), whereas for Chi B, it was driven by both the change in solvation entropy and enthalpy ($-T\Delta S°_{solv} = -5.6 \pm 0.2$, $\Delta H_r° = -4.9 \pm 0.8$ kcal/mol).

Paper III: Substrate positioning in chitinase A, a processive chito-biohydrolase from Serratia marcescens

In Paper III we investigated substrate positioning in ChiA from *S. marcescens*. The role of a conserved tryptophan in subsite −3 together with a putative "+3" binding site were studied by comparing how ChiA and its −3 subsite mutant ChiA-W167A interact with chitooligosaccharides and chitosan. We observed that binding of $(GlcNAc)_5$ to ChiA-W167A occurs predominantly in subsites −2 to "+3", whereas in ChiA, only about 50 % of $(GlcNAc)_5$ binds in this manner. K_m and k_{cat} were determined for both enzymes using $(GlcNAc)_4$ as the substrate and were 333 ± 44 μM and 97 ± 9 s^{-1}, respectively, for the ChiA-W167A mutant, and 9 ± 1 μM and 33 ± 1 s^{-1}, respectively, for ChiA. Partly deacetylated chitooligosaccharides with a DP_n of 8 and average degree of acetylation of 50 % ($F_A = 0.5$) were incubated with both ChiA and ChiA-W167A for 5 or 60 minutes and analyzed by nano-ESI-q-TOF MS and MALDI TOF MS. No oligomers of $DP_n = 8$ were left in solution after 5 minutes

with ChiA, whereas nano-ESI-q-TOF MS spectra of samples incubated with ChiA-W167A revealed oligomers were present in both the solution and in complex with ChiA-W167A after 60 minutes of incubation. By hydrolyzing chitosan to a maximum degree of scission with either ChiA or ChiA-W167A and analyzing the resulting oligomeric products using MALDI-TOF-MS, product sequences were obtained. We observed that oligomeric mixtures formed by ChiA-W167A-mediated hydrolysis were considerably more complex than mixtures generated via ChiA-catalyzed hydrolysis.

Paper IV: The action of the human chitotriosidase on chitosan

The mode of action of HCHT was studied extensively by considering the hydrolysis of high molecular weight chitosans. It was observed that HCHT displays tri-phasic kinetics when catalyzing the hydrolysis of chitosan, with an F_A of 0.62. The initial phase of hydrolysis proceeded until an α-value of approximately 0.05 was achieved, with an apparent rate constant (k_{cat}^{app}) of 86 s^{-1}. The second kinetic phase, corresponded to α-values between 0.05 and 0.13 and was characterized by an 8-fold decrease in the apparent rate constant (k_{cat}^{app} = 11 s^{-1}). The final kinetic phase was characterized by a further 2 – 3-fold reduction in k_{cat}^{app} (= 4 s^{-1}) and lasted until an α-value of 0.33 was reached. Sequence information about the acetylated and deacetylated units in the oligomers formed at different times during hydrolysis indicated that there was a very strong, absolute, and a relatively weak preference for an acetylated unit in the –2, –1, and +1 subsite, respectively. The relative viscosity of the chitosan solution was observed to rapidly decrease during chitinase-catalyzed hydrolysis, suggesting HCHT acts in the endo-mode when hydrolyzing chitosan. By plotting the relative viscosity of the polymer solution (from which the value of α for the polymer fraction, α_{pol}, can be calculated), versus the total number of reducing ends (α_{tot}), the number of cuts (N_{cuts}) per enzyme-substrate complex was calculated. The results indicated that HCHT is processive with an average of 2.5 cuts per enzyme-substrate complex for the hydrolysis of a chitosan with F_A of 0.62.

Paper V: Analysis of productive binding modes reveals differences between human chitinases

We mapped the preferred productive-binding modes of oligosaccharide substrates to HCHT. Productive binding of $(GlcNAc)_6$, $(GlcNAc)_5$, and $(GlcNAc)_4$ to HCHT was analyzed using HPLC under conditions that permitted determination of both the concentrations and the β/α-anomer ratios of substrates and products. Oligomers were observed to bind with a β-anomer preference in the aglycon subsites and with strong binding in the putative "+3" and even "+4" subsites. Binding modes were confirmed by MALDI-TOF analysis.

Paper VI: Analysis of noncovalent chitinase-chitooligosaccharide complexes by infrared matrix-assisted laser desorption/ionization and nano-electrospray ionization mass spectrometry

We developed a novel method to analyze noncovalently bound complexes, which is fast, sensitive and highly specific, using infrared matrix-assisted laser desorption/ionization orthogonal time-of-flight (IR-MALDI o-TOF)-MS. Specific noncovalent complexes between ChiA from *S. marcescens* and CHOS were detected and the relative amount of enzyme with bound oligosaccharides versus free enzyme was essentially identical to that obtained by nano-ESI-quadrupole (q)-TOF-MS. Chitinase-CHOS complexes were not detected when ultraviolet (UV)-MALDI-o-TOF-MS was employed for desorption/ionization.

4. DISCUSSION

4.1 Energetics of ligand binding to family 18 chitinases

A desirable property for an inhibitor is strong binding with the target enzyme as reflected by the free energy change of the interaction. To enhance the binding strength, one can either design an inhibitor that has many favorable intermolecular interactions with the enzyme to increase the enthalpy change, or is rigid so that an unfavorable loss of conformational entropy change is avoided [91]. Even though an increase in the enthalpic term is typically balanced by enthalpy-entropy compensation, evidence suggests that inhibitors that are enthalpically optimized perform better as drugs than ones which have been entropically optimized [92]. In family 18 exo-chitinases, well-defined subsites interact with individual sugar moieties of the substrate and are likely to contribute to different extents to the total free energy change upon binding. Moreover, family 18 chitinases have several subsites whose function is to hold onto the substrate during processive hydrolysis, as well as subsites involved in initial substrate binding and product release, which may all interact differently with inhibitors [24]. This underlines the importance of a detailed knowledge of the energetics of ligand binding, of either an inhibitor or a substrate, for effective inhibitor development. Papers I and II are concerned with thermodynamic characterization of the interactions between different CHOS and ChiB from *S. marcescens* using ITC. Several interesting findings arose from this work. Firstly, the binding of $(GlcNAc)_6$ to ChiB, and allosamidin to ChiB or ChiA, was accompanied by the same change in the free energy ($\Delta G_r^\circ \approx -9.1$ kcal/mol) (Paper II). However, when the individual contributions of the enthalpy and entropy terms to the overall free energy change were considered, it was clear that the thermodynamic signatures were different. Allosamidin binds to ChiA in subsites −3 to −1, which remain attached to the polymeric substrate during processive hydrolysis. This interaction was driven equally by enthalpic ($\Delta H_r^\circ = -5.6 \pm 0.2$

kcal/mol) and solvation entropic changes ($-T\Delta S_{solv}$ = –4.9 ± 0.8 kcal/mol) [24]. Processivity requires a ‘‘sticky” enzyme because this increases the probability that processive sliding of the substrate will occur rather than complete dissociation [72, 132]. This “stickiness” corresponds to favorable enthalpic interactions between the enzyme and the ligand as observed for allosamidin binding to ChiA. Trp^{167} in the –3 subsite has been shown to be important for processivity in ChiA. Baban *et al*. subsequently determined the thermodynamics of allosamidin binding to the mutant ChiA-W167A and estimated that the contribution which Trp^{167} stacking to a sugar moiety made to the overall free energy change and enthalpic change was −1.8 kcal/mol and −4.4 kcal/mol, respectively [24], confirming that Trp^{167} was indeed a “sticky” residue. Allosamidin also binds to subsites −3 to −1, but in ChiB these subsites are associated with product release following the completion of processive hydrolysis. Binding of allosamidin to ChiB was driven by changes in conformational entropy ($-T\Delta S_{conf}$ = −10.8 kcal/mol), which is atypical for binding to glycosyl hydrolases and lectins [133]. Two factors which may contribute to such favorable conformational changes are as follow: Firstly, allosamidin interacts only with residues that have low *B*-factors in the structure of the ligand-free enzyme [73], and secondly, allosamidin is “preformed”, meaning it does not undergo a chair to boat conformational transformation upon binding, and hence the loss in conformational entropy is small. For $(GlcNAc)_6$ binding to ChiB, the interaction was driven by changes in solvation entropy ($-T\Delta S_{solv}$ of −12.7 kcal/mol). This agrees with previous work which showed that $(GlcNAc)_6$ interacts with the entire defined active site of ChiB (80 % with subsites –2 to +4 and 20 % with subsites –3 to +3) [41]. Moreover, this result is consistent with the observation that the interaction between ChiB and allosamidin is accompanied by a smaller $-T\Delta S_{solv}$ of −5.0 kcal/mol, which is as expected since allosamidin only binds three subsites in ChiB. This value is similar to that obtained for allosamidin binding to ChiA ($-T\Delta S_{solv}$ of −4.9 kcal/mol). The energetics of allosamidin binding to Chitinase C (ChiC) of *S. marcescens* were also explored [24]. ChiC is a true endo-chitinase with a shallower and more open substrate-binding cleft than ChiA or ChiB [24, 35, 38, 44, 47]. Thus, ChiC is likely

to be more highly solvated than either ChiA or ChiB, and therefore more water molecules may be expelled upon ligand binding to ChiC. This was shown to be the case for allosamidin binding to ChiC, which was accompanied by a $-T\Delta S_{solv}$ of –9.2 kcal/mol, suggesting that several factors may govern the solvation entropy change besides the length of the ligand.

Whereas the change in conformational entropy was important for allosamidin binding to ChiB ($-T\Delta S_{conf} = -10.8$ kcal/mol), it was almost negligible for $(GlcNAc)_6$ binding ($-T\Delta S_{conf} = -0.1$ kcal/mol). As mentioned above, the *B*-factors for residues in ChiB on the glycon side are low [73], but they are significantly higher for residues on the aglcyon side. Thus, rigidification of the aglycon residues upon $(GlcNAc)_6$ binding may be the reason for the drastic conformational entropy change penalty compared to when binding only occurs on the glycon side. Rigidification of flexible regions upon ligand binding is typical of binding to glycoside hydrolases [134-136]. An additional factor that should be considered is the GlcNAc moiety in the −1 subsite has to undergo the unfavorable conformational change from $^4C_1$ to $^{1,4}B$, which is associated with a free energy penalty of 8 kcal/mol [78]. While, to the best of our knowledge, this conformational entropy change has not been calculated for GlcNAc in CHOS, it has been shown to be less than 11 % (<12 J/mol) of the free energy change for the same conformational transformation of glucose in dextran [137]. Since thermodynamic signatures of inhibitor binding are important for the success of drug development, our results reveal that when developing inhibitors of family 18 chitinases, binding affinity should not be used as the sole selection criterion.

Another important aspect is inhibitor specificity. Allosamidin has been shown to ameliorate asthma, and this is thought to be due to inhibition of AMCase [49]. Nevertheless, allosamidin is not a specific inhibitor and it has also been found to be an excellent inhibitor of HCHT with a $\Delta G_r°$ of – 9.1 kcal/mol (K_d of 0.2 μM) (preliminary results). Since HCHT has a fungistatic effect, it would be beneficial to have an inhibitor that is specific for AMCase and would not inhibit HCHT. One

promising strategy would be to use partially deacetylated CHOS as inhibitors. As discussed in the Introduction, a partially deacetylated CHOS positioned so that a GlcN unit binds in the −1 subsite should function as an inhibitor. This has been shown previously; DADAA is only very slowly degraded by ChiB, whereas ADDAA is not degraded at all due to a preference for an acetylated unit in the active site [122, 130, 138]. In our work (Paper IV), such preferences were also evident for HCHT, and it is likely that this may be the case for AMCase as well. These preferences can be exploited in developing CHOS-based inhibitors that are not affected by the processivity because they bind over the entire active site.

The weak interactions formed upon ligand binding are reflected in the measured enthalpy. For a newly formed weak interaction to contribute positively to the enthalpy, angles and/or distances between the enzyme and ligand need to be optimal to counteract the high enthalpic penalty associated with desolvation of a polar group (about 8 kcal/mol) [139]. If the geometry between the ligand and enzyme is suboptimal, there may be an enthalpic penalty associated with the relatively weak interaction that the same residue forms with water upon binding. The best way to identify an optimal weak interaction is by directly measuring the binding enthalpy using ITC, as described in Paper I. This paper deals with the characterization of the enthalpic and entropic contributions to the interaction between ChiB and CHOS with a DP_n of 3, 4, 5, and 6. Combination of thermodynamic data with information on how the individual CHOS are productively bound, allows the binding energies for individual subsites to be estimated, i.e., −3, −2 to +1 combined, +2, "+3", and "+4". The active-site cleft of ChiB is covered by a path of aromatic residues, Trp^{403}, Trp^{97}, Trp^{220} and Phe^{190} in subsites −2, +1, +2 and "+3" respectively, which stack well with the pyranose rings of the substrate. Sugar-Trp interactions have previously been shown to be relatively strong, with a beneficial enthalpic effect of −3 to −4 kcal/mol [24, 140]. Interestingly, the results showed two different trends. Binding to subsites −2 to +1 yielded a free energy change of −4.7 kcal/mol, which was

dominated by the total enthalpy change of −4.9 kcal/mol. These subsites exhibit several beneficial interactions between the protein and the sugar, which help to stabilize the ligand upon hydrolysis. Hydrogen bonds are formed with Tyr^{214} and Asp^{215}, as well as hydrophobic interactions with Trp^{403} and Trp^{97} [73]. In addition, Asp^{142} is rotated away from Asp^{140} and interacts with the acetoamido group of the −1 GlcNAc. Together, these interactions alleviate the highly unfavorable free energy change of 8 kcal/mol that is associated with distortion of the pyranose ring from a relaxed $^4C_1$ chair conformation to the skewed $^{1,4}B$ boat conformation in the −1 subsite [78]. Surprisingly, we observed that the stacking interactions in glycon subsites +2 (Trp) and "+3" (Phe) were endothermic ($\Delta H_r°$ of 3.9 and 1.8 kcal/mol, respectively) and entirely driven by entropy changes ($-T\Delta S_r°$ of −6.7 and −2.6 kcal/mol, respectively). The stacking in subsite +2 ($\Delta G_r° = -2.7$ kcal/mol) is comparable to the binding affinity of similar Trp-GlcNAc stacking in the +2 subsite of Chit42 from *T. harzianum* ($\Delta G_r° \approx -2.5$ kcal/mol) [141]. The endothermic enthalpic contribution is counterintuitive considering the favorable stacking interactions formed by the aromatic residues [70]. Substrate binding to subsites +2 and "+3" induces considerable conformational changes, and it is conceivable that enthalpically favorable interactions in the apo-enzyme are disrupted upon binding, causing favorable entropic changes [73]. One example of such a disruption is Phe^{190} rotates −91° around χ_1 when stacking with a GlcNAc moiety.

These results illustrate that even though binding may be entropically driven with overall enthalpic penalties, there may still be "local" effects which are enthalpically favorable, e.g., single GlcNAc-aromatic residue stacking.

4.2 Substrate positioning in the active site

Paper III describes an investigation of the factors which affect the positioning of substrates in the active site of ChiA from *S. marcescens*. It has previously been shown that the aromatic residue Trp^{167} in the glycon subsite −3 of ChiA is crucial for

binding to a polymeric substrate and steering processive hydrolysis [68]. The observations that $(GlcNAc)_4$ binds from −2 to +2, and $(GlcNAc)_5$ has an equal distribution between −3 to +2 and −2 to "+3" despite the strong binding of Trp^{167} in −3, together suggest a preference for the −3 to +2 subsites and indicate significant affinity in "+3". Our results show that removal of the strongly bound Trp^{167} clearly affects subsite preferences and positioning of soluble substrates in the active site. By inspecting the crystal structure of ChiA, it is apparent that several residues in the "+3" subsite are candidates for interacting with the ligand, either directly or through a water molecule. In general, four regions of residues are important for creating a "+3" subsite. All of these four regions are in relatively mobile parts of the enzyme, and thus would be liable to undergo conformational changes upon binding in subsite "+3".

ChiA has been shown to degrade chitin in an exo-manner towards the non-reducing end [42] by a processive mechanism [41], resulting in an accumulation of $(GlcNAc)_2$. However, Brurberg *et al.* have reported accumulation of noticeable amounts of GlcNAc upon incubation of ChiA with colloidal chitin, indicating that ChiA possesses some endo-chitinolytic activity towards insoluble substrates [45]. In addition, ChiA has been observed to hydrolyze soluble chitosan in an endo-manner [46]. It is tempting to suggest that the strong interactions in the "+3" subsite contribute to the endo-activity of ChiA. Endo-activity enhances the number of binding sites of an enzyme with the polymer, leading to a more efficient hydrolysis. The strong interactions in the "+3" subsite may also be a part of the product release mechanism. After productive binding, the resulting dimer in +1 and +2 needs to be removed so that the polymer can slide along by two GlcNAc units.

Surprisingly, we observed that binding with $(GlcNAc)_4$, which does not interact directly via a stacking interaction, was also affected by the mutation in subsite −3 with respect to affinity and hydrolytic rate. This indicates that Trp^{167} is important for pulling the substrate out of the solution and into the active site, regardless of ligand size. This is apparent from the 37-fold increase in K_m observed for $(GlcNAc)_4$

binding to ChiA-W167A compared to ChiA. K_m values may not reflect the true dissociation binding constant. However, K_m for $(GlcNAc)_4$ hydrolysis by ChiB has been shown to equal K_d within experimental errors (4 ± 2 μM vs. 2.7 ± 0.2 μM, respectively) [142, 143].

The role of Trp^{167} in substrate positioning was further elucidated by binding partly deacetylated CHOS of DP_n=8 and F_A=0.5 to both the wild type and ChiA-W167A. With ChiA, none of the oligomers in the original solution were detected using nano-ESI-q-TOF-MS and MALDI-TOF-MS after 60 minutes of hydrolysis. In contrast, when ChiA-W167A used, the original oligomers were detected in solution using MALDI-TOF-MS and in complexes with the enzyme using nano-ESI-q-TOF-MS, even after incubating for 60 minutes. The exchange of a Trp with an Ala appears to either change the preference for an acetylated unit in the –3 subsite, or disrupts the aromatic stacking with the sugar moiety, which appears to play a crucial role in overcoming the energetic penalty connected to binding an acetylated sugar in the –1 subsite. Previously, it has been suggested that non-productive binding of partially de-acetylated CHOS is in part due to binding of a deacetylated sugar to the –1 subsite, which would be favorable in terms of binding energies because there would be less need for the sugar to distort from a $^4C_1$ chair conformation to a twisted $^{1,4}B$ boat conformation (representing an energetic penalty of ~ 8 kcal/mol).

The effect of replacing Trp^{167} with deacetylated sugar moieties is illustrated by the ability of ChiA-W167A to hydrolyze chitosan compared to wild-type ChiA. When comparing the products obtained at the end point of chitosan hydrolysis with ChiA or ChiA-W167A, it is clear that the preferences for acetylated units in the –4 and –2 subsites observed for the wild type disappears when Trp^{167} is exchanged with Ala. The data show that Trp – GlcNAc stacking in the –3 subsite rigidifies the protein backbone, which is important for the formation of the network of intermolecular interactions that is necessary for the recognition and positioning of the *N*-acetyl groups before the –1 subsite. Interactions in the undefined "+3" subsite enhance the

binding affinity in aglycon subsites, which is associated with transglycosylation activity.

The results described in Paper III illustrate that one should not just consider the defined subsites known to interact with a ligand when studying the mechanism of hydrolysis. Residues and/or regions of the protein situated outside the defined active site can have a profound impact on the binding and hydrolysis of a substrate.

4.3 Human chitinases

The human chitotriosidase (HCHT) and acidic mammalian chitinase (AMCase) are family 18 chitinases which are involved in the innate immune system, playing a role in anti-parasite responses. In the work described in Papers IV and V, we investigated the binding preferences and mode of action of HCHT. The main conclusions of theses studies were that HCHT has endo-activity on chitosan and is moderately processive. Furthermore, HCHT exhibited strong binding in the "+3" subsite and even had affinity in the "+4" subsite, in addition to strong β-anomer preferences in subsites +2 and "+3". The preferences of HCHT subsites for acetylated versus non-acetylated sugars were assessed by sequence analysis of the oligomeric products, which indicated a very strong, absolute, and a relatively weak preference for an acetylated unit in the –2, –1, and +1 subsites, respectively. The results clearly show that HCHT is endo-active, as suggested previously [50, 54]. Substrate-association is the rate-limiting step in the enzymatic degradation of chitin [132], and thus high affinity subsites would obviously help to facilitate this process. The ability to hydrolyze chitin in an endo-manner, dramatically increases the number of possible binding sites on an enzyme which can interact with a polymer. HCHT hydrolyses chitin in the cell wall of pathogens, which causes a fungistatic effect [62], and the efficiency with which HCHT can do this is probably increased considerably as a result of endo-activity. It is conceivable that binding in an endo fashion, which is particularly challenging, depends on the presence of binding affinities beyond both

the −2 and the +2 subsites. It is interesting to compare HCHT with ChiA from *S. marcescens*, since the latter is fairly well understood. ChiA has a similar stretch of aromatic amino acids to HCHT and AMCase, extending from –6 to +2 (Phe-Tyr-Trp-Trp-Trp-Phe vs. Trp-Tyr-Trp-Trp-Trp-Trp). ChiA shows some resemblance to HCHT in that studies of productive binding of oligomeric substrates indicate the existence of a "+3" subsite. However, it differs from HCHT by having a more open aglycon region (in the "+3" and "+4" area, and presumably a weaker +2 subsite (Phe^{396} replaces Trp^{218}). Aglycon subsite binding strength has been shown to correlate with transglycosylation activity of chitinases [86]. ChiA shows low transglycosylation activity, even under "transglycosylation conditions" [86], whereas HCHT readily transglycosylates at CHOS concentrations of 100 μM, in accordance with the seemingly weaker aglycon subsites in ChiA than HCHT. For ChiA, it has been shown that stacking of a sugar moiety with the Trp-residue in the –3 subsite (Trp^{167} in ChiA, Trp^{31} in HCHT) yields a considerable change in the binding free energy of –1.8 kcal/mol [24]. Therefore, the fact that the pentamer primarily binds from –2 to "+3" despite the presence of Trp^{31}, indicates that the "+3" subsite must have considerable binding affinity.

As mentioned above, ChiA exhibits endo-activity, even though it degrades chitin from the non-reducing end in a processive manner. The directionality of HCHT, or AMCase, has not yet been determined, but it is tempting to speculate that HCHT would resemble ChiA in being an exo-processive chitinase that degrades chitin towards the non-reducing end, with a considerable endo-activity. Furthermore, one might also postulate that the observed transglycosylation activity of HCHT is simply a result of the endo-activity rather than having a biological role *per se*.

Comparing our results for CHOS with DP_n of 6, 5, and 4 binding to HCHT, with those for AMCase obtained by Chuo *et* al [144], it is clear that AMCase has weaker binding in the "+3" subsite than HCHT, as shown by the dominance of –4 to +2

binding of $(GlcNAc)_6$ for AMCase compared to the −3 to "+3" for HCHT. Furthermore, AMCase has only a β-anomer preference in +2, which is weaker than that observed for HCHT. By comparing the structure of HCHT and AMCase it is evident that the active site of HCHT is tighter beyond the +2 subsite. In particular, two regions stand out in HCHT as possible candidates for interacting with the ligand in subsites "+3" and "+4". The first of these comprises three non-conserved amino acids on α-helix 5 (Glu^{188}, Thr^{189}, and Tyr^{190}) and one amino acid on a loop (Gln^{145}) in HCHT, which differ from AMCase. Secondly, there is a SGAAAS sequence at the start of α-helix 6 in HCHT, which is in a position to interact with a sugar in subsite "+3" and "+4" via a water molecule, whereas this corresponds to PTDTGSNAY in AMCase.

The only other known active human chitinase, AMCase, is found in the lungs and stomach of humans and is shown to be up-regulated in lung tissue of asthma patients. Inhibition of AMCase in murine asthma models has been shown to ameliorate symptoms [49]. Since HCHT is a part of the human immune defense system, it is desirable to inhibit AMCase exclusively to preserve the activity of HCHT. To achieve specific inhibition of AMCase, detailed knowledge of the hydrolytic mechanism of both AMCase and HCHT is required. In the work described in Paper IV we investigated the mode of action of HCHT towards the soluble substrate chitosan. The tri-phasic kinetic behavior which was observed for HCHT towards chitosan reveals a fast initial phase, before the reaction rate progressively decreases in the two later kinetic phases. Family 18 chitinases have an absolute preference for an acetylated unit in subsite −1 for hydrolysis. The observed strong preference for a GlcNAc in subsite –2 of HCHT and the relatively weaker preference of +1, probably explains the tri-phasic kinetic behavior of HCHT. As hydrolysis progresses, there will be less chitosan oligomers available, resulting in acetylated units in subsites –2 to +1, and hence the efficiency of hydrolysis will decrease. Moreover, the results strongly suggest that a CHOS with the sequence DADADA from the non-reducing end (where D is a deacetylated unit (GlcN) and A is an acetylated unit (GlcNAc)), will bind unproductively from –3 to "+3". This

should be taken into consideration when attempting to use a partially deacetylated CHOS as an inhibitor of AMCase.

Since chitin is insoluble, the rate-limiting step of hydrolysis for a soluble enzyme is substrate association. To overcome the high penalty associated with binding to an insoluble substrate, many enzymes slide along the polymer chain, performing multiple cuts per association with the substrate. The conserved aromatic residues in the active site of chitinases are known to be crucial for processive hydrolysis [68, 70]. HCHT and AMCase have the same aromatic residues, which have been shown to be important for the processivity of both ChiA, subsite −3 (Trp^{167} corresponding to Trp^{31}), and ChiB, subsite +1 (Trp^{97} corresponding to Trp^{99}), and hence they are both expected to be processive. Our results (Paper IV) confirm that HCHT is processive, supporting the hypothesis that AMCase is processive as well. The processive mode of HCHT is likely to be involved in the fungistatic activity of HCHT because multiple cleavages can occur for each association to the pathogen.

4.4 Studying noncovalent interactions by mass spectrometry

As discussed previously, the main aims of this study were to investigate inhibitor binding to chitinases, and subsequently identify and develop new inhibitors. To achieve these aims, a fast and reliable screening method for assaying inhibitor binding was required. Mass spectrometry is a widely used method, which can provide information on inhibitor identity, binding stoichiometry, strength of interactions, and reaction kinetics. The transfer of noncovalently bound complexes from the condensed phase into the gaseous phase is challenging due to the requirement that intermolecular bonds are maintained during the phase transition. Currently, electrospray ionization (ESI) is the standard mass spectrometric technique used to analyze noncovalent complexes. Cederkvist *et al*. were able to detect intact noncovalent complex between ChiB and pentameric or heptameric CHOS, using

nano-ESI-q-TOF-MS or nano-ESI-Fourier transform (FT)- ion cyclotron resonance (ICR)-MS, respectively [130, 145]. Such techniques have a high degree of mass accuracy, and particularly in the case of FT-ICR, excellent resolution. However, they also have several disadvantages, including the length of time it takes for a single experiment, which precludes their use for fast/high throughput screening, the large amount of sample needed, and their low tolerance to salts and pH variations. To address these problems, we developed a new, robust and fast mass spectrometric method for screening noncovalent enzyme-ligand complexes using infrared (IR)-MALDI-MS (Paper VI). The widely used UV-MALDI-MS approach, employing crystalline, acidic matrixes, has so far failed to provide a means of easily and reproducibly detecting noncovalent complexes. We were able to develop a fast and sensitive screening method for noncovalent complexes employing IR-MALDI o-TOF-MS with liquid glycerol as the matrix. Infrared lasers have an advantage over the more frequently used UV lasers in providing softer transfer to the gas phase and ionization through absorption of energy by the O-H and N-H stretch vibrations. The use of glycerol as a matrix is beneficial because the noncovalent complexes are kept under near physiological conditions prior to ionization, minimizing the risk of complex dissociation.

Compared to nano-ESI techniques, the resolution of the new approach was lower due to glycerol forming adducts with the analyte, causing an increase in *m/z* value and tailing of the peaks. Adduct formation was reduced by adding proton exchange beads to the matrix. Despite this problem, our results clearly show that noncovalent complexes can be detected using relatively small amounts of sample in a fast and simple manner.

5. CONCLUDING REMARKS

The main objective of the work upon which this dissertation is based was to obtain a better understanding of ligand binding to family 18 chitinases. To this end, the work produced the following outcomes:

- Energetics of ligand binding was shown to depend on the nature of the ligand, the chitinase of interest, and where on the chitinase the ligand bound. This is important information for the future development of inhibitors as drug candidates since the relative contributions of the enthalpic and entropic terms are key factors which should be considered.

- Substrate affinity in aglycon subsites for both ChiA and HCHT was shown to be related to endo-activity, which enhances the degradation of insoluble chitin.

- A novel method for fast and simple screening of noncovalent enzyme-ligand complexes was developed, which provides a new tool for drug discovery.

6. REFERENCES

1. Sinnott, M. L. (1990). Catalytic Mechanisms of enzymatic glycosyl transfer. *Chem. Rev. 90*, 1171-1202.

2. Yip, V. L. Y. & Withers, S. G. (2004). Nature's many mechanisms for the degradation of oligosaccharides. *Org. Biomol. Chem. 2*, 2707-2713.

3. Wolfenden, R., Lu, X. D. & Young, G. (1998). Spontaneous hydrolysis of glycosides. *J. Am. Chem. Soc. 120*, 6814-6815.

4. Henrissat, B. (1991). A classification of glycosyl hydrolases based on amino-acid-sequence similarities. *Biochem. J. 280*, 309-316.

5. Gardner, K. H. & Blackwell, J. (1975). Refinement of structure of beta-chitin. *Biopolymers 14*, 1581-1595.

6. Rinaudo, M. (2006). Chitin and chitosan: Properties and applications. *Prog. Polym. Sci. 31*, 603-632.

7. Tharanathan, R. N. & Kittur, F. S. (2003). Chitin - The undisputed biomolecule of great potential. *Criti. Rev. Food Sci. 43*, 61-87.

8. Merzendorfer, H. & Zimoch, L. (2003). Chitin metabolism in insects: structure, function and regulation of chitin synthases and chitinases. *J. Exp. Biol. 206*, 4393-4412.

9. Eijsink, V. G. H., Vaaje-Kolstad, G., Vårum, K. M. & Horn, S. J. (2008). Towards new enzymes for biofuels: lessons from chitinase research. *Trends. Biotechnol. 26*, 228-235.

10. Kurita, K. (2006). Chitin and chitosan: Functional biopolymers from marine crustaceans. *Mar. Biotechnol. 8*, 203-226.

11. Harish Prashanth, K. V. & Tharanathan, R. N. (2007). Chitin/chitosan: modifications and their unlimited application potential - an overview. *Trends Food Sci. Tech. 18*, 117-131.

12. Kawada, M., Hachiya, Y., Arihiro, A. & Mizoguchi, E. (2007). Role of mammalian chitinases in inflammatory conditions. *Keio J Med. 56*, 21-7.

13. Rhoades, J., Gibson, G., Formentin, K., Beer, M. & Rastall, R. (2006). Inhibition of the adhesion of enteropathogenic *Escherichia coli* strains to HT-29 cells in culture by chito-oligosaccharides. *Carbohyd. Polym. 64*, 57-59.

14. You, Y., Park, W. H., Ko, B. M. & Min, B. M. (2004). Effects of PVA sponge containing chitooligosaccharide in the early stage of wound healing. *J. Mat. Sci. 15*, 297-301.

15. Vander, P., Vårum, K. M., Domard, A., El Gueddari, N. E. & Moerschbacher, B. M. (1998). Comparison of the ability of partially *N*-acetylated chitosans and chitooligosaccharides to elicit resistance reactions in wheat leaves. *Plant Physiol. 118*, 1353-1359.

16. Xu, Q., Chao, Y. L. & Wan, Q. B. (2009). Health benefit application of functional oligosaccharides. *Carbohyd. Polym. 77*, 435-441.

17. Aam, B. B., Heggset, E. B., Norberg, A. L., Sørlie, M., Vårum, K. M. & Eijsink, V. G. H. (2010). Production of chitooligosaccharides and their potential applications in medicine. *Marine Drugs. 8*, 1482-1517.

18. Shen, K. T., Chen, M. H., Chan, H. Y., Jeng, J. H. & Wang, Y. J. (2009). Inhibitory effects of chitooligosaccharides on tumor growth and metastasis. *Food. Chem. Toxicol. 47*, 1864-1871.

19. Ribeiro, M. P., Espiga, A., Silva, D., Baptista, P., Henriques, J., Ferreira, C., Silva, J. C., Borges, J. P., Pires, E., Chaves, P. & Correia, I. J. (2009). Development of a new chitosan hydrogel for wound dressing. *Wound Repair Regen. 17*, 817-824.

20. Shahabuddin, M., Toyoshima, T., Aikawa, M. & Kaslow, D. C. (1993). Transmissions-blocking activity of a chitinase inhibitor and activation of malarial parasite chitinase by mosquito protease. *P. Natl. Acad. Sci. USA. 90*, 4266-4270.

21. Chothia, C. & Lesk, A. M. (1986). The relation between the divergence of sequence and structure in proteins. *Embo J. 5*, 823-826.

22. Davies, G. & Henrissat, B. (1995). Structures and mechanisms of glycosyl hydrolases. *Structure 3*, 853-859.

23. Davies, G. J., Wilson, K. S. & Henrissat, B. (1997). Nomenclature for sugar-binding subsites in glycosyl hydrolases. *Biochem. J. 321*, 557-559.

24. Baban, J., Fjeld, S., Sakuda, S., Eijsink, V. G. H. & Sørlie, M. (2010). The roles of three *Serratia marcescens* chitinases in chitin conversion are reflected in different thermodynamic signatures of allosamidin binding. *J. Phys. Chem. B. 114*, 6144-6149.

25. Koshland, D. E. (1953). Stereochemistry and the mechanism of enzymatic reactions. *Biol. Rev. 28*, 416-436.

26. Rye, C. S. & Withers, S. G. (2000). Glycosidase mechanisms. *Curr. Opin. Chem. Biol. 4*, 573-580.

27. Henrissat, B. & Davies, G. (1997). Structural and sequence-based classification of glycoside hydrolases. *Curr. Opin. Struc. Biol. 7*, 637-644.

28. Akagi, K., Watanabe, J., Hara, M., Kezuka, Y., Chikaishi, E., Yamaguchi, T., Akutsu, H., Nonaka, T., Watanabe, T. & Ikegami, T. (2006). Identification of the substrate interaction region of the chitin-binding domain of *Streptomyces griseus* chitinase C. *J. Biochem-Tokyo. 139*, 483-493.

29. Elias, J. A., Homer, R. J., Hamid, Q. & Lee, C. G. (2005). Chitinases and chitinase-like proteins in Th2 inflammation and asthma. *J. Allergy Clin. Immun. 116*, 497-500.

30. Fukamizo, T. (2000). Chitinolytic enzymes catalysis, substrate binding, and their application. *Curr. Prot. Pep. Sci. 1*, 105-124.

31. Monzingo, A. F., Marcotte, E. M., Hart, P. J. & Robertus, J. D. (1996). Chitinases, chitosanases, and lysozymes can be divided into procaryotic and eucaryotic families sharing a conserved core. *Nature Struct. Biol. 3*, 133-140.

32. Garcia-Casado, G., Collada, C., Allona, I., Casado, R., Pacios, L. F., Aragoncillo, C. & Gomez, L. (1998). Site-directed mutagenesis of active site residues in a class I endochitinase from chestnut seeds. *Glycobiology 8*, 1021-1028.

33. Perrakis, A., Tews, I., Dauter, Z., Oppenheim, A. B., Chet, I., Wilson, K. S. & Vorgias, C. E. (1994). Crystal-structure of a bacterial chitinase at 2.3 Ångstrom resolution. *Structure 2*, 1169-1180.

34. Tews, I., Terwisscha van Scheltinga, A. C., Perrakis, A., Wilson, K. S. & Dijkstra, B. W. (1997). Substrate-assisted catalysis unifies two families of chitinolytic enzymes. *J. Am. Chem. Soc. 119*, 7954-7959.

35. Terwisscha van Scheltinga, A. C., Armand, S., Kalk, K. H., Isogai, A., Henrissat, B. & Dijkstra, B. W. (1995). Stereochemistry of chitin hydrolysis by a plant chitinase/lysozyme and X-ray structure of a complex with allosamidin: evidence for substrate assisted catalysis. *Biochemistry 34*, 15619-15623.

36. Vaaje-Kolstad, G., Houston, D. R., Rao, F. V., Peter, M. G., Synstad, B., van Aalten, D. M. F. & Eijsink, V. G. H. (2004). Structure of the D142N mutant of the family 18 chitinase ChiB from *Serratia marcescens* and its complex with allosamidin. *BBA-Prot. Proteom. 1696*, 103-111.

37. Vaaje-Kolstad, G., Horn, S. J., van Aalten, D. M. F., Synstad, B. & Eijsink, V. G. H. (2005). The non-catalytic chitin-binding protein CBP21 from *Serratia marcescens* is essential for chitin degradation. *J. Biol. Chem. 280*, 28492-28497.

38. Suzuki, K., Sugawara, N., Suzuki, M., Uchiyama, T., Katouno, F., Nikaidou, N. & Watanabe, T. (2002). Chitinases A, B, and C1 of *Serratia marcescens* 2170 produced by recombinant *Escherichia coli*: Enzymatic properties and synergism on chitin degradation. *Biosci. Biotechnol. Biochem. 66*, 1075-1083.

39. Watanabe, T., Kimura, K., Sumiya, T., Nikaidou, N., Suzuki, K., Suzuki, M., Taiyoji, M., Ferrer, S. & Regue, M. (1997). Genetic analysis of the chitinase system of *Serratia marcescens* 2170. *J. Bacteriol. 179*, 7111-7117.

40. van Aalten, D. M. F., Synstad, B., Brurberg, M. B., Hough, E., Riise, B. W., Eijsink, V. G. H. & Wierenga, R. K. (2000). Structure of a two-domain chitotriosidase from *Serratia marcescens* at 1.9-angstrom resolution. *P. Natl. Acad. Sci. USA. 97*, 5842-5847.

41. Horn, S. J., Sørlie, M., Vaaje-Kolstad, G., Norberg, A. L., Synstad, B., Vårum, K. M. & Eijsink, V. G. H. (2006). Comparative studies of chitinases A, B and C from *Serratia marcescens*. *Biocatal. Biotransfor. 24*, 39-53.

42. Hult, E. L., Katouno, F., Uchiyama, T., Watanabe, T. & Sugiyama, J. (2005). Molecular directionality in crystalline beta-chitin: hydrolysis by chitinases A and B from *Serratia marcescens* 2170. *Biochem. J. 388*, 851-856.

43. Uchiyama, T., Katouno, F., Nikaidou, N., Nonaka, T., Sugiyama, J. & Watanabe, T. (2001). Roles of the exposed aromatic residues in crystalline chitin hydrolysis by chitinase a from *Serratia marcescens* 2170. *J. Biol. Chem. 276*, 41343-41349.

44. Horn, S. J., Sørbotten, A., Synstad, B., Sikorski, P., Sørlie, M., Vårum, K. M. & Eijsink, V. G. H. (2006). Endo/exo mechanism and processivity of family 18 chitinases produced by *Serratia marcescens*. *FEBS J. 273*, 491-503.

45. Brurberg, M. B., Nes, I. F. & Eijsink, V. G. H. (1996). Comparative studies of chitinases A and B from *Serratia marcescens*. *Microbiol. UK 142*, 1581-1589.

46. Sikorski, P., Sørbotten, A., Horn, S. J., Eijsink, V. G. H. & Vårum, K. M. (2006). *Serratia marcescens* chitinases with tunnel-shaped substrate-binding grooves show endo activity and different degrees of processivity during enzymatic hydrolysis of chitosan. *Biochemistry 45*, 9566-9574.

47. Synstad, B., Vaaje-Kolstad, G., Cederkvist, H., Saua, S. F., Horn, S. J., Eijsink, V. G. H. & Sørlie, M. (2008). Expression and characterization of endochitinase C from *Serratia marcescens* BJL200 and its purification by a one-step general chitinase purification method. *Biosci. Biotechnol. Biochem. 72*, 715-723.

48. Vaaje-Kolstad, G., Westereng, B., Horn, S. J., Liu, Z. L., Zhai, H., Sørlie, M. & Eijsink, V. G. H. (2010). An oxidative enzyme boosting the enzymatic conversion of recalcitrant polysaccharides. *Science 330*, 219-222.

49. Zhu, Z., Zheng, T., Homer, R. J., Kim, Y. K., Chen, N. Y., Cohn, L., Hamid, Q. & Elias, J. A. (2004). Acidic mammalian chitinase in asthmatic Th2 inflammation and IL-13 pathway activation. *Science 304*, 1678-1682.

50. Fusetti, F., von Moeller, H., Houston, D., Rozeboom, H. J., Dijkstra, B. W., Boot, R. G., Aerts, J. & van Aalten, D. M. F. (2002). Structure of human chitotriosidase - Implications for specific inhibitor design and function of mammalian chitinase-like lectins. *J. Biol. Chem. 277*, 25537-25544.

51. Hollak, C. E. M., Vanweely, S., Vanoers, M. H. J. & Aerts, J. M. F. G. (1994). Marked elevation of plasma chitotriosidase activity - A novel hallmark of Gaucher disease. *J. Clin. Invest. 93*, 1288-1292.

52. Ramanathan, M., Lee, W. K. & Lane, A. P. (2006). Increased expression of acidic mammalian chitinase in chronic rhinosinusitis with nasal polyps. *Am. J. Rhinol. 20*, 330-335.

53. Musumeci, M., Bellin, M., Maltese, A., Aragona, P., Bucolo, C. & Musumeci, S. (2008). Chitinase levels in the tears of subjects with ocular allergies. *Cornea 27*, 168-173.

54. Boot, R. G., Blommaart, E. F. C., Swart, E., Ghauharali-van der Vlugt, K., Bijl, N., Moe, C., Place, A. & Aerts, J. (2001). Identification of a novel acidic mammalian chitinase distinct from chitotriosidase. *J. Biol. Chem. 276*, 6770-6778.

55. Zhao, Y. S., Zheng, Q. C., Zhang, H. X., Chu, H. Y. & Sun, C. C. (2009). Analysis of a three-dimensional structure of human acidic mammalian chitinase obtained by homology modeling and ligand binding studies. *J. Mol. Model. 15*, 499-505.

56. Olland, A. M., Strand, J., Presman, E., Czerwinski, R., Joseph-McCarthy, D., Krykbaev, R., Schlingmann, G., Chopra, R., Lin, L., Fleming, M., Kriz, R., Stahl, M., Somers, W., Fitz, L. & Mosyak, L. (2009). Triad of polar residues implicated in pH specificity of acidic mammalian chitinase. *Protein Sci. 18*, 569-578.

57. Tjoelker, L. W., Gosting, L., Frey, S., Hunter, C. L., Le Trong, H., Steiner, B., Brammer, H. & Gray, P. M. (2000). Structural and functional definition of the human chitinase chitin-binding domain. *J. Biol. Chem. 275*, 514-520.

58. Renkema, G. H., Boot, R. G., Au, F. L., Donker-Koopman, W. E., Strijland, A., Muijsers, A. O., Hrebicek, M. & Aerts, J. (1998). Chitotriosidase, a chitinase, and the 39-kDa human cartilage glycoprotein, a chitin-binding lectin, are homologues of family 18 glycosyl hydrolases secreted by human macrophages. *Eur. J. Biochem. 251*, 504-509.

59. Beasley, R., Crane, J., Lai, C. K. W. & Pearce, N. (2000). Prevalence and etiology of asthma. *J. Allergy Clin. Immunol. 105*, S466-S472.

60. Holt, P. G. (1996). Infections and the development of allergy. *Toxicol. Lett. 86*, 205-210.

61. Holt, P. G. (2000). Parasites, atopy, and the hygiene hypothesis: resolution of a paradox? *Lancet 356*, 1699-1701.

62. van Eijk, M., van Roomen, C. P. A. A., Renkema, G. H., Bussink, A. P., Andrews, L., Blommaart, E. F. C., Sugar, A., Verhoeven, A. J., Boot, R. G. & Aerts, J. M. F. G. (2005). Characterization of human phagocyte-derived chitotriosidase, a component of innate immunity. *Int. Immunol. 17*, 1505-1512.

63. Debono, M. & Gordee, R. S. (1994). Antibiotics that inhibit fungal cell-wall development. *Ann. Rev. Microbiol. 48*, 471-497.

64. Papanikolau, Y., Prag, G., Tavlas, G., Vorgias, C. E., Oppenheim, A. B. & Petratos, K. (2001). High resolution structural analyses of mutant chitinase A complexes with substrates provide new insight into the mechanism of catalysis. *Biochemistry-US 40*, 11338-11343.

65. Watanabe, T., Ishibashi, A., Ariga, Y., Hashimoto, M., Nikaidou, N., Sugiyama, J., Matsumoto, T. & Nonaka, T. (2001). Trp122 and Trp134 on the surface of the catalytic domain are essential for crystalline chitin hydrolysis by *Bacillus circulans* chitinase A1. *FEBS Lett. 494*, 74-78.

66. Watanabe, T., Ariga, Y., Sato, U., Toratani, T., Hashimoto, M., Nikaidou, N., Kezuka, Y., Nonaka, T. & Sugiyama, J. (2003). Aromatic residues within the substrate-binding cleft of *Bacillus circulans* chitinase A1 are essential for hydrolysis of crystalline chitin. *Biochem. J. 376*, 237-244.

67. Katouno, F., Taguchi, M., Sakurai, K., Uchiyama, T., Nikaidou, N., Nonaka, T., Sugiyama, J. & Watanabe, T. (2004). Importance of exposed aromatic residues in chitinase B from *Serratia marcescens* 2170 for crystalline chitin hydrolysis. *J. Biochem. 136*, 163-168.

68. Zakariassen, H., Aam, B. B., Horn, S. J., Vårum, K. M., Sørlie, M. & Eijsink, V. G. H. (2009). Aromatic residues in the catalytic center of chitinase A from *Serratia marcescens* affect processivity, enzyme activity, and biomass converting efficiency. *J. Biol. Chem. 284*, 10610-10617.

69. Zakariassen, H., Klemetsen, L., Sakuda, S., Vaaje-Kolstad, G., Vårum, K. M., Sørlie, M. & Eijsink, V. G. H. (2010). Effect of enzyme processivity on the efficacy of a competitive chitinase inhibitor. *Carbohyd. Polym. 82*, 779-785.

70. Horn, S. J., Sikorski, P., Cederkvist, J. B., Vaaje-Kolstad, G., Sørlie, M., Synstad, B., Vriend, G., Vårum, K. M. & Eijsink, V. G. H. (2006). Costs and benefits of processivity in enzymatic degradation of recalcitrant polysaccharides. *P. Natl. Acad. Sci. USA. 103*, 18089-18094.

71. Rouvinen, J., Bergfors, T., Teeri, T., Knowles, J. K. C. & Jones, T. A. (1990). 3-Dimensional structure of cellobiohydrolase-II from *Trichoderma reesei*. *Science 249*, 380-386.

72. Varrot, A., Frandsen, T. P., von Ossowski, I., Boyer, V., Cottaz, S., Driguez, H., Schulein, M. & Davies, G. J. (2003). Structural basis for ligand binding and processivity in cellobiohydrolase Cel6A from *Humicola insolen*s. *Structure 11*, 855-864.

73. van Aalten, D. M. F., Komander, D., Synstad, B., Gåseidnes, S., Peter, M. G. & Eijsink, V. G. H. (2001). Structural insights into the catalytic mechanism of a family 18 exo-chitinase. *P. Natl. Acad. Sci. USA. 98*, 8979-8984.

74. Meyer, J. E. W. & Schulz, G. E. (1997). Energy profile of maltooligosaccharide permeation through maltoporin as derived from the structure and from a statistical analysis of saccharide-protein interactions. *Prot. Sci. 6*, 1084-1091.

75. Breyer, W. A. & Matthews, B. W. (2001). A structural basis for processivity. *Prot. Sci. 10*, 1699-1711.

76. Brameld, K. A., Shrader, W. D., Imperiali, B. & Goddard, W. A. (1998). Substrate assistance in the mechanism of family 18 chitinases: Theoretical studies of potential intermediates and inhibitors. *J. Mol. Biol. 280*, 913-923.

77. Brameld, K. A. & Goddard, W. A. (1998). Substrate distortion to a boat conformation at subsite-1 is critical in the mechanism of family 18 chitinases. *J. Am. Chem. Soc. 120*, 3571-3580.

78. Biarnes, X., Ardevol, A., Planas, A., Rovira, C., Laio, A. & Parrinello, M. (2007). The conformational free energy landscape of beta-D-glucopyranose.

Implications for substrate preactivation in beta-glucoside hydrolases. *J. Am. Chem. Soc. 129*, 10686-10693.

79. Honda, Y., Kitaoka, M. & Hayashi, K. (2004). Kinetic evidence related to substrate-assisted catalysis of family 18 chitinases. *FEBS Lett. 567*, 307-310.

80. Synstad, B., Gåseidnes, S., van Aalten, D. M. F., Vriend, G., Nielsen, J. E. & Eijsink, V. G. H. (2004). Mutational and computational analysis of the role of conserved residues in the active site of a family 18 chitinase. *Eur. J. Biochem. 271*, 253-262.

81. Chipman, D. M., Pollock, J. J. & Sharon, N. (1968). Lysosyme-catalyzed hydrolysis and transglycosylation reactions of bacterial cell wall oligosaccharides. *J. Biol. Chem. 243*, 487-&.

82. Aronson, N. N., Halloran, B. A., Alexeyev, M. F., Zhou, X. E., Wang, Y. J., Meehan, E. J. & Chen, L. Q. (2006). Mutation of a conserved tryptophan in the chitin-binding cleft of *Serratia marcescens* Chitinase A enhances transglycosylation. *Biosci. Biotech. Bioch. 70*, 243-251.

83. Aguilera, B., Ghauharali-van der Vlugt, K., Helmond, M. T. J., Out, J. M. M., Donker-Koopman, W. E., Groener, J. E. M., Boot, R. G., Renkema, G. H., van der Marel, G. A., van Boom, J. H., Overkleeft, H. S. & Aerts, J. M. F. G. (2003). Transglycosidase activity of chitotriosidase: improved enzymatic assay for the human macrphage chitinase. *J. Biol. Chem. 278*, 40911-40916.

84. Taira, T., Fujiwara, M., Dennhart, N., Hayashi, H., Onaga, S., Ohnuma, T., Letzel, T., Sakuda, S. & Fukamizo, T. (2010). Transglycosylation reaction catalyzed by a class V chitinase from cycad, *Cycas revoluta*: A study involving site-directed mutagenesis, HPLC, and real-time ESI-MS. *BBA-Prot. Proteom. 1804*, 668-675.

85. Lü, Y., Yang, H. T., Hu, H. Y., Wang, Y., Rao, Z. H. & Jin, C. (2009). Mutation of Trp137 to glutamate completely removes transglycosyl activity associated with the *Aspergillus fumigatus* AfChiB1. *Glycoconjugate J. 26*, 525-534.

86. Zakariassen, H., Hansen, M. C., Jøranli, I. M., Eijsink, V. G. H. & Sørlie, M. (2011). Mutational effects on transglycosylating activity of family 18 chitinases and construction of a hypertransglycosylating mutant. *Biochemistry*

87. Cooper, A., Johnson, C. M., Lakey, J. H. & Nollmann, M. (2001). Heat does not come in different colours: entropy-enthalpy compensation, free energy windows, quantum confinement, pressure perturbation calorimetry, solvation and the multiple causes of heat capacity effects in biomolecular interactions. *Biophys. Chem. 93*, 215-230.

88. Dunitz, J. D. (1995). Win some, lose some - Enthalpy-entropy compensation in weak intermolecular interactions. *Chem. Biol. 2*, 709-712.

89. Baldwin, R. L. (1986). Temperature-dependence of the hydrophobic interaction in protein folding. *P. Nat. Acad. Sci. 83*, 8069-8072.

90. Murphy, K. P., Xie, D., Thompson, K. S., Amzel, L. M. & Freire, E. (1994). Entropy in biological binding processes - Estimation of translational entropy loss. *Proteins 18*, 63-67.

91. Leavitt, S. & Freire, E. (2001). Direct measurement of protein binding energetics by isothermal titration calorimetry. *Curr. Opin. Struct. Biol. 11*, 560-566.

92. Freire, E. (2008). Do enthalpy and entropy distinguish first in class from best in class? *Drug Discov. Today. 13*, 869-874.

93. Cooper, A. (2005). Heat capacity effects in protein folding and ligand binding: a re-evaluation of the role of water in biomolecular thermodynamics. *Biophys. Chem. 115*, 89-97.

94. Livingstone, J. R., Spolar, R. S. & Record, M. T. (1991). Contribution to the thermodynamics of protein folding from the reduction in water-accessible nonpolar surface-area. *Biochemistry 30*, 4237-4244.

95. Kauzmann, W. (1959). Some factors in the interpretation of protein denaturation. *Adv. Protein Chem. 14*, 1-63.

96. Zakariassen, H. & Sørlie, M. (2007). Heat capacity changes in heme protein-ligand interactions. *Thermochim. Acta 464*, 24-28.

97. Baker, B. M. & Murphy, K. P. (1997). Dissecting the energetics of a protein-protein interaction: The binding of ovomucoid third domain to elastase. *J. Mol. Biol. 268*, 557-569.

98. Hensley, P. (1996). Defining the structure and stability of macromolecular assemblies in solution: The re-emergence of analytical ultracentrifugation as a practical tool. *Structure 4*, 367-373.

99. Freire, E., Mayorga, O. L. & Straume, M. (1990). Isothermal titration calorimetry. *Anal. Chem. 62*, A950-A959.

100. Wiseman, T., Williston, S., Brandts, J. F. & Lin, L. N. (1989). Rapid measurement of binding constants and heat of binding using a new titration calorimeter. *Anal. Biochem. 179*, 131-137.

101. O'Shannessy, D. J. (1994). Determination of kinetic rate and equilibrium binding constants for macromolecular interactions: a critique of the surface plasmon resonance literature. *Curr. Opin. Biotechnol. 5*, 65-71.

102. Szabo, A., Stolz, L. & Granzow, R. (1995). Surface-Plasmon Resonance and its use in biomolecular interaction analysis (BIA). *Curr. Opin. Struc. Biol. 5*, 699-705.

103. Wang, W. J., Kitova, E. N., Sun, J. X. & Klassen, J. S. (2005). Blackbody infrared radiative dissociation of nonspecific protein-carbohydrate complexes produced by nanoelectrospray ionization: The nature of the noncovalent interactions. *J. Am. Soc. Mass Spectrom. 16*, 1583-1594.

104. Kitova, E. N., Bundle, D. R. & Klassen, J. S. (2002). Thermal dissociation of protein-oligosaccharide complexes in the gas phase: Mapping the intrinsic intermolecular interactions. *J. Am. Chem. Soc. 124*, 5902-5913.

105. Bahr, U., Karas, M. & Hillenkamp, F. (1994). Analysis of biopolymers by matrix-assisted laser-desorption ionization (MALDI) mass-spectrometry. *Fresen. J. Anal. Chem. 348*, 783-791.

106. Tanaka, K. (2003). The origin of macromolecule ionization by laser irradiation (Nobel lecture). *Angew. Chem. Int. Edit. 42*, 3860-3870.

107. Fenn, J. B. (2003). Electrospray wings for molecular elephants (Nobel lecture). *Angew. Chem. Int. Edit. 42*, 3871-3894.

108. Ganem, B., Li, Y. T. & Henion, J. D. (1991). Observation of noncovalent enzyme substrate and enzyme product complexes by ion-spray mass-spectrometry. *J. Am. Chem. Soc. 113*, 7818-7819.

109. Loo, J. A. (1997). Studying noncovalent protein complexes by electrospray ionization mass spectrometry. *Mass Spectrom. Rev. 16*, 1-23.

110. Daniel, J. M., Friess, S. D., Rajagopalan, S., Wendt, S. & Zenobi, R. (2002). Quantitative determination of noncovalent binding interactions using soft ionization mass spectrometry. *Int. J. Mass Spectrom. 216*, 1-27.

111. Bolbach, G. (2005). Matrix-assisted laser desorption/ionization analysis of non-covalent complexes: Fundamentals and applications. *Curr. Pharm. Design. 11*, 2535-2557.

112. Kiselar, J. G. & Downard, K. M. (2000). Preservation and detection of specific antibody-peptide complexes by matrix-assisted laser desorption ionization mass spectrometry. *J. Am. Soc. Mass Spectrom. 11*, 746-750.

113. Bich, C. & Zenobi, R. (2009). Mass spectrometry of large complexes. *Curr. Opin. Struc. Biol. 19*, 632-639.

114. Yanes, O., Aviles, F. X., Roepstorff, P. & Jorgensen, T. J. D. (2007). Exploring the "intensity fading" phenomenon in the study of noncovalent interactions by MALDI-TOF mass spectrometry. *J. Am. Soc. Mass Spectrom. 18*, 359-367.

115. Wang, W., Kitova, E. N. & Klassen, J. S. (2005). Nonspecific protein-carbohydrate complexes produced by nanoelectrospray ionization. Factors influencing their formation and stability. *Anal. Chem. 77*, 3060-3071.

116. Sandor, E., Pusztahelyi, T., Karaffa, L., Karanyi, Z., Pocsi, I., Biro, S. & Szentirmai, A. (1998). Allosamidin inhibits the fragmentation of *Acremonium chrysogenum* but does not influence the cephalosporin-C production of the fungus. *FEMS Microbio. Lett. 164*, 231-236.

117. Andersen, O. A., Dixon, M. J., Eggleston, I. M. & van Aalten, D. M. F. (2005). Natural product family 18 chitinase inhibitors. *Nat. Prod. Rep. 22*, 563-579.

118. Gloster, T. M. & Davies, G. J. (2009). Glycosidase inhibition: assessing mimicry of the transition state. *Organ. Biomol. Chem. 8*, 305-320.

119. Sakuda, S., Isogai, A., Matsumoto, S., Suzuki, A. & Koseki, K. (1986). The structure of allosamidin, a novel insect chitinase inhibitor, produced by *Streptomyces sp*. *Tetrahedron Lett. 27*, 2475-2478.

120. Rao, F. V., Houston, D. R., Boot, R. G., Aerts, J., Sakuda, S. & van Aalten, D. M. F. (2003). Crystal structures of allosamidin derivatives in complex with human macrophage chitinase. *J. Biol. Chem. 278*, 20110-20116.

121. Vaaje-Kolstad, G., Vasella, A., Peter, M. G., Netter, C., Houston, D. R., Westereng, B., Synstad, B., Eijsink, V. G. H. & van Aalten, D. M. F. (2004). Interactions of a family 18 chitinase with the designed inhibitor HM508 and its degradation product, chitobiono-delta-lactone. *J. Biol. Chem. 279*, 3612-3619.

122. Cederkvist, F. H., Parmer, M. P., Vårum, K. M., Eijsink, V. G. H. & Sørlie, M. (2008). Inhibition of a family 18 chitinase by chitooligosaccharides. *Carbohyd. Polym. 74*, 41-49.

123. Hirose, T., Sunazuka, T. & Omura, S. (2010). Recent development of two chitinase inhibitors, argifin and argadin, produced by soil microorganisms. *P. Jpn. Acad. B. Phys. 86*, 85-102.

124. Johnson, M. A. & Pinto, B. M. (2002). Molecular mimicry of carbohydrates by peptides. *Aust. J. Chem. 55*, 13-25.

125. Arai, N., Shiomi, K., Yamaguchi, Y., Masuma, R., Iwai, Y., Turberg, A., Kolbl, H. & Omura, S. (2000). Argadin, a new chitinase inhibitor, produced by *Clonostachys sp.* FO-7314. *Chem. Pharm. Bull. 48*, 1442-1446.

126. Shiomi, K., Arai, N., Iwai, Y., Turberg, A., Kolbl, H. & Omura, S. (2000). Structure of argifin, a new chitinase inhibitor produced by *Gliocladium sp*. *Tetrahedron Lett. 41*, 2141-2143.

127. Kumar, A. & Rao, M. (2010). A novel bifunctional peptidic aspartic protease inhibitor inhibits chitinase A from *Serratia marcescens*: Kinetic analysis of inhibition and binding affinity. *BBA.-Gen. Subjects. 1800*, 526-536.

128. Houston, D. R., Shiomi, K., Arai, N., Omura, S., Peter, M. G., Turberg, A., Synstad, B., Eijsink, V. G. H. & van Aalten, D. M. F. (2002). High-resolution structures of a chitinase complexed with natural product cyclopentapeptide. inhibitors: Mimicry of carbohydrate substrate. *P. Natl. Acad. Sci. USA. 99*, 9127-9132.

129. Lipinski, C. A. (2000). Drug-like properties and the causes of poor solubility and poor permeability. *J. Pharmacol. Toxicol. 44*, 235-249.

130. Cederkvist, F., Zamfir, A. D., Bahrke, S., Eijsink, V. G. H., Sørlie, M., Peter-Katalinic, J. & Peter, M. G. (2006). Identification of a high-affinity-binding oligosaccharide by (+) nanoelectrospray quadrupole time-of-flight tandem mass spectrometry of a noncovalent enzyme-ligand complex. *Angew. Chem. Int. Edit. 45*, 2429-2434.

131. Letzel, M. C., Synstad, B., Eijsink, V. G. H., Peter-Katalinić, J. & Peter, M. G. (2000). Libraries of chito-oligosaccharides of mixed acetylation patterns and their interactions with chitinases. *Adv. Chitin Sci. 4*, 545-552.

132. Zakariassen, H., Eijsink, V. G. H. & Sørlie, M. (2010). Signatures of activation parameters reveal substrate-dependent rate determining steps in polysaccharide turnover by a family 18 chitinase. *Carbohyd. Polym. 81*, 14-20.

133. Cederkvist, F. H., Saua, S. F., Karlsen, V., Sakuda, S., Eijsink, V. G. H. & Sørlie, M. (2007). Thermodynamic analysis of allosamidin binding to a family 18 chitinase. *Biochemistry-US 46*, 12347-12354.

134. Davies, G. J., Tolley, S. P., Henrissat, B., Hjort, C. & Schulein, M. (1995). Structures of oligosaccharide-bound forms of the endoglucanase V from *Humicola insolens* at 1.9 angstrom resolution. *Biochemistry 34*, 16210-16220.

135. Varrot, A., Schulein, M. & Davies, G. J. (2000). Insights into ligand-induced conformational change in Cel5A from *Bacillus agaradhaerens* revealed by a catalytically active crystal form. *J. Mol. Biol. 297*, 819-828.

136. Zou, J. Y., Kleywegt, G. J., Stahlberg, J., Driguez, H., Nerinckx, W., Claeyssens, M., Koivula, A., Teerii, T. T. & Jones, T. A. (1999). Crystallographic evidence for substrate ring distortion and protein conformational changes during

catalysis in cellobiohydrolase Cel6A from *Trichoderma reesei*. *Structure 7*, 1035-1045.

137. Haverkamp, R. G., Marshall, A. T. & Williams, M. A. K. (2007). Entropic and enthalpic contributions to the chair-boat conformational transformation in dextran under single molecule stretching. *J. Phys. Chem. B. 111*, 13653-13657.

138. Haebel, S., Bahrke, S. & Peter, M. G. (2007). Quantitative sequencing of complex mixtures of heterochitooligosaccharides by vMALDI-linear ion trap mass spectrometry. *Anal. Chem. 79*, 5557-5566.

139. Cabani, S., Gianni, P., Mollica, V. & Lepori, L. (1981). Group contributions to the thermodynamic preperties of non-ionic organic solutes in dilute aqueous-solution. *J. Sol. Chem. 10*, 563-595.

140. Zolotnitsky, G., Cogan, U., Adir, N., Solomon, V., Shoham, G. & Shoham, Y. (2004). Mapping glycoside hydrolase substrate subsites by isothermal titration calorimetry. *P. Natl. Acad. Sci. USA. 101*, 11275-11280.

141. Lienemann, M., Boer, H., Paananen, A., Cottaz, S. & Koivula, A. (2009). Toward understanding of carbohydrate binding and substrate specificity of a glycosyl hydrolase 18 family (GH-18) chitinase from *Trichoderma harzianum*. *Glycobiology 19*, 1116-1126.

142. Krokeide, I. M., Synstad, B., Gåseidnes, S., Horn, S. J., Eijsink, V. G. H. & Sørlie, M. (2007). Natural substrate assay for chitinases using high-performance liquid chromatography: A comparison with existing assays. *Anal. Biochem. 363*, 128-134.

143. Norberg, A. L., Karlsen, V., Hoell, I. A., Bakke, I., Eijsink, V. G. H. & Sørlie, M. (2010). Determination of substrate binding energies in individual subsites of a family 18 chitinase. *FEBS Lett. 584*, 4581-4585.

144. Chou, Y. T., Yao, S. H., Czerwinski, R., Fleming, M., Krykbaev, R., Xuan, D. J., Zhou, H. F., Brooks, J., Fitz, L., Strand, J., Presman, E., Lin, L., Aulabaugh, A. & Huang, X. Y. (2006). Kinetic characterization of recombinant human acidic mammalian chitinase. *Biochemistry 45*, 4444-4454.

145. Cederkvist, F. H., Mormann, M., Froesch, M., Eijsink, V. G. H., Sørlie, M. & Peter-Katalinić, J. (2010). Concurrent enzyme reactions and binding events for chitinases interacting with chitosan oligosaccharides monitored by high resolution mass spectrometry. *Int. J. Mass Spectrom. doi:10.1016/j.ijms.2010.10.031* |.

PAPER I

FEBS Letters 584 (2010) 4581–4585

journal homepage: www.FEBSLetters.org

Determination of substrate binding energies in individual subsites of a family 18 chitinase

Anne Line Norberg, Vigdis Karlsen, Ingunn Alne Hoell, Ingrid Bakke, Vincent G.H. Eijsink, Morten Sørlie *

Department of Chemistry, Biotechnology, and Food Science, The Norwegian University of Life Sciences, 1432 Ås, Norway

ARTICLE INFO

Article history:
Received 20 September 2010
Revised 11 October 2010
Accepted 13 October 2010
Available online 19 October 2010

Edited by Miguel De la Rosa

Keywords:
Isothermal titration calorimetry
Chitinase
Glycosidase
Subsite energy

ABSTRACT

Thermodynamic parameters for binding of *N*-acetylglucosamine (GlcNAc) oligomers to a family 18 chitinase, ChiB of *Serratia marcescens*, have been determined using isothermal titration calorimetry. Binding studies with oligomers of different lengths showed that binding to subsites −2 and +1 is driven by a favorable enthalpy change, while binding to the two other most important subsites, +2 and +3, is driven by entropy with unfavorable enthalpy. These remarkable unfavorable enthalpy changes are most likely due to favorable enzyme-substrate interactions being offset by unfavorable enthalpic effects of the conformational changes that accompany substrate-binding.

1. Introduction

Chitin, a β-1,4-linked polymer of *N*-acetylglucosamine (GlcNAc), is among the most abundant biopolymers in nature, and hence, of large biological and economical importance. The degradation of chitin to di- and monosaccharides is catalyzed by glycosyl hydrolases called chitinases. Chitin, and, particularly its partially deacetylated and water soluble analog chitosan, are important in the food and feed industry, pharmacological industry, in water purification systems, and as antimicrobial additives [1]. Chitin metabolism is essential in several major plague organisms such as certain fungi, insects and nematodes, and chitin turnover has been associated with the ability of humans to respond to such organisms [2]. Inhibition of chitinases belonging to glycosyl hydrolase family 18 [3] is a target area in the development of medicines for allergic and inflammatory disorders [4,5]. Hydrolytic products of chitin and chitosan, chitooligosaccharides (CHOS), have interesting biological activities [6], for example as elicitors of plant defense against fungal infections [7]. CHOS are known to affect several cellular processes and direct enzymatic inhibition by CHOS has been observed for a prolyl endopeptidase as well as a family 18 chitinase [8–11].

To better understand chitinase functionality and to increase our ability to design inhibitors, it is important to determine how individual subsites contribute to binding of the substrate. Substrate-binding studies in family 18 chitinases [12–14] and family 19 chitinases [15] have been described previously, but several of these were based on modelling only. Very recently, direct measurements of binding affinities have been described for Chit-42 from *Trichoderma harzianum* and for ChiB from *Serratia marcescens* [13,14]. However, so far, there are no direct experimental data showing the free energy changes associated with binding in each of the individual subsites including data that show how these energies divide into enthalpic and entropic terms. In the present study we have used isothermal titration calorimetry (ITC) for direct measurements of the interaction of CHOS with individual subsites of ChiB from *S. marcescens*. Studies of the binding reactions with ITC enable the direct determination of the equilibrium binding association constant (K_a) and ΔH°_r in one single experiment. The results show how different subsites in ChiB contribute to substrate binding and reveal some peculiar features of the binding energetics.

2. Materials and methods

2.1. Chemicals

$(GlcNAc)_6$, $(GlcNAc)_5$, $(GlcNAc)_4$, and $(GlcNAc)_3$ were purchased from Sigma–Aldrich (St. Louis, MO, USA).

2.2. Construction of His_{10}-ChiB-E144Q

The wild-type *chiB* gene was amplified from pMAY2-10 [16] with primer ChiBpET16b-F1 5′-TCGA**CATATG**TCCACACGCAAAGCCGTTATT-3′ (NdeI restriction site is in bold type) and primer

* Corresponding author. Fax: +47 64965901.
E-mail address: morten.sorlie@umb.no (M. Sørlie).

0014-5793/$36.00
doi:10.1016/j.febslet.2010.10.017

ChiBpETM11-R1 5′-CC**CTCGAG**TTACGCTACGCGGCCCACCTT-3′ (XhoI restriction site is in bold type). PCR reactions were conducted with *Phusion* DNA polymerase (Finnzymes, Espoo, Finland) in a PTC-100 Programmable Thermal Cycler (MJ Research Inc., Waltham, MA, USA). The amplification protocol consisted of an initial denaturation cycle of 30 s at 98 °C, followed by 24 cycles of 5 s at 98 °C, 10 s at 70 °C, and 15 s at 72 °C, followed by a final step of 5 min at 72 °C. Amplified fragments were ligated into vector pCR®4Blunt-TOPO®Zero Blunt TOPO (Invitrogen, Carlsbad, CA, USA). The gene fragment was excised from the TOPO vector for insertion into the pET16b expression vector (Novagen, Madison, WI, USA), using NdeI and XhoI restriction sites. The resulting pET16b-His_{10}-ChiB construct was transformed into *Escherichia coli* BL21Star (DE3) (Invitrogen). For construction of a gene encoding His_{10}-ChiB-E144Q (i.e. a variant of ChiB that is inactive due to mutation of the catalytic acid [16]), the pET16b-His_{10}-ChiB construct and a pMAY2-10 variant encoding ChiB-E144Q were digested with BamHI. Cleavage of the latter plasmid resulted in a fragment of approximately 820 bp containing part of the *chiB* gene carrying the E144Q mutation, which was then ligated with the 5090 bp BamHI fragment derived from the cleaved pET16b-His_{10}-ChiB construct. The sequence of the final construct was verified by sequencing. The final construct, pET16b-His_{10}-ChiB-E144Q was transformed into *E. coli* BL21Star (DE3).

2.3. Protein expression and purification

ChiB-E144Q from *S. marcescens* was over-expressed in *E. coli* and purified as described elsewhere [17]. Initial ITC experiments showed that this protein yielded essentially identical binding data as His_{10}-ChiB-E144Q (not shown) and this latter protein was used in all further experiments. His_{10}-ChiB-E144Q was over expressed and purified as follows: *E. coli* BL21Star (DE3) containing the appropriate plasmid was grown at 37 °C in 300 ml LB-medium with 100 μg ml^{-1} ampicillin at 225 rpm, to a cell density of 0.6 at 600 nm. Isopropyl-β-D-thiogalactopyranoside was then added to a final concentration of 0.4 mM, and the cells were further incubated for 4 h at 37 °C, followed by harvesting by centrifugation (9820×*g*, 8 min at 4 °C, Beckman Coulter Avanti J-25, Rotor JA14).

The cells were then subjected to an osmotic shock procedure to produce a periplasmatic extract. First, the cell pellet was resuspended in 15 ml ice-cold spheroplastbuffer and incubated on ice for 5 min. This buffer was made by taking 10 ml 1 M Tris–HCl, pH 8.0, 17.1 g sucrose, 100 μL 0.5 M EDTA, pH 8.0, and 200 μL 50 mM PMSF with a volume adjustment to 100 ml with dH_2O. The cells were then harvested by centrifugation (7741×*g*, 8 min at 4 °C, Beckman Coulter Avanti J-25, Rotor JA25-5), the supernatant was removed, and the pellet was incubated 10 min at room temperature. The pellet was then resuspended in 12.5 ml ice cold, sterile water, and incubated on ice for 45 s before supplementing with 12.5 μL 1 M $MgCl_2$. After centrifugation (7741×*g*, 8 min at 4 °C, Beckman Coulter Avanti J-25, Rotor JA25-5), the supernatant was pressed through a 0.20 μm sterile filter and stored at 4 °C.

Proteins were purified on a Ni-NTA column (0.5 cm in diameter, 2 ml stationary phase in total) using a flow rate of 2.5 ml/min. The column was equilibrated in 20 mM Tris–HCl buffer, pH 8.0, containing 60 mM imidazole and 0.5 M NaCl. The periplasmatic extract was loaded directly onto the column (i.e. without any pH or imidazole adjustment), and the column was washed with approximately 3 column volumes of the starting buffer. The His-tagged protein was then eluted with 20 mM Tris–HCl buffer, pH 8.0, containing 0.5 M imidazole and 0.5 M NaCl. The purified protein was concentrated and transferred to another buffer (100 mM Tris–HCl, pH 8.0) for storage by repeated centrifugations in a 10 000 MWCO Centricon tube (Amicon) at 4000 rpm in a centrifuge with swing out rotor (Beckman Coulter Avanti J-25, Rotor JA14). Enzyme purity was verified by SDS–PAGE and protein concentrations were determined using the Qubit Protein Assay (Invitrogen).

2.4. Isothermal titration calorimetry experiments

ITC experiments were performed with a VP-ITC system from Microcal, Inc (Northampton, MA) [18]. Solutions were thoroughly degassed prior to experiments to avoid air bubbles in the calorimeter. For experiments with $(GlcNAc)_6$ and $(GlcNAc)_5$, typically 15 μM of ChiB-E144Q in 20 mM potassium phosphate buffer (pH 8.0) was placed in the reaction cell with a volume of 1.42 ml, and 500 μM solutions of the ligands in identical buffers as for the protein solutions were placed in the ITC syringe. The concentration of other buffers, HEPES and TRIS at pH 8.0 was also 20 mM. The heats of ionization of these buffers are as follows: potassium phosphate, 1.22 kcal/mol [19], HEPES 5.02 kcal/mol [19], and TRIS 11.2 kcal/mol [20]. For experiments with $(GlcNAc)_4$ and $(GlcNAc)_3$, 30 μM of ChiB-144Q in 20 potassium phosphate buffer (pH 8.0) was placed in the reaction cells and 750 μM and 7 mM solutions of the ligands, respectively, were placed in the syringe. Aliquots of 4 μL were injected into the reaction cell at 140 s intervals with a stirring speed of 260 rpm. The titrations were normally completed after 20–25 injections. The shape of the ITC binding curve is determined by the so-called Wiseman *c*-value [18], which can be expressed as:

$$c = nK_a[M]_t \quad (1)$$

where n is the stoichiometry of the reaction, K_a is the equilibrium binding association constant, and $[M]_t$ is the protein concentration. For three of the four ligands ITC experiments could be optimized to give a *c*-value to be in the range of $10 < c < 1000$. This ensures that K_a can be determined from the Wiseman binding isotherm. Titration of $(GlcNAc)_3$ into ChiB-E144Q yielded a *c*-value of 0.01. Binding thermodynamics can be obtained using ITC even if c is in the range of $0.01 < c < 10$ if a sufficient portion of the binding isotherm is used for analysis [21,22]. This is achieved by ensuring a high molar ratio of ligand vs. protein at the end of the titration, accurate knowledge of the concentrations of both ligand and receptor, an adequate level of signal-to-noise in the data, and known stoichiometry. All these conditions were met, with the possible exception of the stoichiometry issue. Considering the long binding site of ChiB, it is conceivable that two $(GlcNAc)_3$ molecules can bind simultaneously. However, the "Two Sets of Sites Model" did not provide a satisfactory fit between experimental and theoretical data, whereas the "One Sets of Sites Model" did (see below).

2.5. Analysis of calorimetric data

ITC data were collected automatically using the Microcal Origin v.7.0 software accompanying the VP-ITC system [18]. Prior to further analysis, all data were corrected for heat of dilution by subtracting the heat produced by continuing injections of ligand into the reaction cell after completion of the binding reaction. These heats had same magnitudes as of titrating ligand into buffer alone. The data were fitted using a non-linear least-squares algorithm using a single-site binding model employed by the Origin software that accompanies the VP-ITC system. All data from the binding reactions fitted well to a single-site binding model, yielding the stoichiometry (n), equilibrium binding association constant (K_a), and the enthalpy change (ΔH°_r) of the reaction. The value of n was found to be between 0.9 and 1.1 per enzyme molecule for all reactions. The changes in reaction free energy (ΔG°_r) and entropy (ΔS°_r) as well as the dissociation constant (K_d) were calculated using the following relationship:

$$\Delta G^\circ_r = -RT\ln K_a = RT\ln K_d = \Delta H^\circ_r - T\Delta S^\circ_r \quad (2)$$

Errors in ΔH_r°, K_d, and ΔG_r° were obtained as standard deviations of at least three experiments. Errors in ΔS_r° and $-T\Delta S_r^\circ$ were obtained as propagation of errors.

Table 1
Thermodynamic parameters of CHOS binding to ChiB-E144Q derived from ITC. The experiments were performed at $t = 20$ °C in 20 mM potassium phosphate buffer, pH 8.0.

Substrate	K_d[a]	ΔG_r°[b]	ΔH_r°[b]	$-T\,\Delta S_r^\circ$[b]42	ΔS_r°[c]
$(GlcNAc)_6$	0.13 ± 0.09	−9.2 ± 0.3	1.7 ± 0.3	−10.9 ± 0.4	37 ± 1
$(GlcNAc)_5$[d]	0.67 ± 0.20	−8.3 ± 0.1	0.8 ± 0.2	−9.1 ± 0.2	31 ± 1
$(GlcNAc)_4$	2.7 ± 0.19	−7.4 ± 0.2	−1.0 ± 0.1	−6.5 ± 0.2	22 ± 1
$(GlcNAc)_3$	327 ± 22	−4.7 ± 0.2	−4.9 ± 0.9	0.2 ± 0.2	−1 ± 1

[a] μM.
[b] kcal/mol.
[c] cal/K mol.
[d] Performed at 15 °C due to low heat of binding at $t = 20$ °C.

3. Results and discussion

The binding of oligomeric substrates to ChiB-E144Q was studied by ITC at $t = 20$ °C and pH 8.0 in potassium phosphate buffer and the results are summarized in Table 1. Fig. 1 shows typical ITC thermograms and theoretical fits to the experimental data for binding of $(GlcNAc)_6$, $(GlcNAc)_5$, $(GlcNAc)_4$, and $(GlcNAc)_3$. $(GlcNAc)_6$ binds with a K_d of 0.13 ± 0.09 μM (Table 1). The binding is clearly entropically driven ($-T\Delta S_r^\circ = -10.9 \pm 0.4$ kcal/mol and $\Delta S_r^\circ = 37 \pm 1$ cal/K mol) with an enthalpic penalty ($\Delta H_r^\circ = 1.7 \pm 0.3$ kcal/mol). Potential protonation/deprotonation effects coupled to $(GlcNAc)_6$ binding to ChiB-E144Q were investigated by testing the contribution from buffer ionization to ΔH_r° [23]. ITC experiments were carried out as well in HEPES and TRIS, which have different ionization enthalpies compared to potassium phosphate, yielding ΔH_r° of 2.0 ± 0.4 kcal/mol and 1.3 ± 0.3 kcal/mol, respectively, indicating no proton transfer upon binding. For

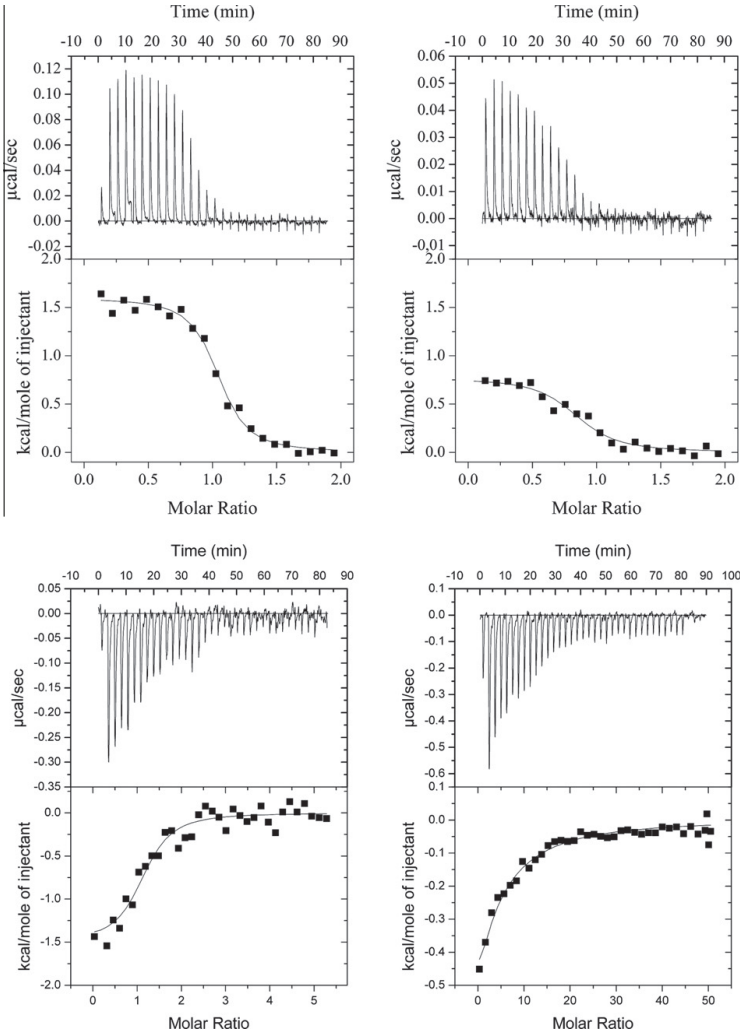

Fig. 1. Thermograms (upper panels) and binding isotherms with theoretical fits (lower panels) obtained for the binding of $(GlcNAc)_6$ (top left), $(GlcNAc)_5$ (top right), $(GlcNAc)_4$ (bottom left), and $(GlcNAc)_3$ (bottom right) to ChiB-E144Q.

$(GlcNAc)_5$ binding, the K_d is 0.67 ± 0.20 μM and the reaction is entropically driven ($-T\Delta S^\circ_r = -9.1 \pm 0.2$ kcal/mol and $\Delta S^\circ_r = 31 \pm 1$ cal/K mol) with a small enthalpic penalty ($\Delta H^\circ_r = 0.8 \pm 0.2$ kcal/mol). $(GlcNAc)_4$ binding is accompanied with a K_d of 2.5 ± 0.19 μM. This reaction is also entropically driven ($-T\Delta S^\circ_r$ = −6.5 ± 0.2 kcal/mol and $\Delta S^\circ_r = 22 \pm 1$ cal/Kmol) with a small enthalpic contribution ($\Delta H^\circ_r = -1.0 \pm 0.1$ kcal/mol). Contrasting with the results for the longer oligomers, $(GlcNAc)_3$ binding to ChiB-E144Q is enthalpically driven with a K_d of 327 ± 22 μM, a ΔH°_r of −4.9 ± 0.9 kcal/mol and a $-T\Delta S^\circ_r = 0.2 \pm 0.2$ kcal/mol (ΔS°_r of −1 ± 1 cal/K mol). The K_d values for binding of $(GlcNAc)_6$, $(GlcNAc)_5$ and $(GlcNAc)_4$ to Chit-42 from *T. harzianum* determined by Lienemann et al. using surface plasmon resonance are approximately 2-, 10- and 5-fold higher than the values reported for ChiB in this study [18].

For ChiB, six subsites, spanning from −3 to + 3 have been described [24] (Fig. 2). The substrate-binding cleft on the catalytic domain is extended by a chitin-binding domain interacting with the reducing end of the sugar chain. Thus, some degree of substrate affinity may be expected in additional aglycon subsites, and this has indeed been observed [25]. Previous studies of ChiB catalyzed hydrolysis of CHOS have shown that $(GlcNAc)_3$ productively binds from −2 to +1, $(GlcNAc)_4$ productively binds from −2 to +2, and that $(GlcNAc)_5$ productively binds from −2 to +3 [25]. The preferential binding of $(GlcNAc)_5$ to subsites −2 to +3 was confirmed by the crystal structure of this ligand in complex with ChiB-E144Q [26]. $(GlcNAc)_6$ productively binds from −3 to +3 (approximately 20 %) and from −2 to "+4" (80%; "+4" denotes a binding position next to the +3 subsite) [25]. Combining this information with the obtained thermodynamic parameters (Table 1) allows for the estimation of binding energies for individual subsites. The calculated free energy, enthalpy, and entropy changes for GlcNAc binding in the individual subsites −3, +2, +3, and "+4", in addition to combined values for binding to the −2, −1, and +1 subsites are shown in Fig. 2.

Interestingly, binding to the −2, −1, and +1 subsites is enthalpically driven. Structural data show that there are many favorable interactions between the sugars and ChiB in these subsites [26]. Apparently, these interactions are not only necessary to overcome the loss of free energy associated with the distortion of the sugar bound in the −1 subsite from the $^4C_1$ chair conformation to the twisted $^{1,4}B$ boat conformation (calculated to amount to ~8 kcal/mol [27]), but also to drive the actual binding. Based on theoretical analysis of kinetic data for substrate conversion, a free energy change of +3.1 kcal/mol has been calculated for the −1 subsite in chitinase-1 from the fungal pathogen *Coccidioides immitis* [12]. A positive ΔG°_r for sugar binding in the −1 subsite is to be expected due to the loss of free energy upon sugar distortion, and is in agreement with observations made in classical studies of substrate affinities in lysozyme [28]. These literature data suggest that the favorable free energy of binding for the joint −2 to +1 subsites shown in Fig. 2 may be the net result of one unfavorable (subsite −1) and two favorable (subsites −2 and +1) interactions.

Like in many other glycosyl hydrolases ligand binding in ChiB involves stacking interactions between the side chains of aromatic amino and sugar moieties (Fig. 2). Binding to subsite +2 involves stacking with Trp^{220} and is relatively strong ($\Delta G^\circ_r = -2.7$ kcal/mol). The binding affinity of this subsite is comparable to the binding affinity generated by a similar Trp-GlcNAc stacking

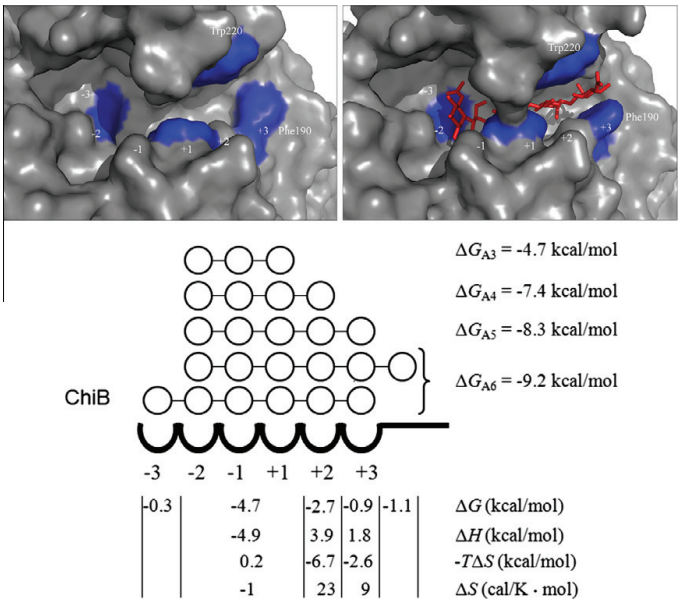

Fig. 2. Upper panel: Crystal structure of ChiB (left, 1e15 [24]) alone and in complex with a $(GlcNAc)_5$ molecule (right, 1e6n [26]), with numbered subsites. Aromatic amino acids interacting with the ligand are colored blue. These are: Trp^{403} (subsite −1/−2), Trp^{97} (+1), Trp^{220} (+2), and Phe^{190} (+3). It is clear that there is significant movement in the active site, especially by Phe^{190}, upon substrate binding. This panel was prepared using the PyMol software (http://www.pymol.org). Lower panel: Energies associated with sugar binding to the individual subsites of ChiB. These energies are derived from the data in Table 1, combined with existing knowledge concerning the binding preferences of the various ligands; see text for details. Since $(GlcNAc)_6$ approximately binds 20% from −3 to +3 and 80% from −2 to "+4" [25], the difference in free energy change of −0.9 kcal/mol between $(GlcNAc)_6$ and $(GlcNAc)_5$ can be shared as −0.3 kcal/mol and −1.1 kcal/mol for the −3 and "+4" subsites, respectively (solved as two equations with two unknowns, *X*, the Δ*G* for subsite −3 and *Y*, the Δ*G* for subsite +4; the equations are $0.2X + 0.8Y = 0.9$ and (referring the experimentally observed binding ratios) $Y = 4X$). Estimates for Δ*H* and Δ*S* for these subsites cannot be made.

interaction in the +2 subsite of Chit42 of *T. harzianum* ($\Delta G^{\circ}_{r} \approx -2.5$ kcal/mol; calculated from the difference in the reported K_d values for $(GlcNAc)_6$ binding to Chit42-WT and Chit42-W246A [13]). However, remarkably, our data show that binding to the +2 subsite is driven by a huge increase in entropy ($-T\Delta S^{\circ}_{r} = -6.7$ kcal/mol) with a relatively large enthalpic penalty ($\Delta H^{\circ}_{r} = 3.9$ kcal/mol). Likewise, binding to subsite +3, involving a strong stacking interaction between Phe^{190} and the sugar is driven by entropy, with an enthalpic penalty. These results are counterintuitive because there are several studies that clearly show the beneficial enthalpic effect (in the order of -3 to -4 kcal/mol) of a Trp-sugar interaction [29,30]. Our data thus show that the beneficial enthalpic effects of the stacking interactions in the +2 and the +3 subsites are somehow offset. Substrate-binding to these subsites induces considerable conformational changes [26], and it is conceivable these changes lead to the disruption of favorable interactions in the apo-enzyme. The rotation of -91° around Phe-190 χ_1 upon substrate binding that results in the stacking interaction with the sugar in the +3 subsite is an example of such a conformational change [26].

In conclusion, in addition to unraveling sugar affinities of individual subsites in ChiB, our results show the importance of detailed studies on ligand-binding thermodynamics for understanding how chitinases bind their ligands. For example, the large and counterintuitive enthalpic penalty associated with ligand binding to subsites +2 and +3 needs to be taken into account in current efforts to design chitinase inhibitors [31].

Acknowledgements

This work was supported by Grants 155518/V00 (ITC instrument), 164653/V40, 140497/I30 and 177542/V30 from the Norwegian Research Council.

References

[1] Synowiecki, J. and Al-Khateeb, N.A. (2003) Production, properties, and some new applications of chitin and its derivatives. Crit. Rev. Food Sci. 43, 145–171.
[2] van Eijk, M., van Roomen, C.P.A.A., Renkema, G.H., Bussink, A.P., Andrews, L., Blommaart, E.F.C., Sugar, A., Verhoeven, A.J., Boot, R.G. and Aerts, J.M.F.G. (2005) Characterization of human phagocyte-derived chitotriosidase, a component of innate immunity. Int. Immun. 17, 1505–1512.
[3] Henrissat, B. and Davies, G.J. (1997) Structural and sequence-based classification of glycoside hydrolases. Curr. Opin. Struct. Biol. 7, 637–644.
[4] Donnelly, L.E. and Barnes, P.J. (2004) Acidic mammalian chitinase – a potential target for asthma therapy. Trends Pharmacol. Sci. 25, 509–511.
[5] Zhu, Z., Zheng, T., Homer, R.J., Kim, Y.K., Chen, N.Y., Cohn, L., Hamid, Q. and Elias, J.A. (2004) Acidic mammalian chitinase in asthmatic Th2 inflammation and IL-13 pathway activation. Science 304, 1678–1682.
[6] Aam, B.B., Heggset, E.B., Norberg, A.L., Sørlie, M., Vårum, K.M. and Eijsink, V.G.H. (2010) Production of chitooligosaccharides and their potential applications in medicine. Marine Drugs 8, 1482–1517.
[7] Roby, D., Gadelle, A. and Toppan, A. (1987) Chitin oligosaccharides as elicitors of chitinase activity in melon plants. Biochem. Biophys. Res. Commun. 143, 885–892.
[8] Rahman, A., Kumar, S.G., Kim, S.W., Hwang, H.J., Baek, Y.M., Lee, S.H., Hwang, H.S., Shon, Y.H., Nam, K.S. and Yun, J.W. (2008) Proteomic analysis for inhibitory effect of chitosan oligosaccharides on 3T3-L1 adipocyte differentiation. Proteomics 8, 569–581.
[9] Nam, K.S., Kim, M.K. and Shon, Y.H. (2007) Inhibition of proinflammatory cytokine-induced invasiveness of HT-29 cells by chitosan oligosaccharide. J. Microbiol. Biotechnol. 17, 2042–2045.
[10] Je, J.-Y., Kim, E.K., Ahn, C.B., Moon, S.H., Jeon, B.T., Kim, B., Park, T.K. and Park, P.J. (2007) Sulfated chitooligosaccharides as prolyl endopeptidase inhibitor. Int. J. Biol. Macromol. 41, 529–533.
[11] Cederkvist, F.H., Parmer, M.P., Vårum, K.M., Eijsink, V.G.H. and Sørlie, M. (2008) Inhibition of a family 18 chitinase by chitooligosaccharides. Carbohyd. Polym. 74, 41–49.
[12] Fukamizo, T., Sasaki, C., Schelp, E., Bortone, K. and Robertus, J.D. (2001) Kinetic properties of chitinase-1 from the fungal pathogen *Coccidioides immitis*. Biochemistry 40, 2448–2454.
[13] Lienemann, M., Boer, H., Paananen, A., Cottaz, S. and Koivula, A. (2009) Towards understanding of carbohydrate binding and substrate specificity of a glycosyl hydrolase 18 family (GH-18) chitinase from *Trichoderma harzianum*. Glycobiology 19, 1116–1126.
[14] Norberg, A. L., Eijsink, V. G. H. and Sørlie, M. (2010) Dissecting factors that contribute to ligand-binding energetics for family 18 chitinases. Thermochim. Acta, doi:10.1016/j.tca.2010.08.013.
[15] Sasaki, C., Itoh, Y., Takehara, H., Kuhara, S. and Fukamizo, T. (2003) Family 19 chitinase from rice (*Oryza sativa* L.): substrate-binding subsites demonstrated by kinetic and molecular modeling studies. Plant Mol. Biol. 52, 43–52.
[16] Brurberg, M.B., Eijsink, V.G.H., Haandrikman, A.J., Venema, G. and Nes, I.F. (1995) Chitinase B from *Serratia marcescens* BJL200 is exported to the periplasm without processing. Microbiology 141, 123–131.
[17] Brurberg, M.B., Nes, I.F. and Eijsink, V.G.H. (1996) Comparative studies of chitinases A and B from *Serratia marcescens*. Microbiology 142, 1581–1589.
[18] Wiseman, T., Williston, S., Brandts, J.F. and Lin, L.N. (1989) Rapid measurement of binding constants and heats of binding using a new titration calorimeter. Anal. Biochem. 179, 131–137.
[19] Fukada, H. and Takahashi, K. (1998) Enthalpy and heat capacity changes for the proton dissociation of various buffer components in 0.1 M potassium chloride. Proteins 33, 159–166.
[20] Todd, M.J. and Gomez, J. (2001) Enzyme kinetics determined using calorimetry: a general assay for enzyme activity? Anal. Biochem. 296, 179–187.
[21] Turnbull, W.B. and Daranas, A.H. (2003) On the value of *c*: can low affinity systems be studied by isothermal titration calorimetry? J. Am. Chem. Soc. 125, 14859–14866.
[22] Zakariassen, H. and Sørlie, M. (2007) Heat capacity changes in heme protein–ligand interactions. Thermochim. Acta 464, 24–28.
[23] Baker, B.M. and Murphy, K.P. (1996) Evaluation of linked protonation effects in protein binding reactions using isothermal titration calorimetry. Biophys. J. 71, 2049–2055.
[24] van Aalten, D.M.F., Synstad, B., Brurberg, M.B., Hough, E., Riise, B.W., Eijsink, V.G.H. and Wierenga, R.K. (2000) Structure of a two-domain chitotriosidase from *Serratia marcescens* at 1.9-angstrom resolution. Proc. Natl. Acad. Sci. USA 97, 5842–5847.
[25] Horn, S.J., Sørlie, M., Vaaje-Kolstad, G., Norberg, A.L., Synstad, B., Vårum, K.M. and Eijsink, V.G.H. (2006) Comparative studies of chitinases A, B and C from *Serratia marcescens*. Biocatal. Biotransfor. 24, 39–53.
[26] van Aalten, D.M.F., Komander, D., Synstad, B., Gåseidnes, S., Peter, M.G. and Eijsink, V.G.H. (2001) Structural insights into the catalytic mechanism of a family 18 exo-chitinase. Proc. Natl. Acad. Sci. USA 98, 8979–8984.
[27] Biarnes, X., Ardevol, A., Planas, A., Rovira, C., Laio, A. and Parrinello, M. (2007) The conformational free energy landscape of â-D-glucopyranose. implications for substrate preactivation in â-glucoside hydrolases. J. Am. Chem. Soc. 129, 10686–10693.
[28] Schindler, M., Assaf, Y., Sharon, N. and Chipman, D.M. (1977) Mechanism of lysozyme catalysis: role of ground-state strain in subsite D in hen egg-white and human lysozymes. Biochemistry 16, 423–431.
[29] Baban, J., Fjeld, S., Sakuda, S., Eijsink, V.G.H. and Sørlie, M. (2010) The roles of three *Serratia marcescens* chitinases in chitin conversion are reflected in different thermodynamic signatures of allosamidin binding. J. Phys. Chem. B 114, 6144–6149.
[30] Zolotnitsky, G., Cogan, U., Adir, N., Solomon, V., Shoham, G. and Shoham, Y. (2004) Mapping glycoside hydrolase substrate subsites by isothermal titration calorimetry. Proc. Natl. Acad. Sci. USA 101, 11275–11280.
[31] Andersen, O.A., Nathubhai, A., Dixon, M.J., Eggleston, I.M. and Van Aalten, D.M. (2008) Structure-based dissection of the natural product cyclopentapeptide chitinase inhibitor argifin. Chem. Biol. 15, 295–301.

PAPER II

Thermochimica Acta 511 (2010) 189–193

Contents lists available at ScienceDirect

Thermochimica Acta

journal homepage: www.elsevier.com/locate/tca

Dissecting factors that contribute to ligand-binding energetics for family 18 chitinases

Anne Line Norberg, Vincent G.H. Eijsink, Morten Sørlie*

Department of Chemistry, Biotechnology and Food Science, Norwegian University of Life Sciences, P.O. Box 5003, N-1432 Ås, Norway

ARTICLE INFO

Article history:
Received 29 June 2010
Received in revised form 11 August 2010
Accepted 12 August 2010
Available online 19 August 2010

Keywords:
Isothermal titration calorimetry
Chitinase
Inhibition
Conformational changes

ABSTRACT

Inhibition of family 18 chitinases has several interesting applications. To this regard, it is important to understand the dependency of binding energetics with respect to the nature of the ligand as well as the chitinase. We have studied the binding of hexameric *N*-acetylglucosamine $(GlcNAc)_6$ to both glycon and aglycon subsites in chitinase B (ChiB) of *Serratia marcescens* and we compare the results with binding of allosamidin to ChiB (glycon subsites only, where products are released) and to chitinase A (ChiA) of *S. marcescens* (glycon subsites only, where polymeric substrates bind). The ΔG_r° values for the three binding processes were identical within experimental errors (−38 kJ/mol) while binding was driven by different factors, being solvation entropy ($-T\Delta S_{solv}^\circ$ = −52.3 ± 1.5 kJ/mol), conformational entropy ($-T\Delta S_{conf}^\circ$ −45.2 ± 2.0 kJ/mol) [27], and equal contributions of ΔH_r° and $-T\Delta S_{solv}^\circ$ (−23.4 ± 0.9 and −20.4 ± 3.1 kJ/mol) [29], respectively.

1. Introduction

Chitin, an insoluble linear polysaccharide consisting of repeated units of β-1,4-*N*-acetylglucosamine (GlcNAc), is common as a structural polymer in crustaceans, arthropods, fungi, and parasitic nematodes. Chitinases, the enzymes that degrade chitin, belong to the glycoside hydrolase enzyme families 18 and 19 [1]. As a consequence of the known and putative biological roles of chitinases, especially family 18 chitinases [2,3], inhibition of these enzymes is a target for the development of plant protecting compounds [4,5] and medicines for allergic and inflammatory disorders [6,7].

When designing inhibitors, it is important know and understand the energetics of the inhibitor–enzyme interaction. As an example, for FDA-approved HIV-1 protease inhibitors as well as statins, two classes of drugs for which complete thermodynamic information has been published, data suggest that best-in-class compounds that come into the market after several years are enthalpically better optimized than the original first-in class compounds, indicating that optimizing binding enthalpies is more favorable than optimizing binding entropies [8]. It is especially interesting to determine binding energetics of chitooligosaccharide (CHOS) based inhibitors since substrate based inhibitors hold a tremendous advantage in being very specific towards chitinases, and hence not likely to interfere with other enzymatic systems. The binding strength of such inhibitors can be tuned with the length of the oligomer (i.e. longer bind stronger) [9,10].

Binding of known family 18 chitinase CHOS-based inhibitors occurs in glycon subsites of the active site only or in both glycon and aglycon subsites (subsites are labeled according to the nomenclature for sugar-binding subsites in glycosyl hydrolases, where glycon subsites denoted $-n$, binding to the non-reducing end of the substrate and aglycon subsites are denoted $+n$, binding to the reducing end, with cleavage taking place between the −1 and +1 subsite [11]). As an example, Fig. 1 shows the overall structures and the subsites of chitinase A (ChiA) and chitinase B (ChiB) from *Serratia marcescens* that are the target enzymes used in this study. Known CHOS-based inhibitors bind to glycon subsites only: allosamidin [12] and CHOS thiazolines [9] that are intermediate analogues and CHOS lactones [13] that are transition state analogues. These CHOS-derivatives bind to the glycon subsites because the conformation of the sugar moiety at the "reducing end" of the oligomer resembles the structure of the transition state (^{4}E conformation) and thus has high affinity for the −1 subsite. In principle, it should be possible to develop CHOS-based inhibitors that bind to the whole of the active site, but this requires that the sugar moiety binding to the −1 subsite does not have an *N*-acetyl group [2]. Family 18 chitinases have an absolute preference for an *N*-acetylglucosamine sugar in the −1 subsite of the active site due to the need for the carbonyl group to act as a nucleophile in the first step of the hydrolysis [14].

To obtain more insight in the binding energetics of whole active site-binding inhibitors, we have studied the energetics for binding of $(GlcNAc)_6$ (Fig 2.) to ChiB-E144Q. From previous work, it is known that $(GlcNAc)_6$ binds to subsites −2 to +3 (with an "overhang" in

* Corresponding author. Tel.: +47 64965902; fax: +47 64965901.
E-mail address: morten.sorlie@umb.no (M. Sørlie).

0040-6031/$ – see front matter © 2010 Elsevier B.V. All rights reserved.
doi:10.1016/j.tca.2010.08.013

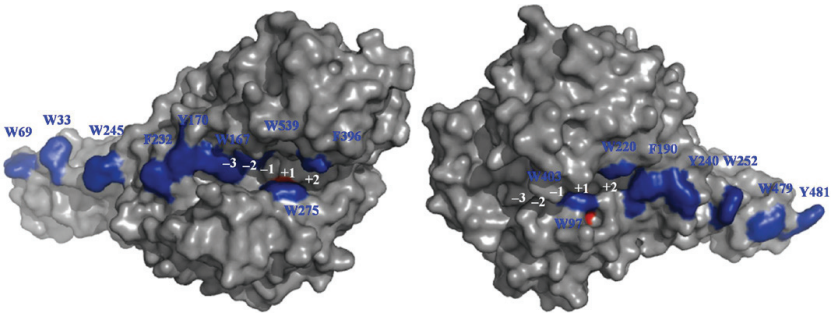

Fig. 1. Crystal structures of ChiA (left, [16] 1ctn), ChiB (right, [17] 1e15). Highlighted in blue are aromatic amino acids that are important for substrate binding; the catalytic acids, Glu^{315} and Glu^{144}, are colored red. These enzymes degrade chitin in a processive manner from the reducing end (ChiA; the polymeric substrate binds to glycon subsites) or the non-reducing end (ChiB; the polymeric substrate binds to aglycon subsites) [18]. (For interpretation of the references to color in this figure legend, the reader is referred to the web version of the article.)

subsite "+4") and subsites −3 to +3 in ChiB [15]. We compare the results with data previously obtained for binding of the glycon-binding inhibitor allosamidin (Fig. 2) to both ChiB and ChiA.

2. Experimental

2.1. Proteins and chemicals

ChiB-E144Q from *S. marcescens* were over expressed in *Escherichia coli* and purified as described elsewhere [19,20]. $(GlcNAc)_6$ was purchased from Sigma–Aldrich (St. Louis, MO, U.S.A.).

2.2. Isothermal titration calorimetry experiments

ITC experiments were performed with a VP-ITC system from Microcal, Inc. (Northampton, MA) [21]. Solutions were thoroughly degassed prior to experiments to avoid air bubbles in the calorimeter. Standard ITC conditions were 250 μM of $(GlcNAc)_6$ in the syringe and 15 μM of ChiB-E144Q in the reaction cell in 20 mM potassium phosphate buffer of pH 6.0, 7.0, and 8.0, respectively. Aliquots of 8 μL were injected into the reaction cell at 180 s intervals at temperatures of 15, 17.5, 20, and 37 °C with a stirring speed of 260 rpm. The titrations were normally complete after 22–27 injections. At least three independent titrations were performed for each binding reaction. As a control experiment, 30 μM $(GlcNAc)_6$ was incubated with ChiB-E144Q (15 μM) for 75 min (equal the time for an ITC measurement) and analyzed using normal phase HPLC as described by Krokeide et al. to ensure that there are no enzymatic hydrolysis of $(GlcNAc)_6$ [22].

2.3. Analysis of calorimetric data

ITC data were collected automatically using the Microcal Origin v.7.0 software accompanying the VP-ITC system [21]. Prior to further analysis, data were corrected for heat of dilution by subtracting the heat remaining after saturation of binding sites on the enzyme. Data were fitted using a non-linear least-squares algorithm using a single-site-binding model employed by the Origin software that accompanies the VP-ITC system. All data from the binding reactions fitted well with the single-site-binding model yielding the stoichiometry (n), equilibrium binding association constant (K_a), and the reaction enthalpy change (ΔH_r°) of the reaction. The value of n was found to be between 0.9 and 1.1 for all reactions. The reaction free energy change (ΔG_r°) and the reaction entropy change (ΔS_r°) were calculated from the relation described in Eq. (1).

$$\Delta G_r^\circ = -RT \ln K_a = \Delta H_r^\circ - T\Delta S_r^\circ \quad (1)$$

Errors are reported as standard deviations of at least three experiments at each temperature. A description of how the entropic term is parameterized has been described in detail previously [23,24].

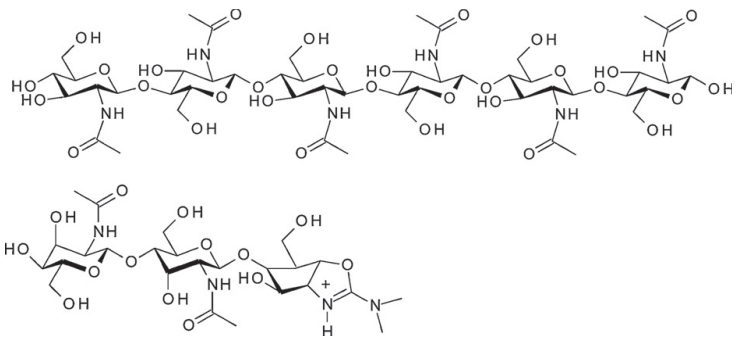

Fig. 2. Molecular structures of $(GlcNAc)_6$ (top) and allosamidin (bottom).

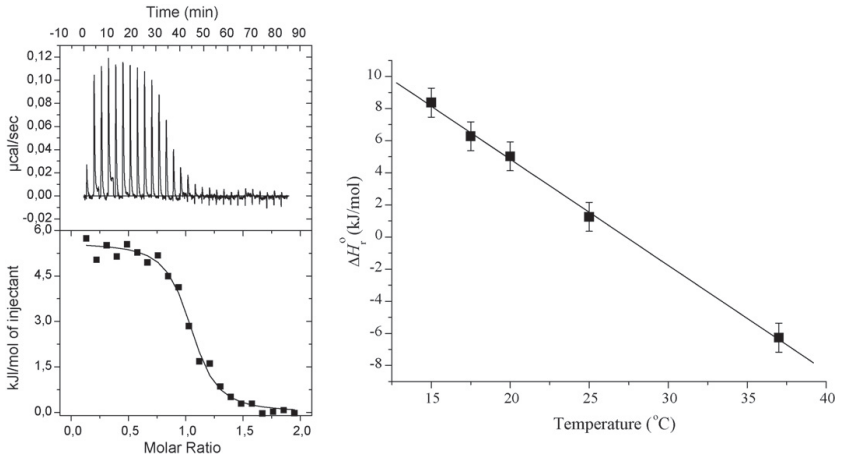

Fig. 3. Left panel, thermograms (top) and binding isotherms (bottom) for the titration of $(GlcNAc)_6$ (at $t = 20\,^\circ C$). Right panel, temperature dependence of $(GlcNAc)_6$ binding to ChiB-E144Q at pH 6.0. The plot of ΔH_r° vs. temperature yields the change of heat capacity (ΔC_p) as the slope. The value of ΔC_p is -661 ± 20 J/K mol.

3. Results and discussion

3.1. Binding of $(GlcNAc)_6$ to ChiB-E144Q

The binding of $(GlcNAc)_6$ to ChiB-E144Q in 20 mM potassium phosphate at different temperatures (15-37 °C) and at a pH of 6.0 was studied by ITC. Fig. 2 shows a typical ITC thermogram and theoretical fit to the experimental data $t = 20\,^\circ C$. At this temperature, $(GlcNAc)_6$ binds with a $\Delta G_r^\circ = -38.0 \pm 1.3$ kJ/mol (Table 1). The binding is clearly entropically driven ($-T\Delta S_r^\circ = -43.0 \pm 1.8$ kJ/mol) with an enthalpic penalty ($\Delta H_r^\circ = 5.0 \pm 1.2$ kJ/mol). Determination of the temperature dependence of ΔH_r° yields the change in the reaction heat capacity ($\Delta C_{p,r}^\circ$). The change in reaction heat capacity for $(GlcNAc)_6$ binding to ChiB-E144Q was found to be -661 ± 20 J/K mol (Fig. 3). $(GlcNAc)_6$ binding to ChiB-E144Q was also analyzed at pH 7.0 and 8.0. The results show that the change in pH had only small effects on binding ($\Delta G_r^\circ = -36.0 \pm 1.5$ and 38.5 ± 1.8 kJ/mol, respectively) and little variation in the enthalpic and entropic terms ($\Delta H_r^\circ = 6.3 \pm 1.2$ and 7.1 ± 1.8 kJ/mol, respectively, and $-T\Delta S_r^\circ = -42.3 \pm 1.9$ and -45.6 ± 2.5 kJ/mol, respectively). Furthermore, there was little variation in the change in heat capacity with respect to pH as well with $\Delta C_{p,r}$ being -711 ± 29 J/K mol at pH 8.0 (not determined at pH 7.0).

ΔS_r° can be parameterized into three terms as shown in Equation 2 [25].

$$\Delta S_r^\circ = \Delta S_{solv}^\circ + \Delta S_{mix}^\circ + \Delta S_{conf}^\circ \quad (2)$$

As explained in the legend to Table 1, ΔS_{solv}° may be derived from $\Delta C_{p,r}^\circ$ [26–28] and ΔS_{mix} represent a fixed known "cratic" term [25], meaning that ΔS_{conf}° can be derived from ΔS_r°. The results, summarized in Table 1, show that at pH 6.0 $-T\Delta S_{solv}^\circ$ equals -52.3 ± 1.5 kJ/mol, the loss of translational entropy ($-T\Delta S_{mix}^\circ$) equals 9.7 kJ/K mol and the entropic effect of conformational changes, $-T\Delta S_{conf}^\circ$, equals -0.4 ± 2.3 J/K mol.

3.2. Differences in binding energetics

The free energies of binding for $(GlcNAc)_6$ and allosamidin to ChiB are identical within experimental errors. Both binding reactions come with an enthalpic penalty ($\Delta H_r^\circ = 5.0$ and 18.5 kJ/mol, respectively), and are thus entropically driven ($-T\Delta S_r^\circ = -43.0 \pm 1.8$ and -56.5 ± 1.7 kJ/mol, respectively). One would expect the longer ligand $(GlcNAc)_6$ that binds to six subsites to displace more solvent molecules than the shorter allosamidin that only binds to three subsites. This is reflected in $-T\Delta S_{solv}^\circ$ values of -52.3 ± 1.5

Table 1
Thermodynamic parameters for binding of $(GlcNAc)_6$ and allosamidin binding to ChiB[a] and for allosamidin binding to ChiA[a] at $t = 20\,^\circ C$, as determined by isothermal titration calorimetry.

ΔG_r° [b]	ΔH_r° [b]	$-T\Delta S_r^\circ$ [b]	$-T\Delta S_{solv}^\circ$ [b,c]	$-T\Delta S_{conf}^\circ$ [b,d]	ΔS_r° [e]	$\Delta C_{p,r}^\circ$ [e,f]
ChiB-$(GlcNAc)_6$						
-38.0 ± 1.3	5.0 ± 1.2	-43.0 ± 1.8	-52.3 ± 1.5	-0.4 ± 2.3	147 ± 4	-661 ± 20
ChiB-allosamidin[a]						
-38.0 ± 1.0	18.5 ± 0.9	-56.5 ± 1.7	-21.0 ± 1.1	-45.2 ± 2.0	193 ± 4	-263 ± 16
ChiA-allosamidin[b]						
-39.3 ± 0.9	-23.4 ± 0.9	-15.9 ± 1.7	-20.4 ± 3.1	-5.2 ± 3.5	54 ± 4	-255 ± 52

[a] The values at $t = 20\,^\circ C$ are calculated from the ones at $t = 30\,^\circ C$ by using the temperature dependence on ΔH_r° and ΔS_r°, from Cederkvist et al. [22] and Baban et al. [28], respectively, to be able to compare to those of the $(GlcNAc)_6$–ChiB-E144Q binding that has low ΔH_r° at $t = 30\,^\circ C$.
[b] kJ/mol.
[c] $\Delta S_{solv}^\circ = \Delta C_p \ln(T_{293\ K}/T_{385\ K})$ [25–27].
[d] Derived using $\Delta S_r^\circ = \Delta S_{solv}^\circ + \Delta S_{mix}^\circ + \Delta S_{conf}^\circ$ where $\Delta S_{mix}^\circ = R\ln(1/55.5) = -33$ J/K mol ("cratic" term) [24].
[e] J/K mol.
[f] These data are derived from the temperature dependence of ΔH_r°.

and -21.0 ± 1.1 kJ/mol, respectively, i.e. a much more favorable $-T\Delta S^{\circ}_{solv}$ for the hexamer. Interestingly, there is a huge difference in the conformational entropy change. While binding of $(GlcNAc)_6$ to ChiB results in $-T\Delta S^{\circ}_{conf}$ of -0.4 ± 2.3 kJ/mol, allosamidin binding to the same protein is accompanied with an $-T\Delta S^{\circ}_{conf}$ of -45.2 ± 2.0 kJ/mol. One obvious explanation for this great difference is that long ligands are more flexible than short, and that the conformational entropy loss upon binding for this reason will be greater. Similar trends have been observed for the binding of xylosaccharides to xylanases [10]. Another explanation may be that the allosamizoline group in allosamidin is preformed while −1 sugar in $(GlcNAc)_6$ must undergo a chair – boat conformational transformation and, hence, lose conformational entropy. While this conformational entropy change to our knowledge has not been calculated for GlcNAc in CHOS, it has been shown to be less than 11% (<12 J/K mol) of the free energy change for the same conformational transformation for glucose in dextran [30].

Another factor may be the topology and the structure of the ligand-binding sites of the enzymes. ChiB contains several loops with relatively high *B*-factors that primarily interact with ligands binding in aglycon subsites, and not in the glycon subsites where allosamidin binds [31]. Rigidification of these loops upon binding of $(GlcNAc)_6$ may contribute to the relatively unfavorable ΔS°_{conf} for binding of this hexamer. Support for this comes from allosamidin binding to ChiA. For this interaction, $-T\Delta S^{\circ}_{solv}$ (-20.4 ± 3.1 kJ/mol) is the same as for binding to ChiB (-21.0 ± 1.1 kJ/mol) but $-T\Delta S^{\circ}_{conf}$ is 40 kJ/mol less favorable than for ChiB (-5.2 ± 3.5 kJ/mol vs. -45.2 ± 2.0 kJ/mol) [23,29]. Even though allosamidin binds to glycon subsites in both chitinases, the difference is that allosamidin binds to ChiA in "substrate-binding sites" (i.e., where the chitin chain would be binding during processive hydrolysis) compared to "product-binding sites" in ChiB (i.e., where chitobiose is released from the enzyme during processive hydrolysis). Judged from the structure, flexible loops interacting with the polymeric substrate are less prominent in ChiA than in ChiB, but ChiA does indeed contain some inserted loops absent in ChiB that are affected by substrate binding in the glycon subsites [32]. Thus, one could a priori expect relatively unfavorable – $T\Delta S^{\circ}_{conf}$ terms for hexamer binding to ChiB and allosamidin binding to ChiA, as is indeed observed.

Effective enzymes need to make sure that their products are not bound too strongly. The occurrence of aromatic residues in the active site clefts of ChiA and ChiB indicate that the enzymes are optimized to bind the polymeric substrate (in glycon subsites in ChiA and in aglycon subsites in ChiB), while the product is bound more loosely [18,33]. Indeed, our previous studies, summarized in Table 1, show that binding of allosamidin to substrate-binding subsites in ChiA is accompanied by a favorable enthalpic change in contrast to what is observed binding to product binding sites in ChiB (-23.4 ± 0.9 kJ/mol vs. 18.5 ± 0.9 kJ/mol, respectively). Surprisingly, the characterization of binding of $(GlcNAc)_6$ to ChiB in the present study showed only a minor enthalpic improvement as compared to binding of allosamidin, and the overall enthalpic term still disfavors binding. Structural studies show that $(GlcNAc)_6$ has several favorable interactions in the aglycon subsites [31]. Somewhat unexpectedly, it is only the favorable effect of ΔS_{solv} that drives binding of $(GlcNAc)_6$.

Lastly, the binding of $(GlcNAc)_6$ to ChiB-144Q was not dependent of pH contrasting to what is observed for the binding of allosamidin to both ChiA and ChiB where the binding enthalpy changes decreases with increasing pH [23,29]. The pH dependencies for the latter interactions have been attributed to the deprotonation of the Asp^{313}–Glu^{315} and Asp^{142}–Glu^{144} diads for ChiA and ChiB, respectively, and the formation of favorable electrostatic–electrostatic interactions with the positively charged allosamizoline group of allosamidin [23,29]. For the $(GlcNAc)_6$–ChiB interaction, this cannot only be due to the fact that there are no titratable groups on the ligands, but must also imply that the titratable groups remaining in the catalytic center of ChiB after mutating the catalytic Glu^{144} to a non-titratable glutamine are not significantly titrated in the pH 6.0–8.0 range. This is in accordance with the results of previous experimental and bioinformatics studies showing that only remaining titratable group with a pK_a in or near the physiological pH interval is Asp^{142} and that this residue has a distorted pK_a value near, and possibly well above 8.0 [20].

4. Concluding remarks

The results described in this work show that binding energetics for ligands to family 18 chitinases greatly depend on both the nature of ligand and details of the active site architecture of the enzyme. To some extent, the observed energetics can be explained by chemical considerations and structural information on ligand binding, but, on the other hand, the energetics of binding of $(GlcNAc)_6$ showed some surprising features. This whole active site-binding compound showed good affinity, comparable with that of allosamidin, but did not show the expected favorable enthalpic term in binding energetics. The two active human chitinases, chitotriosidase (HCHT) and acidic mammalian chitinase (AMCase) that are possible therapeutic targets [7,34] contain many aromatic residues in both their glycon and aglycon subsites, but the roles of these residue e.g. in determining processivity and its direction agree not yet known. Future rational inhibitor design will require more in-depth knowledge of the enzymes in addition to the type of measurements described in this study.

Acknowledgements

We are grateful for the funding from the Norwegian Research Council for a research grant (Project 177542/V30) and the ITC instrument (Project 155518/V00).

References

[1] B. Henrissat, G.J. Davies, Structural and sequence-based classification of glycoside hydrolases, Curr. Opin. Struct. Biol. 7 (1997) 637–644.
[2] F.H. Cederkvist, M.P. Parmer, K.M. Vårum, V.G.H. Eijsink, M. Sørlie, Inhibition of a family 18 chitinase by chitooligosaccharides, Carbohydr. Polym. 74 (2008) 41–49.
[3] O.A. Andersen, A. Nathubhai, M.J. Dixon, I.M. Eggleston, D.M. Van Aalten, Structure-based dissection of the natural product cyclopentapeptide chitinase inhibitor argifin, Chem. Biol. 15 (2008) 295–301.
[4] H. Izumida, M. Nishijima, T. Takadera, A.M. Nomoto, H. Sano, The effect of chitinase inhibitors, cyclo(Arg-Pro) against cell separation of Saccharomyces cerevisiae and the morphological change of Candida albicans, J. Antibiot. (Tokyo) 49 (1996) 829–831.
[5] J. Saguez, F. Dubois, C. Vincent, J.C. Laberche, B.S. Sangwan-Norreel, P. Giordanengo, Differential aphicidal effects of chitinase inhibitors on the polyphagous homopteran Myzus persicae (Sulzer), Pest. Manage. Sci. 62 (2006) 1150–1154.
[6] L.E. Donnelly, P.J. Barnes, Acidic mammalian chitinase—a potential target for asthma therapy, Trends Pharmacol. Sci. 25 (2004) 509–511.
[7] Z. Zhu, T. Zheng, R.J. Homer, Y.K. Kim, N.Y. Chen, L. Cohn, Q. Hamid, J.A. Elias, Acidic mammalian chitinase in asthmatic Th2 inflammation and IL-13 pathway activation, Science 304 (2004) 1678–1682.
[8] E. Freire, Do enthalpy and entropy distinguish first in class from best in class? Drug Discov. Today 13 (2008) 869–874.
[9] J.M. Macdonald, C.A. Tarling, E.J. Taylor, R.J. Dennis, D.S. Myers, S. Knapp, G.J. Davies, S.G. Withers, Chitinase inhibition by chitobiose and chitotriose thiazolines, Angew. Chem. Int. Ed. Engl. 49 (2010) 2599–2602.
[10] G. Zolotnitsky, U. Cogan, N. Adir, V. Solomon, G. Shoham, Y. Shoham, Mapping glycoside hydrolase substrate subsites by isothermal titration calorimetry, Proc. Natl. Acad. Sci. U.S.A. 101 (2004) 11275–11280.
[11] G.J. Davies, K.S. Wilson, B. Henrissat, Nomenclature for sugar-binding subsites in glycosyl hydrolases, Biochem. J. 321 (1997) 557–559.
[12] S. Sakuda, A. Isogai, S. Matsumoto, A. Suzuki, K. Koseki, The structure of allosamidin, a novel insect chitinase inhibitor, produced by Streptomyces Sp, Tetrahedron Lett. 27 (1986) 2475–2478.

[13] G. Vaaje-Kolstad, A. Vasella, M.G. Peter, C. Netter, D.R. Houston, B. Westereng, B. Synstad, V.G. Eijsink, D.M. Van Aalten, Interactions of a family 18 chitinase with the designedinhibitor HM508, and its degradation product,chitobiono-delta-lactone, J. Biol. Chem. (2004).
[14] A.C. Terwisscha van Scheltinga, S. Armand, K.H. Kalk, A. Isogai, B. Henrissat, B.W. Dijkstra, Stereochemistry of chitin hydrolysis by a plant chitinase/lysozyme and X-ray structure of a complex with allosamidin: evidence for substrate assisted catalysis, Biochemistry 34 (1995) 15619–15623.
[15] S.J. Horn, M. Sørlie, G. Vaaje-Kolstad, A.L. Norberg, B. Synstad, K.M. Vårum, V.G.H. Eijsink, Comparative studies of chitinases A, B and C from *Serratia marcescens*, Biocatal. Biotransform. 24 (2006) 39–53.
[16] A. Perrakis, I. Tews, Z. Dauter, A.B. Oppenheim, I. Chet, K.S. Wilson, C.E. Vorgias, Crystal structure of a bacterial chitinase at 2.3 A resolution, Structure 2 (1994) 1169–1180.
[17] D.M.F. van Aalten, B. Synstad, M.B. Brurberg, E. Hough, B.W. Riise, V.G.H. Eijsink, R.K. Wierenga, Structure of a two-domain chitotriosidase from *Serratia marcescens* at 1.9-angstrom resolution, Proc. Natl. Acad. Sci. U.S.A. 97 (2000) 5842–5847.
[18] H. Zakariassen, B.B. Aam, S.J. Horn, K.M. Varum, M. Sorlie, V.G. Eijsink, Aromatic residues in the catalytic center of chitinase A from *Serratia marcescens* affect processivity, enzyme activity, and biomass converting efficiency, J. Biol. Chem. 284 (2009) 10610–10617.
[19] M.B. Brurberg, I.F. Nes, V.G.H. Eijsink, Comparative studies of chitinases A and B from *Serratia marcescens*, Microbiology 142 (1996) 1581–1589.
[20] B. Synstad, S. Gåseidnes, D.M.F. van Aalten, G. Vriend, J.E. Nielsen, V.G.H. Eijsink, Mutational and computational analysis of the role of conserved residues in the active site of a family 18 chitinase, Eur. J. Biochem. 271 (2004) 253–262.
[21] T. Wiseman, S. Williston, J.F. Brandts, L.N. Lin, Rapid measurement of binding constants and heats of binding using a new titration calorimeter, Anal. Biochem. 179 (1989) 131–137.
[22] I.-M. Krokeide, B. Synstad, S. Gåseidnes, S.J. Horn, V.G.H. Eijsink, M. Sørlie, Natural substrate assay for chitinases using high-performance liquid chromatography: a comparison with existing assays, Anal. Biochem. 363 (2007) 128–134.
[23] F.H. Cederkvist, S.F. Saua, V. Karlsen, S. Sakuda, V.G.H. Eijsink, M. Sørlie, Thermodynamic analysis of allosamidin binding to a family 18 chitinase, Biochemistry 46 (2007) 12347–12354.
[24] H. Zakariassen, M. Sørlie, Heat capacity changes in heme protein–ligand interactions, Thermochim. Acta 464 (2007) 24–28.
[25] B.M. Baker, K.P. Murphy, Dissecting the energetics of a protein–protein interaction: the binding of ovomucoid third domain to elastase, J. Mol. Biol. 268 (1997) 557–569.
[26] R.L. Baldwin, Temperature dependence of the hydrophobic interaction in protein folding, Proc. Natl. Acad. Sci. U.S.A. 83 (1986) 8069–8072.
[27] K.P. Murphy, P.L. Privalov, S.J. Gill, Common features of protein unfolding and dissolution of hydrophobic compounds, Science 247 (1990) 559–561.
[28] K.P. Murphy, Hydration and convergence temperatures—on the use and interpretation of correlation plots, Biophys. Chem. 51 (1994) 311–326.
[29] J. Baban, S. Fjeld, S. Sakuda, V.G.H. Eijsink, M. Sørlie, The roles of three *Serratia marcescens* chitinases in chitin conversion are reflected in different thermodynamic signatures of allosamidin binding, J. Phys. Chem. B 114 (2010) 6144–6149.
[30] R.G. Haverkamp, A.T. Marshall, M.A.K. Williams, Entropic and enthalpic contributions to the chair—boat conformational transformation in Dextran under single molecule stretching, J. Phys. Chem. B 111 (2007) 13653–13657.
[31] D.M.F. van Aalten, D. Komander, B. Synstad, S. Gåseidnes, M.G. Peter, V.G.H. Eijsink, Structural insights into the catalytic mechanism of a family 18 exo-chitinase, Proc. Natl. Acad. Sci. U.S.A. 98 (2001) 8979–8984.
[32] Y. Papanikolau, G. Prag, G. Tavlas, C.E. Vorgias, A.B. Oppenheim, K. Petratos, High resolution structural analyses of mutant chitinase A complexes with substrates provide new insight into the mechanism of catalysis, Biochemistry 40 (2001) 11338–11343.
[33] H. Zakariassen, V.G.H. Eijsink, M. Sørlie, Signatures of activation parameters reveal substrate-dependent rate determining steps in polysaccharide turnover by a family 18 chitinase, Carbohydr. Polym. 81 (2010) 14–20.
[34] F. Fusetti, H. von Moeller, D. Houston, H.J. Rozeboom, B.W. Dijkstra, R.G. Boot, J.M.F.G. Aerts, D.M.F. van Aalten, Structure of human chitotriosidase. Implications for specific inhibitor design and function of mammalian chitinase-like lectins, J. Biol. Chem. 277 (2002) 25537–25544.

PAPER III

FEBS Letters 585 (2011) 2339–2344

journal homepage: www.FEBSLetters.org

Substrate positioning in chitinase A, a processive chito-biohydrolase from *Serratia marcescens*

Anne Line Norberg [a], Anette I. Dybvik [b], Henrik Zakariassen [a], Michael Mormann [c], Jasna Peter-Katalinić [c], Vincent G.H. Eijsink [a], Morten Sørlie [a,*]

[a] Department of Chemistry, Biotechnology and Food Science, Norwegian University of Life Sciences, P.O. Box 5003, N-1432 Ås, Norway
[b] Department of Biotechnology, Norwegian University of Science and Technology, Trondheim, Norway
[c] Institute of Medical Physics and Biophysics, Westphalian Wilhelms University of Münster, Robert-Koch-Str. 31, D-48149 Münster, Germany

ARTICLE INFO

Article history:
Received 6 April 2011
Revised 2 June 2011
Accepted 3 June 2011
Available online 12 June 2011

Edited by Miguel De la Rosa

Keywords:
Subsite affinities
Endo-activity
Product displacement
Family 18 chitinases

ABSTRACT

The contributions of the –3 subsite and a putative +3 subsite to substrate positioning in ChiA from *Serratia marcescens* have been investigated by comparing how ChiA and its –3 subsite mutant W167A interact with soluble substrates. The data show that Trp – GlcNAc stacking in the –3 subsite rigidifies the protein backbone supporting the formation of the intermolecular interaction network that is necessary for the recognition and positioning of the *N*-acetyl groups before the –1 subsite. The +3 subsite exhibits considerable substrate affinity that may promote endo-activity in ChiA and/or assist in expelling dimeric products from the +1 and +2 subsites during processive hydrolysis.

1. Introduction

Chitin, a β-1,4-linked linear polymer of *N*-acetyl-glucosamine (GlcNAc), is the second most abundant biopolymer in nature, after its analogue cellulose, acting as a structuring biomaterial in fungi, crustaceans and arthropods [1]. In the polymer, each residue is rotated 180 degrees relative to its neighbors. Chitinases, the enzymes that degrade chitin in nature, belong to glycosyl hydrolase families 18 and 19 [2]. Due to the crystalline nature of chitin, substrate accessibility is energetically demanding and enzyme-substrate association is considered the rate limiting step of hydrolysis [3,4]. In addition to a catalytic domain, many chitinases contain at least one additional substrate-binding domain that may help the enzyme in attaching to its substrate. The enzymes may bind in an exo- (binding at chain ends) or endo- (binding at random, internal, positions) fashion, and each of these binding modes may be combined with some degree of processivity [5]. Processive family 18 chitinases are thought to bind mainly in an exo-fashion when acting on crystalline substrates [6] but have the potential to bind in an endo-fashion, as is clearly seen when the enzymes act on chitosan, a soluble polymeric chitin-derivative [7].

In order to bind to and guide the insoluble substrate into the active site cleft, many chitinases, including all those that are known to act processively, have a path of conserved solvent exposed aromatic residues leading from the chitin binding domain to the active site cleft [8–12] (Fig. 1). The aromatic residues interact with the pyranose rings through stacking interactions [13,14]. They are thought to play an important role in binding of the crystalline substrate [12,15] and they are critical for the "sliding" of the polymeric substrate during processive action [10,16].

Chitinase A (ChiA) from *Serratia marcescens* hydrolyses chitin from reducing chain ends in an exo-prossesive manner [6,11,17]. ChiA has several aromatic residues in its –6 to –3 glycon subsites as well as on the surface of its chitin binding domain that extends the surface binding cleft to the side where the non-reducing end of the polymeric substrate binds [18]. Recently, it was shown that Trp^{167} in subsite –3 (Fig. 1), interacting with the polymeric and "sliding" part of the substrate, is of particular importance for the processive action for ChiA [11].

After a processive hydrolytic event, a dimeric product needs to dissociate from subsites +1 and +2. Before dissociation, the dimeric product stacks with a Trp residue in +1 (Trp275) and a Phe residue in +2 (Phe396) (Fig. 1). Even though it has been suggested that there are no subsites beyond +2 in ChiA [18,19], the length of the active site cleft itself suggest that there is a "+3" subsite, and possibly even a "+4" subsite, as seen by the addition of a modeled

* Corresponding author. Fax: +47 64965901.
E-mail address: morten.sorlie@umb.no (M. Sørlie).

0014-5793/$36.00
doi:10.1016/j.febslet.2011.06.002

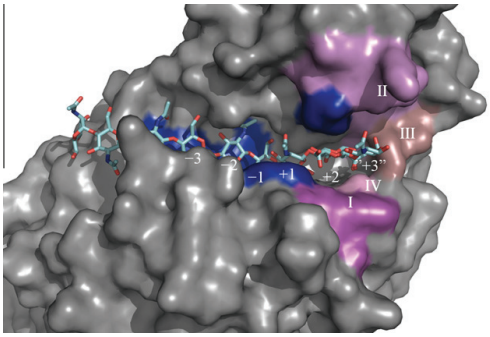

Fig. 1. Crystal structure of the active site of ChiA in complex with a $(GlcNAc)_8$ molecule bound to subsites −6 to +2, with numbered subsites (1ehn) [35]. In addition, two GlcNAc moieties bound to subsites +2 and "+3" in a complex of ChiB with $(GlcNAc)_5$ (1e6n) [36] are shown in a position that was derived after superposing the two structures. Four aromatic amino acids interacting with the ligand and located near the catalytic center are colored blue. These are: Trp^{167} (subsite −3), Trp^{539} (subsite −1/−2), Trp^{275} (+1), and Phe^{396} (+2). Four regions in ChiA that potentially could interact with a GlcNAc moiety bound to a putative +3 subsite are labeled using roman numbers and colored: I (magenta), $G^{318}G^{319}K^{320}G^{321}$, II (violet), $F^{392}Y^{393}G^{394}A^{395}F^{396}D^{397}L^{398}K^{399}N^{400}$, III (dirty violet), $T^{416}A^{417}Y^{418}$, and IV (pink), K^{369}. See text for further discussion.

GlcNAc moiety (Fig. 1). Moreover, studies of the cleavage patterns obtained with oligomeric substrates have indicated that ChiA may indeed have sugar affinity beyond the +2 subsite [19,20]. For example, in one study it was concluded that $(GlcNAc)_5$ binds productively to the −3 to +2 and to the −2 to +3 subsites at approximately equal frequencies [20], despite the strong stacking interaction in the −3 subsite (which represents a free energy change of −1.8 kcal/mol [21]). This puzzling result may be taken to suggest that there indeed is some sort of +3 subsite. The function of this subsite remains somewhat elusive.

To gain further insight into the importance of the −3 and (putative) +3 subsite in ChiA and to understand structural factors steering substrate positioning in ChiA in general, we have studied productive and inhibitory binding of fully acetylated and partially de-acetylated chito-oligosaccharides and polymers to the wild-type enzyme and to the W167A mutant. To analyze hydrolytic and binding events, we have used standard enzymological methods as well as advanced mass spectrometry based analyses. The results provide novel insight into the intricate substrate-binding mechanisms of processive glycoside hydrolases.

2. Materials and methods

2.1. Chemicals

$(GlcNAc)_6$, $(GlcNAc)_5$ and $(GlcNAc)_4$ were purchased from Seikagaku (Japan, Tokyo). Chitin from crab shell was purchased from Sigma–Aldrich (St. Louis, MO, USA).

2.2. Protein expression and purification

ChiA-W167A and ChiA wildtype (WT) from *S. marcescens* were over-expressed and purified as described elsewhere [11].

2.3. Preparation of partly de-acetylated chito-oligosaccharides

Partly de-acetylated chito-oligosaccharides were prepared using chitosanase ScCsn46A (Swiss-Prot Q9RJ88) as described earlier [22]. Chitosans with a fraction of *N*-acetylated units (F_A) of 0.32 were prepared by homogeneous de-*N*-acetylation of chitin [23]. Chitosan (as chitosan hydrochloride) was dissolved in water to 20 mg/ml and incubated with shaking in room temperature, over night. An equivalent volume of 0.08 M sodium acetate buffer, pH 5.5 (containing 0.2 M NaCl), and 0.2 mg BSA was added. Chitosan solutions (final concentration of 10 mg/ml) were incubated in a shaking water bath at 37 °C, and the degradation reactions were started by adding 0.5 μg ScCsn46A per mg chitosan. After 52 h, the samples were immersed in boiling water for 5 min, followed by a centrifugation to remove potential precipitates.

Chitosan and chito-oligosaccharides (CHOS) were separated on three XK 26 columns, connected in series, packed with Superdex™ 30 (Pharmacia Biotech, Uppsala, Sweden), with an overall dimension of 2.60 × 180 cm [24]. The buffer used was 0.15 M ammonium acetate, pH 4.5. The elution buffer was pumped through the system using a LC-10ADvp pump (Shimadzu GmbH, Duisburg, Germany) delivering the buffer at a flow rate of 0.8 ml/min. The relative amounts of oligomers were monitored with a refractive index (RI) detector (Shodex RI-101, Shodex Denko GmbH, Dusseldorf, Germany), coupled to a CR 510 Basic Data logger (Campbell Scientific Inc., Logan, UT, U.S.A.). For characterization of isolated chito-oligomers, fractions of 3.2 ml were collected using a fraction collector. Peaks were assigned using NMR as described previously [24]. Fractions containing oligomers of DP8 were pooled and freeze dried prior to further analysis. Using NMR, the average fraction of acetylated sugars (F_A) in the DP8 sample was determined to be 0.5.

2.4. Nano-ESI-q-TOF mass spectrometry

Nano-ESI-q-TOF Mass Spectrometry was used to study complex formation between partly de-acetylated chito-oligosaccharides (60 μM) and ChiA WT or ChiA-W167A (both at 5 μM) after 5 and 60 min of incubation. Screening for complex formation and top-down analysis of detected complexes were performed as described earlier [25]. For all experiments the following parameters were used: the ion-source temperature was set at 80 °C, desolvation gas was used at a flow rate of 100 l/h, a potential of 900 V was applied to the capillary tip, and the sampling cone voltage was set to 80 V. For collision-induced dissociation (CID)-analysis, the parent ion was selected by the first quadrupole where about ten scans were acquired under the following conditions: the low- and high-mass resolution of the quadrupole for isolation where set to 0; the ion acceleration voltage was set to 4 eV. The parent ion was subsequently fragmented in the collision cell using argon as collision gas at a nominal pressure of 23 psi and initial ion acceleration voltage of 10 V that was increased stepwise during continuous signal acquisition. The MS and MS/MS signals were recorded on the orthogonal TOF analyzer over a range of m/z 100–5000 at a scan rate of 2.0 s/scan. All scans were displayed in a single spectrum.

2.5. Matrix assisted laser desorption/ionization mass spectrometry

MALDI TOF and MALDI TOF-TOF mass spectrometry were used to determine the composition and sequence of partly de-acetylated chito-oligosaccharides (60 μM) before and after interaction with 5 μM ChiA-WT or ChiA-W167A for 5 and 60 min. For sequence determination reducing end derivatization was applied as described earlier by Bahrke et al. [26]. Mass spectrometric conditions were as described by Cederkvist et al. [27].

2.6. HPLC analysis of the degradation of $(GlcNAc)_6$, $(GlcNAc)_5$ and $(GlcNAc)_4$

Chito-oligosaccharides (Seikagaku Corp., Tokyo, Japan) were separated with regard to size and anomeric configuration by normal phase HPLC using a Waters Acquity UPLC BEH-amide 1.7 μM 2.1 × 50 mm column (Waters Cooperation). $(GlcNAc)_6$,

$(GlcNAc)_5$ and $(GlcNAc)_4$ were dissolved in 20 mM ammonium acetate, pH 6.1, to a concentration of 500 μM. ChiA-W167A were added to a concentration of 0.25 μM, and the reactions were incubated for 20 s at 37°, 600 rpm. The reactions were then stopped by adding an equal volume of 100% acetonitrile. The reaction products were immediately analyzed by isocratic ultra high performance liquid chromatography (UHPLC). Typically, 1 μl reaction mixture was injected and the column was eluted isocratically at 0.4 ml/min with 76% (v/v) acetonitrile at 30 °C. Chito-oligosaccharides were monitored by measuring absorbance at 210 nm and quantified by comparing peak areas with peak areas obtained from samples with known concentrations. Using these standard samples, it was established that there was a linear correlation between peak area and oligosaccharide concentration within the concentration range used in this study. Data for wild type ChiA, obtained using an essentially identical procedure, were taken from a previous study [28].

2.7. Kinetic analysis

The kinetic constants k_{cat} and K_m for ChiA-W167A were determined using the $(GlcNAc)_4$ substrate [28], which, at the substrate concentrations and in the time frames used for kinetic analysis is predominantly (>95%) converted to two $(GlcNAc)_2$. Reaction mixtures with 8 different $(GlcNAc)_4$ concentrations varying from 2 to 250 μM, in 20 mM sodium acetate buffer, pH 6.1 and 0.1 mg/ml BSA (final concentrations) were pre-incubated in a 37 °C water bath for 10 min before the reactions were started by adding purified enzyme (10 nM final concentration) and a total reaction volume of 1.0 ml. After starting the reaction, samples of 50 μl were withdrawn at regular time intervals over a total period of 2–25 min, and the enzyme was inactivated by adding 50 μL acetonitrile. All of the reactions were run in duplicate, and all of the samples were stored at –20 °C until UHPLC analysis. Reaction conditions were such that the rate of hydrolysis of $(GlcNAc)_4$ was essentially constant over time, with the $(GlcNAc)_4$ concentration always staying above 80% of the starting concentration. The slopes of plots of 0.5 times the $(GlcNAc)_2$ concentration versus time were taken as the hydrolysis rate. The rates were plotted versus substrate concentration in a Michaelis-Menten plot and the experimental data were fitted to the Michaelis-Menten equation by nonlinear regression using the Origin v7.0 (OriginLab Corporation, Northampton, MA).

2.8. Degradation of chitosan

A 20 mg/ml chitosan solution (in doubly distilled H_2O) was mixed with equal volumes of buffer (0.08 M NaAc, 0.2 M NaCl, pH 5.5, and 0.1 mg/ml bovine serum albumin, giving a final chitosan concentration of 10 mg/ml. Hydrolysis was carried out at 37.0 °C in a shaking incubator using an enzyme concentration of 5 μg/ml. Degradation was allowed to proceed to a maximum degree of scission. The reactions were stopped by lowering the pH to 2.5 by the addition of 1.0 M HCl and immersing the samples in boiling water for 2 min. Sequence analyses of resulting CHOS were performed as described in Section 2.5.

3. Results and discussion

3.1. The putative +3 subsite

Previous studies of binding of $(GlcNAc)_{4-6}$ to ChiA revealed several competing productive binding modes for $(GlcNAc)_6$ (–4 to +2, –3 to +3, and –2 to +4) and $(GlcNAc)_5$ (–2 to +3, –3 to +2), whereas $(GlcNAc)_4$ was found to bind only from -2 to +2 [20]. These observations suggest the presence of a +3 subsite. 70% of the dimers obtained when incubating ChiA with $(GlcNAc)_5$ had the β-anomer configuration (in equilibrium this would be 40%), indicating approximately equal preferences for binding to –3 to +2 and to –2 to +3 [20]. Fig. 2 shows that about 90% of the dimers produced upon incubating $(GlcNAc)_5$ with ChiA-W167A have the β-anomer configuration, showing that the pentamer now predominantly binds from –2 to +3 and confirming the presence of considerable substrate affinity in positive subsites beyond +2. Studies with $(GlcNAc)_6$ confirmed a shift in the ratio of productive binding events towards events that involve more of the positive subsites (results not shown).

Fig. 1 highlights regions of ChiA that might interact with sugars in positive subsites beyond +2. Each of these regions contain residues that would seem able to form hydrogen bonds with a +3 sugar, either directly or via a water molecule. The $G^{318}G^{319}K^{320}G^{321}$ sequence (region I in Fig. 1) containing K^{320} is intriguing because it is an insert relative to many other family 18 chitinases and because the presence of three glycines suggests large conformational flexibility. The $F^{392}Y^{393}G^{394}A^{395}F^{396}D^{397}L^{398}K^{399}N^{400}$ and $T^{416}A^{417}Y^{418}$ sequences (region II and III in Fig. 1, respectively) contain several residues potentially capable of hydrogen bonding. Judged by B-factors, these residues are all in relatively mobile parts of the enzyme, meaning that their involvement in substrate binding could be facilitated by conformational adaptation. Finally, K^{369} is situated in a position to interact with the glycosidic bond between the GlcNAc moieties in +2 and +3 [18].

Studies with both crystalline chitin [29] and chitosan [7] indicate that ChiA has significant endo-activity. Endo-binding is beneficial because for most substrates, the number of "exo-binding sites" (i.e., chain ends) is much lower than the number of "endo-binding sites". Clearly, affinity in positive subsites beyond +2 would be beneficial for an endo-type of substrate association. Another possible role of a +3 subsite could be in promotion of product displacement. During processive hydrolysis, the dimeric product bound to the +1 and +2 subsites needs to dissociate before the polymeric chain can slide by two sugar units to become the new substrate. It is conceivable that affinity in the +3 region could promote displacement and subsequent release of the dimeric prod-

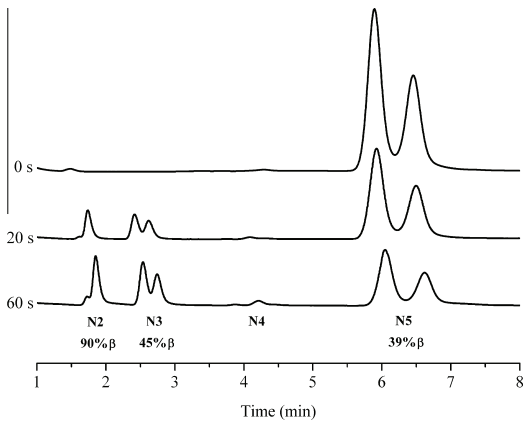

Fig. 2. UHPLC chromatograms showing products released after partial hydrolysis of $(GlcNAc)_5$ (500 μM) with 0.25 μM ChiA-W167A after t = 0 s (top), 20 s (middle), and 60 s (bottom). Each oligosaccharide produces two peaks representing the α- and β-anomer, the α-anomer eluting first. The equilibrium α:β ratio is approximately 60:40. Enzymatic cleavage generates β-anomeric chain ends. The α:β ratio of the individual oligomers was the same at both t = 20 s and 60 s. Reactions were set up with very short incubation times and product mixtures were analyzed immediately to prevent newly formed reducing ends from reaching anomeric equilibrium prior to the UPLC analysis.

uct. It is tempting to speculate that the highly flexible side chain of K^{320} could play a "pulling" role.

3.2. The −3 subsite

The crystal structure of ChiA-W167A as well as ChiA-W167A in complex with allosamidin has been determined previously (pdb file 1 × 6 l and 1 × 6*n*) revealing no other structural change than the removal of the indole side chain at position 167. To further explore the role of Trp^{167} in substrate positioning, k_{cat} and K_m were determined for $(GlcNAc)_4$ and found to be 97 ± 9 s^{-1} and 333 ± 44 μM (Fig. S1; corresponding wild-type values are 33 ± 1 s^{-1} and 9 ± 1 μM [28]). $(GlcNAc)_4$ is a substrate that does not interact with Trp167 in its productive binding mode, occupying subsites −2 to +2 [20]. Even so, the results show considerable mutational effects on the kinetic parameters. In particular, there is a dramatic 37-fold increase in the K_m value. Substrate affinity may to some extent be reflected in the Michaelis-Menten constant K_m, and if so, this suggests that even though there is no direct binding to Trp^{167} during hydrolysis, this residue takes part in guiding the substrate from the solution and into the active site of ChiA. Similar roles have been proposed for aromatic residues in glycon-binding positions that are more remote from the catalytic center [9].

The effect of Trp^{167} in substrate positioning is also reflected in interactions with partly de-acetylated oligomeric substrates. When partly de-acetylated chito-oligosaccharides of degree of polymerization (DP) of 8 and an average degree of acetylation of 50% (F_A 0.5) were incubated for 5 and 60 min with ChiA-WT, all were degraded to shorter fragments as shown by nano-ESI-q-TOF-MS and MALDI-TOF-MS (Fig. 3A and Fig. S2). In contrast, when ChiA-W167A was incubated with the same substrate, several CHOS of DP8 remained in solution after 5 and even 60 min of incubation time (Fig. S2). For ChiA-W167A only, the nano-ESI-q-TOF mass spectra (Fig. 3B) revealed complexes of ChiA-W167A with DP8 CHOS, indicating formation of non-productive complexes. Collision-induced dissociation and MS/MS experiments showed that three different DP8 oligomers, D_4A_4, D_3A_5 and D_5A_3, were bound to the enzyme (Fig. 3C). Sequencing of the remaining CHOS in the reaction mixture [26,27] showed that all contained two or more consecutive acetylated sugars (Table S1) meaning that these CHOS could be cleaved by the wild-type enzyme [17] (Table S1).

Previously, it has been suggested that non-productive binding of partially de-acetylated CHOS is due to binding of a deacetylated sugar to the −1 subsite [25]. Such binding would be non-productive because of the involvement of the acetamidogroup of the −1 sugar in catalysis, [30]. Apparently, formation of non-productive complexes is promoted by removal of Trp^{167}, since substrates that can be cleaved by the wild-type enzyme remain un-cleaved. It thus seems that for partially deacetylated substrates aromatic stacking with Trp^{167} plays a crucial role in overcoming the energetic penalty connected to binding an acetylated sugar in the −1 subsite.

When acting on chitosan, the hydrolytic rate of ChiA-W167A decreases relatively rapidly [11], which is likely due to the reduced ability to cleave partly deacetylated substrates demonstrated above. As a final check of the role of Trp167 in substrate binding and positioning, we analyzed products obtained after degrading a chitosan with a degree of acetylation of 66% with ChiA-WT or ChiA-W167A, to a maximum degree of scission [11]. An impression of product sequences was obtained by sequencing the DP5 product fraction using reducing end labeling and MALDI-TOF-TOF-MS/MS analysis [26]. The results, depicted in Table 1, reveal a clear preference for an acelytated unit in subsites −4 and −2, in addition to the absolute preference in −1, for ChiA-WT while the ChiA-W167 mutant has no strong preferences. Such preferences are likely central in recognizing and orienting the *N*-acetyl groups before the −1 subsite.

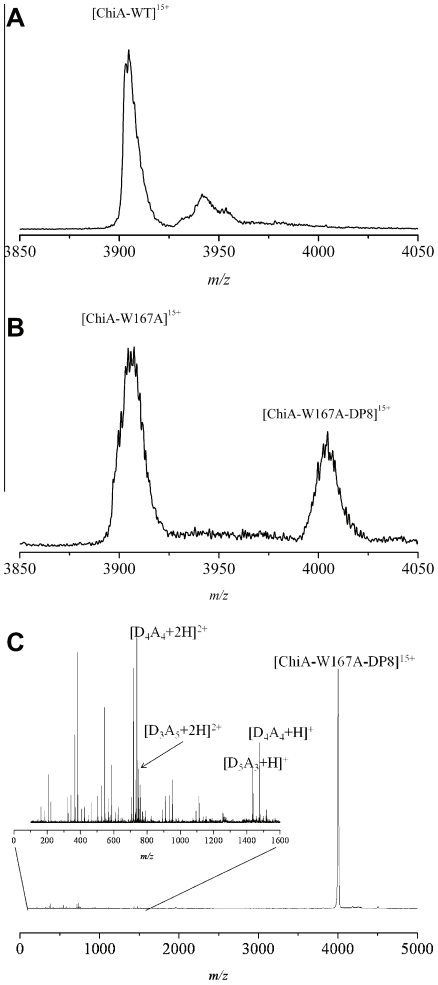

Fig. 3. Nano-ESI-q-TOF spectra of reaction mixtures obtained after incubating a CHOS-DP8 mixture (60 μM, F_A = 0.50) with ChiA variants (5 μM) for 60 min at room temperature. Panel A shows the results after incubating the DP8 material with ChiA-WT; the spectrum displays the free enzyme and a broad peak corresponding to ChiA-WT binding to hydrolysis products. There is no signal for a complex of ChiA-WT with DP8 CHOS. Panel B shows the results after incubating the DP8 material with ChiA-W167A and displays two dominating signals. Deconvolution yielded a molecular weight of 58 434 ± 3 Da for the free enzyme (theoretical value 58 435 Da) and an average mass of 60 088 ± 3 Da (theoretical value for the enzyme complexed to CHOS DP8 with an F_A 0.5 would be 60 035 Da). The latter complexes (at *m*/*z* 4005.89) were subjected to collision-induced dissociation and the resulting MS/MS spectrum showed all three types of DP8 oligomers present in the original mixture, D_4A_4, D_3A_5 and D_5A_3, were bound to the enzyme (Panel C).

In addition to aromatic stackings, there are other important intermolecular interactions in subsites −4, −3, and −2 (Fig. 4). Arg172 and Gly171 interact with the carbonyl oxygen while Ser210, and to a lesser extent Glu208 and His229, interact with O6 subsite −4. In subsite −3, there is a hydrogen bond between Thr276 and the carbonyl oxygen in addition to a hydrophobic interaction between the methyl of the *N*-acetyl group with Leu277 and His229. Moreover, there is a bifurcated hydrogen bond between Arg172 and Glu473 with O6. In subsite −2, Trp 275 and

Table 1
Sequence determination of CHOS of DP = 5 obtained after hydrolysis of chitosan (F_A 0.66) with ChiA-WT and ChiA-W167A to a maximum degree of scission [11].

CHOS	m/z	CHOS	Sequence	
			WT	W167A
Pentamer	1124.252	D3A2	–	DADDA-▲
			–	DDDAA-▲
	1166.265	D2A3	DADAA-▲	ADADA-▲
			–	ADDAA-▲
			–	DDAAA-▲
	1208.269	D1A4	AADAA-▲	ADAAA-▲

▲ represents the reducing end tag.

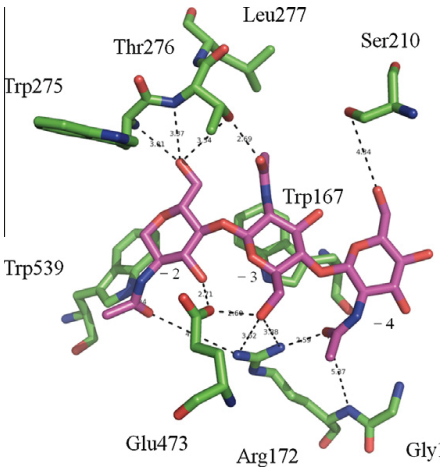

Fig. 4. Crystal structure of the active site of ChiA (1ehn) [35] highlighting non-aromatic interactions in subsites –4, –2, and –2 that are likely to be important in the recognizing and orientation of *N*-acetyl groups.

Thr276 hydrogen bonds with O6 via the backbone while Trp275 forms a hydrogen bond with O6 through the side chain as well. Trp539 and Arg172 interact with the carbonyl oxygen and there is an interaction Glu473 with O3. Arg172 and Glu473 are especially interesting since these interact with several GlcNAc moieties, all three and the –2 and –3, respectively, and that they can form strong electrostatic – dipole interactions. The removal of Trp^{167} may result in an increase in protein dynamics, and hence disruptions of the interactions discussed above that are responsible for substrate positioning, as there is no longer a fixing of the protein backbone through the stacking with the GlcNAc moiety in the –3 subsite. Support for this is the 5 cal/K mol increase in entropy change when allosamidin binds to ChiA-W167A compared to ChiA-WT [21]. It has been observed through NMR and ITC measurements that when the distance of the protein backbone and the ligand is extended, the entropy change rises due to an increase in protein dynamics [31–33].

4. Concluding remarks

Our results show that there is considerable substrate-binding affinity in what could be called a +3 subsite. This affinity may contribute to ChiA's endo-activity. Endo-enzymes have typically open active site clefts [5], while ChiA takes advantage of a deep substrate cleft to degrade chitin in exo-processive manner [6,17]. Substrate-association is the rate-limiting step in enzymatic degradation of chitin [3], and it is quite conceivable that the most challenging binding mode of all, namely binding in an endo-fashion for a typical exo-enzyme, depends on the presence of binding affinities beyond both the −2 and the +2 subsites where there will be less steric hindrance. Being able to hydrolyze chitin in an endo-manner increases the enzymes number of possible binding sites on a polymer dramatically. The affinity in the +3 subsite may also assist in expelling dimeric products from the +1 and +2 subsites during processive hydrolysis.

Trp^{167} in the –3 subsite is a strong binding residue and it appears that its stacking to the substrate rigidifies the protein backbone supporting the formation of the intermolecular interaction network between enzyme and substrate that is necessary for the recognition and positioning of the *N*-acetyl groups before the –1 subsite were these takes part in the substrate assisted hydrolysis of the substrate. Moreover, Trp^{167} also seems crucial for providing the binding energy that is needed to promote energetically unfavorable binding of an acetylated sugar in the –1 subsite for partially deacetylated substrates. The results also suggest that Trp^{167} is important for recruiting substrates to the catalytic center, in line with what has been suggested for a similar residue (Trp^{48}) in the family 18 chitinase Chit-42 of *Trichoderma harzianum* [34].

Acknowledgments

This work was supported by grants 164653/V40, 140497/I30 and 177542/V30 from the Norwegian Research Council.

Appendix A. Supplementary data

Supplementary data associated with this article can be found, in the online version, at doi:10.1016/j.febslet.2011.06.002.

References

[1] Kurita, K. (2006) Chitin and chitosan: functional biopolymers from marine crustaceans. Mar. Biotechnol. 8, 203–226.
[2] Henrissat, B. and Davies, G.J. (1997) Structural and sequence-based classification of glycoside hydrolases. Curr. Opin. Struct. Biol. 7, 637–644.
[3] Zakariassen, H., Eijsink, V.G.H. and Sørlie, M. (2010) Signatures of activation parameters reveal substrate-dependent rate determining steps in polysaccharide turnover by a family 18 chitinase. Carbohyd. Polym. 81, 14–20.
[4] Beckham, G.T. and Crowley, M.F. (2011) Examination of the α-chitin structure and decrystallization thermodynamics at the nanoscale. J. Phys. Chem. B. 115, 4516–4522.
[5] Davies, G. and Henrissat, B. (1995) Structures and mechanisms of glycosyl hydrolases. Structure 3, 853–859.
[6] Hult, E.L., Katouno, F., Uchiyama, T., Watanabe, T. and Sugiyama, J. (2005) Molecular directionality in crystalline beta-chitin: hydrolysis by chitinases A and B from Serratia marcescens 2170. Biochem. J. 388, 851–856.
[7] Sikorski, P., Sørbotten, A., Horn, S.J., Eijsink, V.G.H. and Vårum, K.M. (2006) Serratia marcescens chitinases with tunnel-shaped substrate-binding grooves show endo activity and different degrees of processivity during enzymatic hydrolysis of chitosan. Biochemistry 45, 9566–9574.
[8] Katouno, F., Taguchi, M., Sakurai, K., Uchiyama, T., Nikaidou, N., Nonaka, T., Sugiyama, J. and Watanabe, T. (2004) Importance of exposed aromatic residues in chitinase B from Serratia marcescens 2170 for crystalline chitin hydrolysis. J. Biochem. 136, 163–168.
[9] Uchiyama, T., Katouno, F., Nikaidou, N., Nonaka, T., Sugiyama, J. and Watanabe, T. (2001) Roles of the exposed aromatic residues in crystalline chitin hydrolysis by chitinase a from Serratia marcescens 2170. J. Biol. Chem. 276, 41343–41349.
[10] Horn, S.J. et al. (2006) Costs and benefits of processivity in enzymatic degradation of recalcitrant polysaccharides. Proc. Natl. Acad. Sci. USA 103, 18089–18094.
[11] Zakariassen, H., Aam, B.B., Horn, S.J., Vårum, K.M., Sørlie, M. and Eijsink, V.G.H. (2009) Aromatic residues in the catalytic center of chitinase A from *Serratia marcescens* affect processivity, enzyme activity, and biomass converting efficiency. J. Biol. Chem. 284, 10610–10617.
[12] Watanabe, T. et al. (2003) Aromatic residues within the substrate-binding cleft of Bacillus circulans chitinase A1 are essential for hydrolysis of crystalline chitin. Biochem. J. 376, 237–244.
[13] Hu, G.H., Oguro, A., Li, C.Z., Gershon, P.D. and Quiocho, F.A. (2002) The "cap-binding slot" of an mRNA cap-binding protein: Quantitative effects of

aromatic side chain choice in the double-stacking sandwich with cap. Biochemistry 41, 7677–7687.
[14] Quiocho, F.A. (1989) Protein–carbohydrate interactions – basic molecular-features. Pure Appl. Chem. 61, 1293–1306.
[15] Watanabe, T., Ishibashi, A., Ariga, Y., Hashimoto, M., Nikaidou, N., Sugiyama, J., Matsumoto, T. and Nonaka, T. (2001) Trp122 and Trp134 on the surface of the catalytic domain are essential for crystalline chitin hydrolysis by Bacillus circulans chitinase A1. FEBS Lett. 494, 74–78.
[16] Varrot, A., Frandsen, T.P., von Ossowski, I., Boyer, V., Cottaz, S., Driguez, H., Schulein, M. and Davies, G.J. (2003) Structural basis for ligand binding and processivity in cellobiohydrolase Cel6A from Humicola insolens. Structure 11, 855–864.
[17] Horn, S.J., Sørbotten, A., Synstad, B., Sikorski, P., Sørlie, M., Vårum, K.M. and Eijsink, V.G.H. (2006) Endo/exo mechanism and processivity of family 18 chitinases produced by Serratia marcescens. FEBS J. 273, 491–503.
[18] Papanikolau, Y., Prag, G., Tavlas, G., Vorgias, C.E., Oppenheim, A.B. and Petratos, K. (2001) High resolution structural analyses of mutant chitinase A complexes with substrates provide new insight into the mechanism of catalysis. Biochemistry 40, 11338–11343.
[19] Aronson, N.N., Halloran, B.A., Alexyev, M.F., Amable, L., Madura, J.D., Pasupulati, L., Worth, C. and Van Roey, P. (2003) Family 18 chitinase-oligosaccharide substrate interaction: subsite preference and anomer selectivity of Serratia marcescens chitinase A. Biochem. J. 376, 87–95.
[20] Horn, S.J., Sørlie, M., Vaaje-Kolstad, G., Norberg, A.L., Synstad, B., Vårum, K.M. and Eijsink, V.G.H. (2006) Comparative studies of chitinases A, B and C from Serratia marcescens. Biocatal. Biotrans. 24, 39–53.
[21] Baban, J., Fjeld, S., Sakuda, S., Eijsink, V.G.H. and Sørlie, M. (2010) The roles of three serratia marcescens chitinases in chitin conversion are reflected in different thermodynamic signatures of allosamidin binding. J. Phys. Chem. B 114, 6144–6149.
[22] Heggset, E.B., Dybvik, A.I., Hoell, I.A., Norberg, A.L., Sørlie, M., Eijsink, V.G.H. and Vårum, K.M. (2010) Degradation of chitosans with a family 46 chitosanase from Streptomyces coelicolor A3(2). Biomacromolecules 11, 2487–2497.
[23] Sannan, T., Kurita, K. and Iwakura, Y. (1976) Studies on chitin: 2. Effect of deacetylation on solubility. Makromol. Chem. 177, 3589–3600.
[24] Sørbotten, A., Horn, S.J., Eijsink, V.G.H. and Vårum, K.M. (2005) Degradation of chitosans with chitinase B from Serratia marcescens. Production of chito-oligosaccharides and insight into enzyme processivity. FEBS J. 272, 538–549.
[25] Cederkvist, F.H., Zamfir, A.D., Bahrke, S., Eijsink, V.G.H., Sørlie, M., Peter-Katalinicï, J. and Peter, M.G. (2006) Identification of a high-affinity-binding oligosaccharide by (+) nanoelectrospray quadrupole time-of-flight tandem mass spectrometry of a noncovalent enzyme-ligand complex. Angew. Chem. Int. Ed. Engl. 45, 2429–2434.
[26] Bahrke, S., Einarsson, J.M., Gislason, J., Haebel, S., Letzel, M.C., Peter-Katalinic, J. and Peter, M.G. (2002) Sequence analysis of chitooligosaccharides by matrix-assisted laser desorption ionization postsource decay mass spectrometry. Biomacromolecules 3, 696–704.
[27] Cederkvist, F.H., Parmer, M.P., Vårum, K.M., Eijsink, V.G.H. and Sørlie, M. (2008) Inhibition of a family 18 chitinase by chitooligosaccharides. Carbohyd. Polym. 74, 41–49.
[28] Krokeide, I.M., Synstad, B., Gåseidnes, S., Horn, S.J., Eijsink, V.G.H. and Sørlie, M. (2007) Natural substrate assay for chitinases using high-performance liquid chromatography: a comparison with existing assays. Anal. Biochem. 363, 128–134.
[29] Brurberg, M.B., Nes, I.F. and Eijsink, V.G.H. (1996) Comparative studies of chitinases A and B from Serratia marcescens. Microbiology 142, 1581–1589.
[30] Tews, I., Terwisscha van Scheltinga, A.C., Perrakis, A., Wilson, K.S. and Dijkstra, B.W. (1997) Substrate-assisted catalysis unifies two families of chitinolytic enzymes. J. Am. Chem. Soc. 119, 7954–7959.
[31] Krishnamurthy, V.M., Bohall, B.R., Semetey, V. and Whitesides, G.M. (2006) The paradoxical thermodynamic basis for the interaction of ethylene glycol, glycine, and sarcosine chains with bovine carbonic anhydrase II: an unexpected manifestation of enthalpy/entropy compensation. J. Am. Chem. Soc. 128, 5802–5812.
[32] Krishnamurthy, V.M., Kaufman, G.K., Urbach, A.R., Gitlin, I., Gudiksen, K.L., Weibel, D.B. and Whitesides, G.M. (2008) Carbonic anhydrase as a model for biophysical and physical-organic studies of proteins and protein–ligand binding. Chem. Rev. 108, 946–1051.
[33] Stückmann, H., Bronowska, A., Syme, N.R., Thompson, G.S., Kalverda, A.P., Warriner, S.L. and Homans, S.W. (2008) Residual ligand entropy in the binding of p-substituted benzenesulfonamide ligands to bovine carbonic anhydrase II. J. Am. Chem. Soc. 130, 12420–12426.
[34] Lienemann, M., Boer, H., Paananen, A., Cottaz, S. and Koivula, A. (2009) Towards understanding of carbohydrate binding and substrate specificity of a glycosyl hydrolase 18 family (GH-18) chitinase from Trichoderma harzianum. Glycobiology 19, 1116–1126.
[35] Papanikolau, Y., Prag, G., Tavlas, G., Vorgias, C.E., Oppenheim, A.B. and Petratos, K. (2001) High resolution structural analyses of mutant chitinase A complexes with substrates provide new insight into the mechanism of catalysis. Biochemistry-US 40, 11338–11343.
[36] van Aalten, D.M.F., Komander, D., Synstad, B., Gåseidnes, S., Peter, M.G. and Eijsink, V.G.H. (2001) Structural insights into the catalytic mechanism of a family 18 exo-chitinase. Proc. Natl. Acad. Sci. USA 98, 8979–8984.

PAPER IV

The Action of the Human Chitotriosidase on Chitosan

Kristine Bistrup Eide[a], Anne Line Norberg[a], Ellinor Bævre Heggset[b], Anne Rita Lindbom[a], Kjell Morten Vårum[b], Vincent G.H. Eijsink[a] and Morten Sørlie[a,*]

[a]*Department of Chemistry, Biotechnology and Food Science, Norwegian University of Life Sciences, PO Box 5003, N-1432 Ås, Norway.*

[b]*Department of Biotechnology, Norwegian University of Science and Technology, Trondheim, Norway.*

*Corresponding author: Tel: +47 64965902; fax: 47 64965901; e-mail: morten.sorlie@umb.no

ABSTRACT

Chitotriosidase (HCHT) is one of two family 18 chitinases produced by humans, the other being acidic mammalian chitinase (AMCase). The enzyme is thought to be part of the human defense mechanism against fungal parasites but its precise role and the details of its enzymatic properties have not yet been fully unraveled. We have studied properties of HCHT by analyzing how the enzyme acts on high molecular-weight chitosans, soluble co-polymers of β-(1, 4)-linked *N*-acetylglucosamine (GlcNAc, A) and glucosamine (GlcN, D). Using methods that have previously been used previously for in-depth studies of the chitinolytic machinery of bacterial family 18 enzymes, we show that HCHT degrades chitosan primarily via an endo-processive mechanism, as would be expected on the structural features of its substrate-binding cleft. The preferences of HCHT subsites for acetylated versus non-acetylated sugars were assessed by sequence analysis of obtained oligomeric products showing a very strong, absolute, and a relative weak preference for an acetylated unit in the –2, –1, +1 subsite, respectively. The latter information is important for the design of inhibitors that are specific for the human chitinases and also provide insight into what kind of products may be formed *in vivo* upon administration of chitosan-containing medicines or food products.

Keywords: Human chitinase; chitosan; chitin; processivity; chitotriosidase.

1. Introduction

Chitin, an insoluble linear polysaccharide consisting of repeated units of β-1,4-*N*-linked acetylgucosamine [$(GlcNAc)_n$], is common as a structural polymer in crustaceans, arthropods, fungi, and parasitic nematodes. The metabolism of chitin in nature is controlled by enzymatic systems that produce and break down chitin, primarily chitin synthases and chitinases, respectively. Chitinases are thought to play important roles in anti-parasite responses in several life forms, including humans (Herrera-Estrella & Chet, 1999; Palli & Retnakaran, 1999; Shibata, Foster, Metzger & Myrvik, 1997; van Eijk et al., 2005). Even though chitin and chitin synthases have not been found in humans, we produce two active chitinases that are categorized as family 18 chitinases based on sequence-based classification of glycoside hydrolases (Henrissat & Davies, 1997). These two enzymes are called acidic mammalian chitinase (AMCase) (Boot et al., 2001) and human chitotriosidase (HCHT) (Renkema, Boot, Muijsers, Donker-Koopman & Aerts, 1995) and both are believed to play roles in anti-parasite responses (Elias, Homer, Hamid & Lee, 2005; Herrera-Estrella, 1999; Van Eijk, Scheij, Van Roomen, Speijer, Boot & Aerts, 2007). While AMCase is found in the stomach (Boot et al., 2001), in tears (Musumeci, Bellin, Maltese, Aragona, Bucolo & Musumeci, 2008), sinus mucosa (Ramanathan, Lee & Lane, 2006), and lungs (Zhu et al., 2004), HCHT is primarily expressed in activated human macrophages (Hollak, Vanweely, Vanoers & Aerts, 1994).

HCHT is up-regulated in a series of diseases and medical conditions such as Gaucher's disease (Hollak, Vanweely, Vanoers & Aerts, 1994), sarcoidosis

(Bargagli et al., 2007; Brunner, Scholl-Burgi & Zimmerhackl, 2007), cardiovascular risk (Artieda et al., 2007), coronary artery disease (Karadag, Kucur, Isman, Hacibekiroglu & Vural, 2008), primary prostate cancer and benign prostatic hyperplasia (Kucur et al., 2008), nonalcoholic steatohepatitis (Malaguarnera, Rosa, Zambito, dell'Ombra, Marco & Malaguarnera, 2006), and Niemann-Pick disease (Wajner et al., 2004). The only currently known physiological implications of the elevated HCHT levels are a better defense against chitin-containing pathogens (van Eijk et al., 2005) and the triggering of human macrophage activation by HCHT-mediated chitin and chitosan degradation (Gorzelanny, Poppelmann, Pappelbaum, Moerschbacher & Schneider, 2010).

HCHT is synthesized and secreted as a 50-kDa protein in human macrophages. A considerable portion of produced enzyme is routed to lysosomes and processed into a 39-kDa isoform, lacking the C-terminal chitin binding domain (Renkema et al., 1997). The 39 kDa catalytic domain comprises a $(\beta/\alpha)_8$ barrel with a so called α/β insertion domain that contributes to endorsing the enzyme with a deep catalytic cleft (Fusetti et al., 2002) (Fig. 1B). The catalytic acid, Glu-140, is located at the end of the conserved DxxDxDxE motif that includes strand β4 of the $(\beta/\alpha)_8$ barrel. The substrate-binding cleft of HCHT extends over one face of the enzyme and is lined with solvent exposed aromatic residues (Fig 1B.) (Fusetti et al., 2002). Whereas some chitinases with such deep clefts have long loops that form a "roof" over the substrate-binding cleft (van Aalten, Komander, Synstad, Gåseidnes, Peter & Eijsink, 2001; van Aalten et al., 2000), such a "roof" is absent in HCHT (Fig. 1).

Family 18 chitinases employ a substrate-assisted catalytic mechanism in which the *N*-acetyl group of the sugar bound in the –1 subsite (Synstad, Gåseidnes, van Aalten, Vriend, Nielsen & Eijsink, 2004; Terwisscha van Scheltinga, Armand, Kalk, Isogai, Henrissat & Dijkstra, 1995; Tews, Terwisscha van Scheltinga, Perrakis, Wilson & Dijkstra, 1997; van Aalten, Komander, Synstad, Gåseidnes, Peter & Eijsink, 2001). Because of this, family 18 chitinases have an absolute preference for acetylated units in the –1 subsite. This may be exploited in the design of inhibitors based on partially acetylated chito-oligosaccharides (CHOS). CHOS whose preferred binding mode places a deacetylated unit in subsite –1 will bind non-productively, and hence serve as an inhibitor (Cederkvist, Parmer, Vårum, Eijsink & Sørlie, 2008). CHOS bear great promise as building blocks for chitinase inhibitors, because they are natural products and potentially highly selective (Aam, Heggset, Norberg, Sørlie, Vårum & Eijsink, 2010).

While family 18 chitinases share this special catalytic mechanism, family members may differ in many other aspects. One variable concerns their tendency to cleave the polymeric substrate at chain ends (exo-action) or at random positions (endo-action). Both modes of action may occur in combination with processivity, which implies that the enzyme remains attached to the substrate in between subsequent hydrolytic reactions (Rouvinen, Bergfors, Teeri, Knowles & Jones, 1990). Another variable within the family 18 chitinases concerns the binding affinities and selectivity of their individual subsites. To analyze these characteristics, studies on the degradation of chitosan, the water soluble partially deacetylated polymeric chitin analogue, have shown to be useful (Horn et al., 2006a; Horn et al.,

2006b; Sikorski, Sørbotten, Horn, Eijsink & Vårum, 2006; Sørbotten, Horn, Eijsink & Vårum, 2005).

Being a part of the innate immune system and associated with so many diseases, detailed knowledge of the mechanistic properties of HCHT is of great interest. Several studies of the properties of HCHT have appeared in the literature (Boot, Renkema, Strijland, van Zonneveld & Aerts, 1995; Gorzelanny, Poppelmann, Pappelbaum, Moerschbacher & Schneider, 2010; van Eijk et al., 2005), but issues related to the mode of action and subsite-binding preferences have so far received limited attention. Insight in subsite-binding preferences is particularly important because inhibition of human chitinases is of medical interest. Inhibition of AMCase has been suggested as a therapeutic strategy against asthma (Zhu et al., 2004), while there is no evidence that inhibition of HCHT will be beneficial. In fact, due to the beneficial fungistatic effect of HCHT, inhibition of this enzyme could be unfavorable. Thus, there is a need to develop inhibitors that are selective for AMCase, and to do so, insight in the binding preferences of both AMCase and HCHT is required. Here, we describe novel insights into the enzymatic properties of HCHT derived from an in-depth analysis of HCHT action on chitosan.

2. Materials and Methods

2.1. Materials.

Chitin was isolated from shrimp shells as described previously (Hackman, 1954) and milled in a hammer mill to pass through a 0.1 mm sieve. Chitosans with different fractions of *N*-acetylated units (F_A) were prepared by homogenous de-*N*-acetylation of chitin (Sannan, Kurita & Iwakura, 1976). The characteristics of the chitosans used in this study are given in Table 1. ChiB was purified as described previously (Brurberg, Eijsink, Haandrikman, Venema & Nes, 1995).

2.2. HCHT expression and purification.

Pichia pastoris Cells expressing the 39 kDa form of HCHT (REF) were grown in 100 mL buffered glycerol-complex (BMGY) medium at 28 ºC for 24 hours and 10 mL of this culture was used to inoculate 500 mL fresh BMGY. After incubation for 48 hours at 30 ºC and 200 rpm, cells were harvested through centrifugation at 3500 rpm for 30 min at 20 ºC. Subsequently, pellets were resuspended in 500 mL fresh BMGY and incubated for additional 120 hours at 30 ºC and 200 rpm. Every 24 hour 5 mL of high quality methanol were added to the culture. After 4 additions of methanol, cells were harvested through centrifugation for 30 minutes at 3500 rpm and 20 ºC. HCHT is secreted into the culture medium and is present in the supernatant after centrifugation. The supernatant was filtered through a 0.22 µm filter and concentrated using a Vivaflow 200 PES, 10 000 MWCO, until a total volume of 30-50 mL. Concentrated supernatant was dialysed against 50 mM sodium acetate pH 4.2 at 4 ºC for 72 hours in order to get rid of components from the medium. HCHT was then purified using ion exchange

chromatography with a HiTrap CM FF 5 mL column (GE Healthcare), using 50 mM sodium acetate pH 4.2 as running buffer and a flow of 5 mL/min. The protein was eluted from the column by applying a linear gradient to 100% 50 mM sodium acetate pH 6.5 over 20 column volumes, and detected using UV-detection. The contents of the collected fractions were analyzed using SDS-PAGE. Fractions containing HCHT were pooled and concentrated to approximately 2mg/mL by centrifugation at 4000 rpm for approximately 20 minutes in Amicon centrifuge tubes 10 000 MWCO. Enzyme purity was analyzed by SDS-PAGE and found to be over 95% in all cases (Fig. S1). Protein concentrations were determined by using the Quant-It protein assay kit and a Qubit fluorometer from invitrogen (CA, USA).

2.3. Degradation of high molecular mass chitosan with F_A = 0.62, F_A = 0.49, F_A = 0.35 and F_A = 0.18.

Chitosan was dissolved in 80 mM sodium acetate buffer pH 5.5 to a final concentration of 10 $mgmL^{-1}$ as described previously (Sørbotten, Horn, Eijsink & Vårum, 2005). Chitosan with F_A = 0.62 was depolymerized by adding 0.075 μg HCHT pr mg chitosan. Samples were taken at various time points between 2.5 and 12960 minutes after starting the reaction and enzyme activity was stopped by adjusting the pH to 2.5 with 5 M HCl followed by boiling for 2 minutes (Sørbotten, Horn, Eijsink & Vårum, 2005). Chitosans with F_A = 0.49, 0.35 or 0.18 were depolymerized (as described above) to a maximum degree of scission (α). The degree of scission was determined by NMR (see below) and was considered

maximal after it had been established that addition of fresh enzyme to the reaction mixtures did not yield a further increase in the degree of scission.

2.4. Size exclusion chromatography of chitosan oligomers.

Oligomers produced from the enzymatic depolymerization of chitosan were separated on three columns packed with Superdex^{TM} 30 from GE Healthcare, coupled in series (overall dimensions 2.60 x 180 cm), as described previously (Sørbotten, Horn, Eijsink & Vårum, 2005). Fractions of 4 mL were collected for further analyses of the depolymerization products. Using this method, oligomers are separated by DP only, except for oligomers with the lower DPs (< DP = 5), where there also is some separation according to sugar composition; see results section and (Sørbotten, Horn, Eijsink & Vårum, 2005).

2.5. 2-Aminoacridone derivatization and sequence determination of chito-oligosaccharides.

In order to determine the sequence of chitosan oligomers, the oligosaccharides were derivatized by reductive amination of the reducing end with 2-aminoacridone (AMAC), as described previously (Bahrke et al., 2002; Cederkvist, Parmer, Vårum, Eijsink & Sørlie, 2008). Sequencing of chitosan oligomers was performed using MALDI-TOF/TOF mass spectrometry as described earlier (Cederkvist, Parmer, Vårum, Eijsink & Sørlie, 2008).

2.6. Nuclear Magnetic Resonance spectroscopy.

Samples from enzymatically depolymerized chitosan were freeze dried and solved in D_2O, after which the pD was adjusted to 4.2 using DCl. The ^{1}H-NMR spectra were obtained at 85 ºC at 300 mHz (Oxford NMR^{300}, Varian) (Smidsrød, Vårum, Grasdalen & Anthonsen, 1991; Vårum, Holme, Izume, Stokke & Smidsrød, 1996). The deuterium resonance was used as a field-frequency lock, and the chemical shifts were referenced to internal sodium 3-(trimethylsilyl)propionate-d4 (0.00 p.p.m.). The ^{1}H-NMR spectra were used to determine the degree of scission, α, as described previously (Sørbotten, Horn, Eijsink & Vårum, 2005).

2.7. Simultaneous determination of relative viscosity and reducing ends.

Chitosan with an F_A of 0.62 was dissolved to a final concentration of 1 mgmL^{-1} in 40 mM acetate buffer pH 5.4 containing 0.1 M NaCl. HCHT was added to a final concentration of 10 ngmL^{-1}. Determination of the relative viscosity of the polymer solution and determination of the total number of reducing ends using the MBTH method (Horn & Eijsink, 2004) were performed as described previously (Sikorski, Sørbotten, Horn, Eijsink & Vårum, 2006).

2.8. Matrix assisted laser desorption/ionization mass spectrometry.

MS spectra were acquired using an UltraflexTM TOF/TOF mass spectrometer (Bruker Daltonik GmbH, Bremen, Germany) with gridless ion optics under control of Flexcontrol 4.1. For sample preparation, 1 µl of the reaction products was mixed with 1 µl 10% 2,5-Dihydroxybenzoic acid (DHB) in 30% ethanol and spotted onto a MALDI target plate. The MS experiments were conducted using an accelerating potential of 20 kV in the reflectron mode.

3. Results and discussion

3.1 Degradation of high molecular mass chitosans with HCHT; subsite-preferences.

High molecular chitosan (M_r = 140 000) with F_A 0.62 was degraded with HCHT to different degrees of scission, indicated by α, the fraction of glycosidic linkages that has been cleaved by the enzyme. The degree of scission at any time point of the reaction was determined by monitoring the increase in reducing end resonances relative to resonances from internal protons in a ^{1}H-NMR spectrum of the reaction mixture (Sørbotten, Horn, Eijsink & Vårum, 2005). Fig. 2 shows the time course for the reaction and reveals tri-phasic kinetics. The initial phase of hydrolysis continues to an α-value of approximately 0.05 with an apparent rate constant (k_{cat}^{app}) of 86 s^{-1}. The second kinetic phase, in the α range from 0.05 to 0.13, shows an 8-fold decrease in the apparent rate constant (k_{cat}^{app} = 11 s^{-1}), whereas the final kinetic phase shows another 2 – 3-fold reduction (k_{cat}^{app} 4 s^{-1}). This latter phase

253 continues until the degree of scission reaches 0.33, which is the observed maximum
254 α value.
255 Fig. 3 shows chromatograms for SEC of the reaction mixtures obtained
256 after HCHT degradation of chitosan with F_A of 0.62 to α = 0.03, 0.08, and 0.13; Fig.
257 4A shows a chromatogram for α = 0.33. High molecular chitosan (DP >40) is eluted
258 in the void peak at approximately 550 minutes, while chitosan oligomers are eluted
259 in separate peaks from 700-1200 minutes. Generally, oligomers are separated by DP
260 only, but at low DP some separation according to sugar composition (acetylated, A,
261 versus deacetylated, D) is observed as indicated in Fig. 3. The DP3 to DP6 fractions
262 were subjected to sequence analysis and the results are shown in Table 2. The
263 reducing ends of the observed products reflect binding preferences in the – subsites,
264 whereas the non-reducing ends of the products reflect binding preferences in the +
265 subsites. The combining the data of Fig. 3 with the sequence data of Table 2 shows
266 that early on in the reaction cleavage almost exclusively occurs in the sequence **AA-**
267 **A** bound to subsites -2 to +1. Almost all products have **AA** on their reducing ends in
268 all phases of hydrolysis indicating that there is a strong preference for an acetylated
269 unit in the –2 subsite. Products ending at **–DA** were observed in the dimer and trimer
270 fractions, at the very end of the reaction only (Fig. 4A, Table 2). Significant amounts
271 of products with a **D** at the non-reducing end appear earlier in the reaction indicating
272 that the preference for an acetylated unit in the +1 subsite is not as strong as in the –
273 2 subsite. These preferences may help to explain the multiphasic kinetic behavior
274 described above (Fig. 2). As the hydrolysis reaction progresses, the reaction will
275 slow down because optimal cleavage sites, containing the **AA-A** stretch as well as

perhaps adjacent sequence features that cannot be resolved from the present data, will decrease.

Three other high molecular mass chitosans with F_A of 0.49, 0.35, and 0.18 were also incubated with HCHT and extensively depolymerized to maximum α. As expected based on the clear preferences for acetylated units discussed above, the size distribution of the product mixtures shifted towards higher oligomer lengths and the maximum α became lower for substrates with lower F_A values (Fig. 4). It has previously been shown that chitinases that use aromatic side chains to interact with their substrate are more "tolerant" for deacetylation than chitinases that primarily bind the substrate through specific hydrogen bonds involving polar side chains (Heggset, Hoell, Kristoffersen, Eijsink & Vårum, 2009). This is due to the fact that aromatic residues stack with the hydrophobic faces of the sugars, an interaction type that is less specific than hydrogen bonds that may involve the *N*-acetyl groups. Clearly, both the structural data shown in Fig. 1 and the observations displayed in Fig. 4 show that HCHT belongs to the former category. The ability of HCHT to degrade chitosans with low F_A should be noted, since such chitosans have several (potential) applications in human food (Synowiecki & Al-Khateeb, 2003).

3.2 Determination of endo/exo mode.

By studying the relative viscosity of the chitosan solution during chitinase-catalyzed hydrolysis, it is possible to determine whether the enzymes act in an endo- or an exo-fashion. Endo-acting enzymes will reduce viscosity much faster than exo-

299 acting enzymes (see (Sikorski, Sørbotten, Horn, Eijsink & Vårum, 2006) for a
300 detailed discussion). Acid hydrolysis of chitosan is used as a model for the endo-
301 mode because this process introduces random cleavages along the polymer chain.
302 Another control for endo-activity is chitinase B (ChiB) from *Serratia marcescens*
303 for which highly detailed studies have shown that endo-type of action is
304 predominant when acting on chitosan. Fig. 5 displays relative viscosity over time for
305 a chitosan solution (F_A = 0.62) hydrolyzed by acid, ChiB, and HCHT. In all three
306 cases relative viscosity was quickly reduced, indicating that HCHT acts in the endo-
307 mode when hydrolyzing chitosan.
308 Fig. 1 shows that HCHT, ChiA and ChiB have relatively deep substrate-
309 binding clefts, a property that is often considered to be indicative of exo-activity
310 and/or processivity (Davies & Henrissat, 1995). Nevertheless all three enzymes were
311 found to predominantly act in an endo-mode when hydrolyzing chitosan (Fig.
312 5;(Sikorski, Sørbotten, Horn, Eijsink & Vårum, 2006)). It should be noted that the
313 enzymes may behave differently when acting on crystalline chitin. For example,
314 there are indications that solid β-chitin fibrils are degraded from the reducing end by
315 ChiA and the non-reducing end by ChiB (Hult, Katouno, Uchiyama, Watanabe &
316 Sugiyama, 2005). Studies with ChiA have shown that substrate association is the
317 rate determining step in the hydrolysis of chitin, whereas product release is rate
318 determining when the substrate is soluble chitosan (Zakariassen, Eijsink & Sørlie,
319 2010). This implies that association to a soluble substrate is much less energetically
320 demanding than association to an insoluble substrate. In the crystalline substrate, the
321 ends of the polysaccharide chains are the most accessible, and are thus likely to be

highly preferred by the enzymes. Soluble substrates have much better accessibility, and the number of potential "internal" binding sites heavily outnumbers the number of chain ends. Thus, endo-activity is likely to become dominant, even for enzymes that have an intrinsic tendency to act in an exo-mode. So far is not known whether HCHT acts in an exo- fashion of chitin. For comparison, enzymes of the ChiC-type (Fig. 1C) have much more open and shallow substrate-binding clefts than HCHT and are considered true endo-acting enzymes.

3.3. Processivity.

ChiA and ChiB (Fig. 1A and 1D) are both processive enzymes that degrade chitin chains in opposite directions, while cleaving off GlcNAc dimers (Horn et al., 2006a; Hult, Katouno, Uchiyama, Watanabe & Sugiyama, 2005; Zakariassen, Aam, Horn, Vårum, Sørlie & Eijsink, 2009). For ChiB, mutational studies have shown that Trp^{97} and Trp^{220} in the +1 and +2 aglycon subsites, respectively, are important for the enzyme's processive action on chitosan (Horn et al., 2006a). ChiA also has aromatic residues at these positions (Trp^{275} & Phe^{396}), but their mutation had only a limited affect on processivity. Instead, processivity in ChiA depends heavily on the presence of Trp^{167} in the –3 glycon subsite (Zakariassen, Aam, Horn, Vårum, Sørlie & Eijsink, 2009). HCHT has an aromatic residue (Trp) in all these three positions and also contains other aromatic residues found in glycon subsites in ChiA. Thus, in terms of the "aromatic signature" of the substrate-binding cleft, HCHT resembles

ChiA. HCHT is expected to be processive and it might seem that the enzyme degrades chains from their reducing ends, as does ChiA.

The degree of processivity of HCHT was assessed by plotting the relative viscosity of the polymer solution from which the α of the polymer fraction, α_{pol}, may be calculated, versus the total number of reducing ends (α_{tot}) (Fig. 6). The inverse of the slopes of the lines shown in Fig. 6 represent the number of cuts (N_{cuts}) per formation of an enzyme-substrate complex (Sikorski, Sørbotten, Horn, Eijsink & Vårum, 2006). The observed number of cuts is expressed as relative number, where N_{cuts} observed for acid hydrolysis is set to 1. The results indicate that HCHT is processive with an average of 2.5 cuts per formation of enzyme-substrate complex during hydrolysis of a chitosan with F_A of 0.62. The same numbers are 9.1 and 3.4 cuts per formation of enzyme-substrate complex for ChiA and ChiB, respectively (Sikorski, Sørbotten, Horn, Eijsink & Vårum, 2006). As a control, the value for ChiB was also determined and found to be 3.6 (Fig. 6) in good accordance with the work of Sikorski *et al*.

Processivity in family 18 chitinases leads to a diagnostic product profile dominated by even-numbered products early on in the reaction with chitosan (Eijsink, Vaaje-Kolstad, Vårum & Horn, 2008; Gorzelanny, Poppelmann, Pappelbaum, Moerschbacher & Schneider, 2010; Sørbotten, Horn, Eijsink & Vårum, 2005). HCHT showed this clear dominance of even-numbered only very early in the reaction (insert in Fig. 3A). The ratio between the size of an even-numbered peak and an odd-number peak may serve for a relative quantification of processivity; in this study, the DP6 and DP7 peaks were used. At α below 0.01 the DP6/DP7 ratio

was about 3, but it rapidly decreased via 1.5 at $\alpha = 0.03$ to about 1.3 at $\alpha = 0.08$ (Fig. 3). For ChiA and ChiB the DP6/DP7 ratios at $\alpha \approx 0.08$ are approximately 4 and 3, respectively (Horn et al., 2006b). The initial dominance of even numbered products for HCHT has also been detected by Gorzelanny et al. (Gorzelanny, Poppelmann, Pappelbaum, Moerschbacher & Schneider, 2010) using a completely different approach based on the use of electrophoresis and MS. Another characteristic feature of endo-acting processive enzymes is the slow disappearance of the polymer peak. This is indeed the case for HCHT, where disappearance of this peak is much slower (at $\alpha > 0.13$, Fig. 3) than for non-processive endo-acting family 18 chitinases such as ChiC from *S. marcescens* where the polymer peak disappears at $\alpha \approx 0.05$ (Horn et al., 2006b). For ChiA and ChiB, the polymer peak disappears at $\alpha \approx 0.20$. The combination of slow disappearance of the polymer peak (Fig. 3) and a clear endo-activity (Fig. 5) coupled with an initial dominance of even-numbered products and an estimated 2.5 cuts per formation of enzyme-substrate suggest that HCHT is processive, albeit possibly to a lesser degree than ChiA and ChiB.

It is conceivable that the analysis of processivity in HCHT to some extent is disturbed by transglycosilation. HCHT is known to have relatively high transglycosilation activity and recent mutational work on ChiA has shown that the introduction of a Trp at position +2 drastically increase transglycosilating activity (Zakariassen, Hansen, Jøranli, Eijsink & Sørlie, 2011). This Trp is naturally present in HCHT, whose active site is highly similar to that of the engineered hypertransglycosilating ChiA mutant. Perhaps, the rapid disappearance of the

dominance of even-numbered products during the course of the reaction is somehow linked to increased occurrence of transglycosilation.

3.4. Concluding remarks

In the present study, we provide insight into how HCHT acts on chitosan, which is useful to understand enzyme properties such as endo- vs exo-action, processivity, and substrate binding preferences. This information is important for further work on understanding the roles of human chitinases, the faith of chitosan-containing food products or medicines, and the development of inhibitors that are specific for certain chitinases. HCHT acts on fungal cell walls (van Eijk et al., 2005) and it is conceivable that its processive mechanism contributes to its fungistatic effect. Association to the insoluble polymer is the rate-determining step in chitin hydrolysis (Zakariassen, Eijsink & Sørlie, 2010) and a processive mode allows for more hydrolytic events to take place upon each association compared to a non-processive mechanism. The ability to bind in an endo-mode may also promote substrate-binding since the enzyme may not be dependent of finding chain ends.

HCHT is called chitotriosidase most likely because in the original studies it was found to release 4-methylumberriuferyl from the artificial substrate 4-methylumbelliferyl-β-D-*N*-*N*'-*N*''-triacetylchitotriose. In retrospect, it is clear that chitinase action of artificial substrates is not a good way to determine the mode of action of these enzymes (Brurberg, Nes & Eijsink, 1996; Krokeide, Synstad, Gåseidnes, Horn, Eijsink & Sørlie, 2007). Also, naming an enzyme that *produces*

chitotriose chitotriosidase is somewhat strange. Regardless of formal considerations, it must be noted that the present data clearly show that the main hydrolysis product is chitobiose, i.e. the A-A- dimer (Fig. 4, F_A = 0.62 experiment). This is fully consistent with HCHT acting as a "normal" processive enzyme. Formally, in analogy with nomenclature used in the cellulose field, it would probably be better to refer to the enzyme as chitobiohydrolase.

Acknowledgments

The *Pichia pastoris* cells producing the 39 kDa form of HCHT gene were a kind gift from Prof. Daan M.F. van Aalten, University of Dundee. This work was supported by Grants 164653/V40, 178428/V40, and 177542/V30 from the Norwegian Research Council.

Reference List

Artieda, M., Cenarro, A., Ganan, A., Lukic, A., Moreno, E., Puzo, J., Pocovi, M., & Civeira, F. (2007). Serum chitotriosidase activity, a marker of activated macrophages, predicts new cardiovascular events independently of C-reactive protein. *Cardiology, 108*(4), 297-306.

Bahrke, S., Einarsson, J. M., Gislason, J., Haebel, S., Letzel, M. C., Peter-Katalinic, J., & Peter, M. G. (2002). Sequence analysis of chitooligosaccharides by matrix-assisted laser desorption ionization postsource decay mass spectrometry. *Biomacromolecules, 3*(4), 696-704.

Bargagli, E., Margollicci, M., Perrone, A., Luddi, A., Perari, M. G., Bianchi, N., Refini, R. M., Grosso, S., Volterrani, L., & Rottoli, P. (2007). Chitotriosidase analysis in bronchoalveolar lavage of patients with sarcoidosis. *Sarcoidosis Vasc. Diff., 24*(1), 59-64.

Berth, G., & Dautzenberg, H. (2002). The degree of acetylation of chitosans and its effect on the chain conformation in aqueous solution. *Carbohydr. Polym., 47*(1), 39-51.

Boot, R. G., Blommaart, E. F. C., Swart, E., Ghauharali-van der Vlugt, K., Bijl, N., Moe, C., Place, A., & Aerts, J. (2001). Identification of a novel acidic mammalian chitinase distinct from chitotriosidase. *J. Biol. Chem., 276*(9), 6770-6778.

Boot, R. G., Renkema, G. H., Strijland, A., van Zonneveld, A. J., & Aerts, J. M. F. G. (1995). Cloning of a cDNA Encoding Chitotriosidase, a Human Chitinase Produced by Macrophages. *J. Biol. Chem., 270*(44), 26252-26256.

Brunner, J., Scholl-Burgi, S., & Zimmerhackl, L. B. (2007). Chitotriosidase as a marker of disease activity in sarcoidosis. *Rheumatol. Int., 27*(12), 1171-1172.

Brurberg, M. B., Eijsink, V. G. H., Haandrikman, A. J., Venema, G., & Nes, I. F. (1995). Chitinase B from Serratia marcescens BJL200 is exported to the periplasm without processing. *Microbiology, 141*, 123-131.

Brurberg, M. B., Nes, I. F., & Eijsink, V. G. H. (1996). Comparative studies of chitinases A and B from Serratia marcescens. *Microbiology, 142*, 1581-1589.

Cederkvist, F. H., Parmer, M. P., Vårum, K. M., Eijsink, V. G. H., & Sørlie, M. (2008). Inhibition of a Family 18 Chitinase by Chitooligosaccharides. *Carbohyd.Polym., 74*, 41-49.

Davies, G., & Henrissat, B. (1995). Structures and mechanisms of glycosyl hydrolases. *Structure, 3*(9), 853-859.

Eijsink, V. G. H., Vaaje-Kolstad, G., Vårum, K. M., & Horn, S. J. (2008). Towards new enzymes for biofuels: lessons from chitinase research. *Trends Biotechnol., 26*(5), 228-235.

Elias, J. A., Homer, R. J., Hamid, Q., & Lee, C. G. (2005). Chitinases and chitinase-like proteins in TH2 inflammation and asthma. *J. Allergy Clin. Immun., 116*(3), 497-500.

Fusetti, F., von Moeller, H., Houston, D., Rozeboom, H. J., Dijkstra, B. W., Boot, R. G., Aerts, J. M. F. G., & van Aalten, D. M. F. (2002). Structure of Human Chitotriosidase. Implications for Specific Inhibitor Design and Function of Mammalian Chitinase-Like Lectins. *J. Biol. Chem., 277*(28), 25537-25544.

Gorzelanny, C., Poppelmann, B., Pappelbaum, K., Moerschbacher, B. M., & Schneider, S. W. (2010). Human macrophage activation triggered by chitotriosidase-mediated chitin and chitosan degradation. *Biomaterials, 31*(33), 8556-8563.

Hackman, R. H. (1954). Studies on chitin. I. Enzymic degradation of chitin and chitin esters. *Aust J Biol Sci, 7*(2), 168-178.

Heggset, E. B., Hoell, I. A., Kristoffersen, M., Eijsink, V. G., & Vårum, K. M. (2009). Degradation of chitosans with chitinase G from Streptomyces coelicolor A3(2): production of chito-oligosaccharides and insight into subsite specificities. *Biomacromolecules, 10*(4), 892-899.

Henrissat, B., & Davies, G. (1997). Structural and sequence-based classification of glycoside hydrolases. *Curr Opin Struct Biol, 7*(5), 637-644.

Herrera-Estrella, A., & Chet, I. (1999). Chitinases in biological control. *EXS, 87*, 171-184.

Herrera-Estrella, A. C., Ilan. (1999). Chitinases in biological control. *Chitin and Chitinases, 87*, 171-184.

Hollak, C. E. M., Vanweely, S., Vanoers, M. H. J., & Aerts, J. (1994). Marked Elevation of Plasma Chitotriosidase Activity - a Novel Hallmark of Gaucher Disease. *J. Clin. Invest., 93*(3), 1288-1292.

Horn, S. J., & Eijsink, V. G. H. (2004). A reliable reducing end assay for chito-oligosaccharides. *Carbohyd.Polym., 56*(1), 35-39.

Horn, S. J., Sikorski, P., Cederkvist, J. B., Vaaje-Kolstad, G., Sørlie, M., Synstad, B., Vriend, G., Vårum, K. M., & Eijsink, V. G. H. (2006a). Costs and benefits of processivity in enzymatic degradation of recalcitrant polysaccharides. *Proc.Natl.Acad.Sci U.S.A, 103*(48), 18089-18094.

Horn, S. J., Sørbotten, A., Synstad, B., Sikorski, P., Sørlie, M., Vårum, K. M., & Eijsink, V. G. H. (2006b). Endo/exo mechanism and processivity of family 18 chitinases produced by Serratia marcescens. *FEBS J., 273*(3), 491-503.

Hult, E. L., Katouno, F., Uchiyama, T., Watanabe, T., & Sugiyama, J. (2005). Molecular directionality in crystalline beta-chitin: hydrolysis by chitinases A and B from Serratia marcescens 2170. *Biochem. J., 388*(Pt 3), 851-856.

Karadag, B., Kucur, M., Isman, F. K., Hacibekiroglu, M., & Vural, V. A. (2008). Serum chitotriosidase activity in patients with coronary artery disease. *Circ. J., 72*(1), 71-75.

Krokeide, I. M., Synstad, B., Gåseidnes, S., Horn, S. J., Eijsink, V. G. H., & Sørlie, M. (2007). Natural substrate assay for chitinases using high-performance liquid chromatography: A comparison with existing assays. *Anal. Biochem., 363*(1), 128-134.

Kucur, M., Isman, F. K., Balci, C., Onal, B., Hacibekiroglu, M., Ozkan, F., & Ozkan, A. (2008). Serum YKL-40 levels and chitotriosidase activity as potential biomarkers in primary prostate cancer and benign prostatic hyperplasia. *Urol. Oncol., 26*(1), 47-52.

Malaguarnera, L., Rosa, M. D., Zambito, A. M., dell'Ombra, N., Marco, R. D., & Malaguarnera, M. (2006). Potential role of chitotriosidase gene in nonalcoholic fatty liver disease evolution. *Am. J. Gastroenterol., 101*(9), 2060-2069.

Musumeci, M., Bellin, M., Maltese, A., Aragona, P., Bucolo, C., & Musumeci, S. (2008). Chitinase levels in the tears of subjects with ocular allergies. *Cornea, 27*(2), 168-173.

Palli, S. R., & Retnakaran, A. (1999). Molecular and biochemical aspects of chitin synthesis inhibition. *EXS, 87*, 85-98.

Perrakis, A., Tews, I., Dauter, Z., Oppenheim, A. B., Chet, I., Wilson, K. S., & Vorgias, C. E. (1994). Crystal structure of a bacterial chitinase at 2.3 A resolution. *Structure., 2*(12), 1169-1180.

Ramanathan, M., Lee, W. K., & Lane, A. P. (2006). Increased expression of acidic mammalian chitinase in chronic rhinosinusitis with nasal polyps. *Am. J. Rhinol., 20*(3), 330-335.

Renkema, G. H., Boot, R. G., Muijsers, A. O., Donker-Koopman, W. E., & Aerts, J. M. F. G. (1995). Purification and Characterization of Human Chitotriosidase, a Novel Member of the Chitinase Family of Proteins. *J. Biol. Chem., 270*(5), 2198-2202.

Renkema, G. H., Boot, R. G., Strijland, A., DonkerKoopman, W. E., vandenBerg, M., Muijsers, A. O., & Aerts, J. (1997). Synthesis, sorting, and processing into distinct isoforms of human macrophage chitotriosidase. *Eur. J. Biochem., 244*(2), 279-285.

Rouvinen, J., Bergfors, T., Teeri, T., Knowles, J. K., & Jones, T. A. (1990). Three-dimensional structure of cellobiohydrolase II from Trichoderma reesei. *Science, 249*(4967), 380-386.

Sannan, T., Kurita, K., & Iwakura, Y. (1976). Studies on chitin, 2‡. Effect of deacetylation on solubility
Macromol. Chem., 177(12), 3589-3600.

Shibata, Y., Foster, L. A., Metzger, W. J., & Myrvik, Q. N. (1997). Alveolar macrophage priming by intravenous administration of chitin particles, polymers of N-acetyl-D-glucosamine, in mice. *Infect.Immun., 65*(5), 1734-1741.

Sikorski, P., Sørbotten, A., Horn, S. J., Eijsink, V. G. H., & Vårum, K. M. (2006). Serratia marcescens chitinases with tunnel-shaped substrate-binding grooves show endo activity and different degrees of processivity during enzymatic hydrolysis of chitosan. *Biochemistry, 45*(31), 9566-9574.

Smidsrød, O., Vårum, K. M., Grasdalen, H., & Anthonsen, M. W. (1991). Determination of the degree of _N-acetylation and the distribution of _N-acetyl groups in partially _N-deacetylated chitins (chitosans) by high-field n.m.r. spectroscopy. S. 17-23.

Synowiecki, J., & Al-Khateeb, N. A. (2003). Production, properties, and some new applications of chitin and its derivatives. *Crit.Rev.Food Sci., 43*(2), 145-171.

Synstad, B., Gåseidnes, S., van Aalten, D. M. F., Vriend, G., Nielsen, J. E., & Eijsink, V. G. H. (2004). Mutational and computational analysis of the role of conserved residues in the active site of a family 18 chitinase. *Eur.J.Biochem., 271*(2), 253-262.

Sørbotten, A., Horn, S. J., Eijsink, V. G. H., & Vårum, K. M. (2005). Degradation of chitosans with chitinase B from Serratia marcescens. Production of chito-oligosaccharides and insight into enzyme processivity. *FEBS J, 272*(2), 538-549.

Terwisscha van Scheltinga, A. C., Armand, S., Kalk, K. H., Isogai, A., Henrissat, B., & Dijkstra, B. W. (1995). Stereochemistry of chitin hydrolysis by a plant chitinase/lysozyme and X-ray structure of a complex with allosamidin: evidence for substrate assisted catalysis. *Biochemistry, 34*(48), 15619-15623.

Tews, I., Terwisscha van Scheltinga, A. C., Perrakis, A., Wilson, K. S., & Dijkstra, B. W. (1997). Substrate-assisted catalysis unifies two families of chitinolytic enzymes. *J. Am. Chem. Soc., 119*(34), 7954-7959.

Uchiyama, T., Katouno, F., Nikaidou, N., Nonaka, T., Sugiyama, J., & Watanabe, T. (2001). Roles of the exposed aromatic residues in crystalline chitin hydrolysis by chitinase a from Serratia marcescens 2170. *J. Biol. Chem., 276*(44), 41343-41349.

Van Eijk, M., Scheij, S., Van Roomen, C., Speijer, D., Boot, R. G., & Aerts, J. M. (2007). TLR- and NOD2-dependent regulation of human phagocyte-specific chitotriosidase. *Febs Lett., 581*(28), 5389-5395.

van Eijk, M., van Roomen, C. P. A. A., Renkema, G. H., Bussink, A. P., Andrews, L., Blommaart, E. F. C., Sugar, A., Verhoeven, A. J., Boot, R. G., & Aerts, J. M. F. G. (2005). Characterization of human phagocyte-derived chitotriosidase, a component of innate immunity. *Int.Immun., 17*(11), 1505-1512.

van Aalten, D. M. F., Komander, D., Synstad, B., Gåseidnes, S., Peter, M. G., & Eijsink, V. G. H. (2001). Structural insights into the catalytic mechanism of a family 18 exo-chitinase. *Proc.Natl.Acad.Sci.U.S.A, 98*(16), 8979-8984.

van Aalten, D. M. F., Synstad, B., Brurberg, M. B., Hough, E., Riise, B. W., Eijsink, V. G. H., & Wierenga, R. K. (2000). Structure of a two-domain chitotriosidase from Serratia marcescens at 1.9-angstrom resolution. *Proc.Natl.Acad.Sci.U.S.A, 97*(11), 5842-5847.

Vårum, K. M., Holme, H. K., Izume, M., Stokke, B. T., & Smidsrød, O. (1996). Determination of enzymatic hydrolysis specificity of partially N-acetylated chitosans. *BBA-Gen. Subjects, 1291*(1), 5-15.

Wajner, A., Michelin, K., Burin, M. G., Pires, R. F., Pereira, M. L. S., Giugliani, R., & Coelho, J. C. (2004). Biochemical characterization of chitotriosidase enzyme: comparison between normal individuals and patients with Graucher and with Niemann-Pick diseases. *Clin. Biochem., 37*(10), 893-897.

Zakariassen, H., Eijsink, V. G. H., & Sørlie, M. (2010). Signatures of activation parameters reveal substrate-dependent rate determining steps in polysaccharide turnover by a family 18 chitinase. *Carbohyd.Polym., 81*(1), 14-20.

Zakariassen, H., Hansen, M. C., Jøranli, M., Eijsink, V. G. H., & Sørlie, M. (2011). Mutational Effects on Transglycosylating Activity of Family 18 Chitinases and Construction of a Hypertransglycosylating Mutant. *Biochemistry, 50*, 5693-5703.

Zakariassen, H., Aam, B. B., Horn, S. J., Vårum, K. M., Sørlie, M., & Eijsink, V. G. H. (2009). Aromatic residues in the catalytic center of chitinase A from *Serratia marcescens* affect processivity, enzyme activity, and biomass converting efficiency. *J Biol.Chem., 284*(16), 10610-10617.

Zhu, Z., Zheng, T., Homer, R. J., Kim, Y. K., Chen, N. Y., Cohn, L., Hamid, Q., & Elias, J. A. (2004). Acidic Mammalian Chitinase in Asthmatic Th2 Inflammation and IL-13 Pathway Activation. *Science, 304*(5677), 1678-1682.

Aam, B. B., Heggset, E. B., Norberg, A. L., Sørlie, M., Vårum, K. M., & Eijsink, V. G. H. (2010). Production of Chitooligosaccharides and Their Potential Applications in Medicine. *Marine Drugs, 8*, 1482-1517.

The abbrevations used are: HCHT, Human Chitotriosidase; AMCase, acidic mammalian chitinase; ChiA, chitinase A from *Serratia marcescens*; ChiB, chitinase B from *Serratia marcescens*; GlcNAc or A, *N*-acetylated glucosamine; D, Glucosamine; CHOS, Chito-oligosaccharides; DP, degree of polymerization; F_A, fraction of acetylated sugar monomers; SEC, Size-exclusion chromatography

Table 1. Characterization of Chitosans[a]

chitosan (F_a)	[η] (mL/g)	MW
0.18	800	257 000
0.35	730	233 000
0.49	746	238 000
0.62	865	280 000

[a] Fraction of acetylated units (F_A), intrinsic viscosities ([η]), and average molecular weight (MW) of the chitosans. The molecular weights were calculated from the intrinsic viscosity vs. molecular weight relationship (Berth & Dautzenberg, 2002).

Table 2.

Sequences of the isolated oligomers of different length obtained after hydrolysis of high molecular chitosan, $F_A = 0.62$, at different degrees of scission.[a]

DP_n	Species	**α = 0.03**	**α = 0.08**	**α = 0.13**	**α = 0.33**
DP3	A3	AAA	AAA	AAA	
	A2D	DAA	DAA	DAA	DAA
					ADA
	AD2				ADD
DP4	A4	AAAA	AAAA	AAAA	
	A3D	DAAA	DAAA	DAAA	
				ADAA	ADAA
	D2A2				DDAA
DP5	A4D	AADAA	ADAAA	ADAAA	
		ADAAA		AADAA	
	A3D2		DADAA	DADAA	ADDAA
			DDAAA	DDAAA	
	A2D3				DDDAA
DP6	A5D	AAADAA	AAADAA	AADAAA	
		AADAAA	AAADAA	ADAAAA	
	A4D2	ADADAA	DADAAA	DAADAA	
		ADDAAA	ADADAA	ADADAA	
	A3D3		DDDAAA	DADDAA	ADDDAA
			DADDAA	DDDAAA	DDADAA
				DDADAA	
	A2D4				DDDDAA

[a]Note that the sequencing method is based on labeling of the reducing end and that sequences therefore are determined "from the reducing end" (Bahrke et al., 2002). When two different sugars appear in a certain position, ambiguities are introduced for the "remaining" sequence towards the non-reducing end. The sequences shown are those that are compatible with the mass spectra and not all shown sequences may

actually occur. For example, the pentamer fraction at alpha = 0.13 only contains products ending at -ADAA and –DAAA but it is not certain that all four given pentamer sequences actually occur. For the hexamer fraction ambiguities of course are even larger.

Fig. 1.

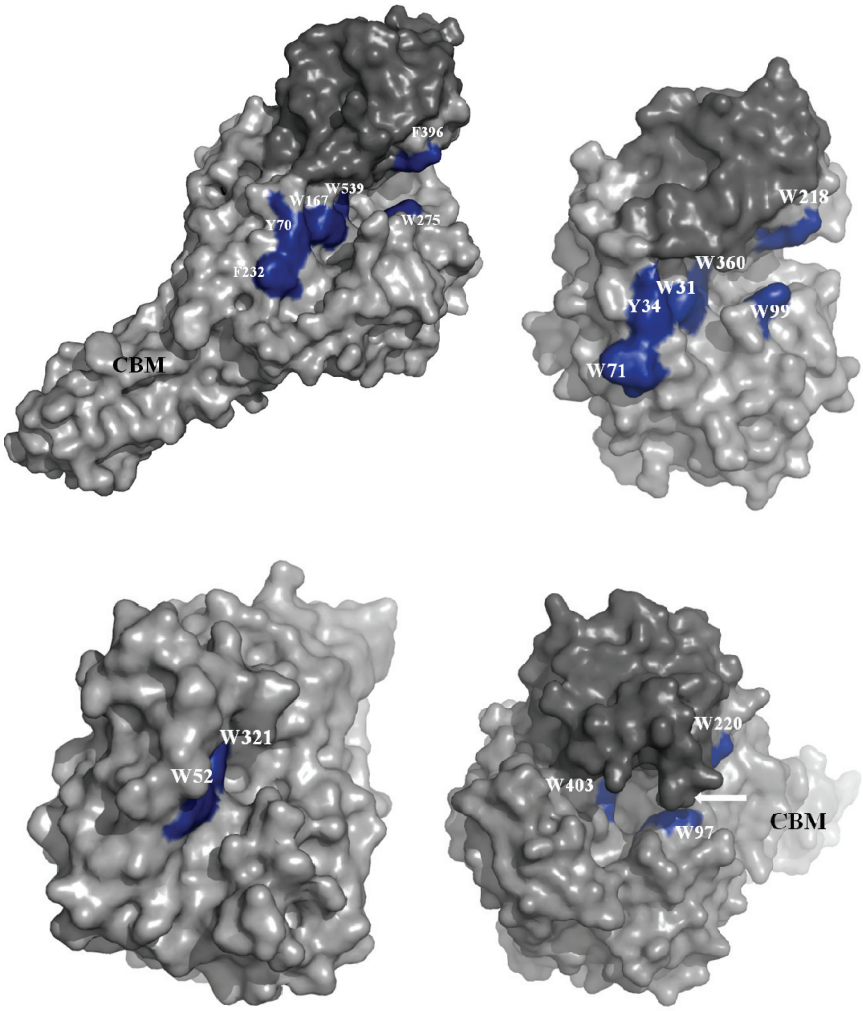

Fig 1. Crystal structures of: A ChiA from *S. marcescens* ((Perrakis et al., 1994); pdb code 1ctn), B: the 39 kDa from of HCHT ((Fusetti et al., 2002); pdb code 1guv), C: the catalytic domain of ChiC from *L. lactis* (pdb code 3ian; this domain has 67 % sequence identity with ChiC from *S. marcescens*), and D: ChiB from *S. marcescens* ((van Aalten et al., 2000); pdb code 1e15). The structures have been aligned by the

position of their (conserved) catalytic centers, meaning that the substrate-binding clefts are shown in the same view. ChiA, ChiB, and HCHT contain the $\alpha + \beta$ insertion domain (a darker grey) and have deep substrate binding clefts, while ChiC has a more shallow and open substrate-binding cleft. The side chains of up to six solvent exposed aromatic amino acids in equivalent structural positions are shown in blue. HCHT has all six of these: it has an aromatic motif the in –6 to –3 glycon subsites similar to the aromatic motif in ChiA (W71, Y34, W31), the same Trp-Trp motif in the +1 and +2 aglycon subsites as ChiB (W99, W218) and a Trp (W321) at the bottom of the –1 subsite that is fully conserved in all family 18 chitinases (labeled W539 in ChiA, W403 in ChiB, and W321 in ChiC, respectively). Aromatic amino acids in the substrate-binding clefts are known to be important for substrate-binding (Uchiyama, Katouno, Nikaidou, Nonaka, Sugiyama & Watanabe, 2001) and for a processive mode of action (Horn et al., 2006a; Zakariassen, Aam, Horn, Vårum, Sørlie & Eijsink, 2009). Note the "roof" over that active site cleft in ChiB (indicated by an arrow). Both ChiA and ChiB contain a chitin-binding domain (indicated by "CBM"), with opposite orientations relative to the catalytic domain; this domain is clearly visible for ChiA but largely hidden for ChiB.

Fig. 2.

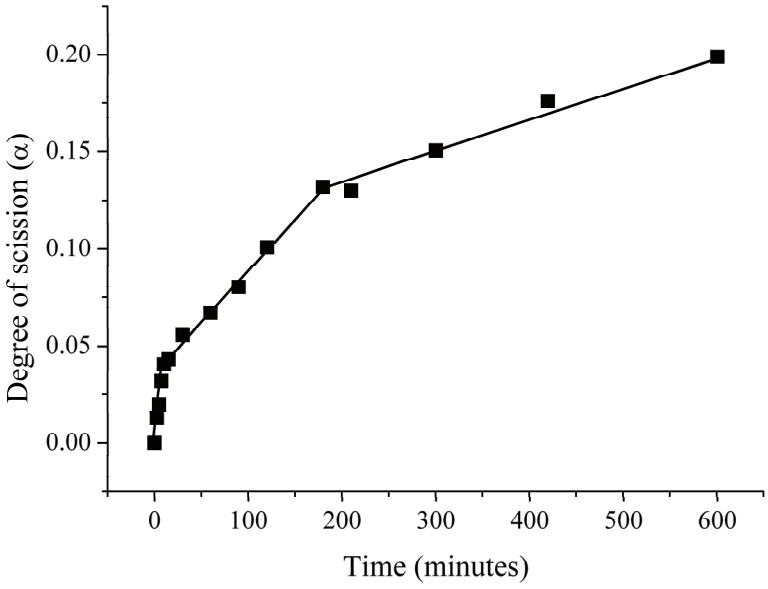

Fig 2. Time course for degradation of chitosan F_A 0.62 with HCHT. The graph shows the degree of scission (α = the fraction of cleaved glycosidic bonds) as a function of time. The graph shows three kinetic phases yielding apparent rate constants (k_{cat}^{app}) of 86 s^{-1}, 11 s^{-1}, and 4 s^{-1}, respectively. The last phase extends until α reaches 0.33.

Fig. 3.

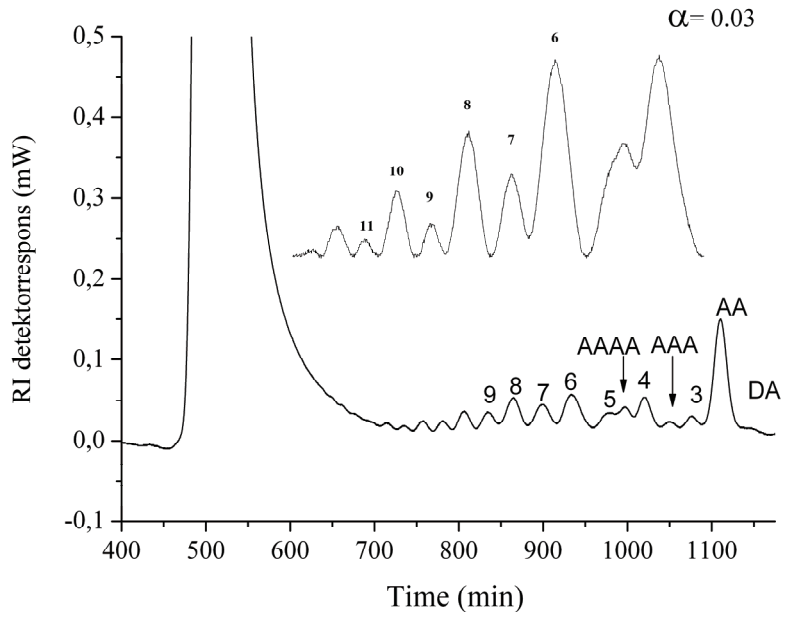
α= 0.03
RI detektorrespons (mW)
Time (min)
AA
AAAA
AAA
DA

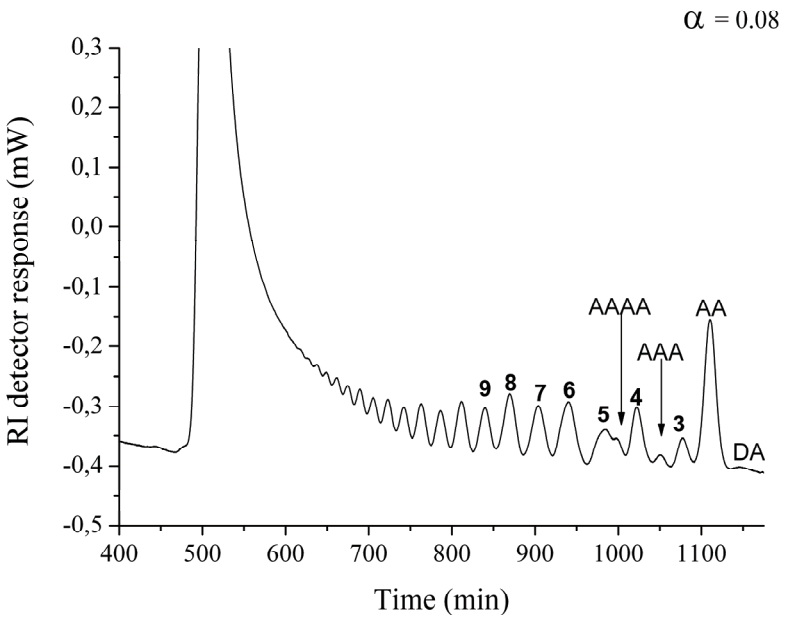
α = 0.08
RI detector response (mW)
Time (min)
AAAA
AA
AAA
DA

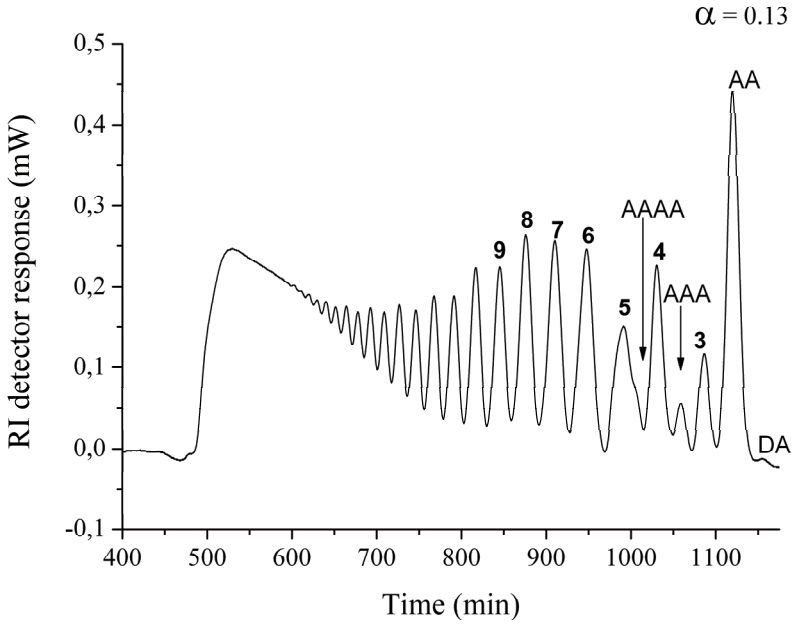

Fig. 3. Size exclusion chromatograms of oligomers obtained after degradation of chitosan (F_A = 0.62) to different degrees of scission (α) by HCHT. Peaks are labeled with DP-values or, in case of monocomponent peaks with known content) with the sequence of the oligomer; the large top to the left represents the void top, containing material with a DP larger than approximately 40 (see Sørbotten et al., 2005 for a detailed description of how the chromatograms are interpreted). The insert for SEC chromatogram for α = 0.03 is resulting oligomers at α below 0.01. A picture for maximally degraded chitosan (α = 0.33) is provided in Fig. 4.

Fig. 4.

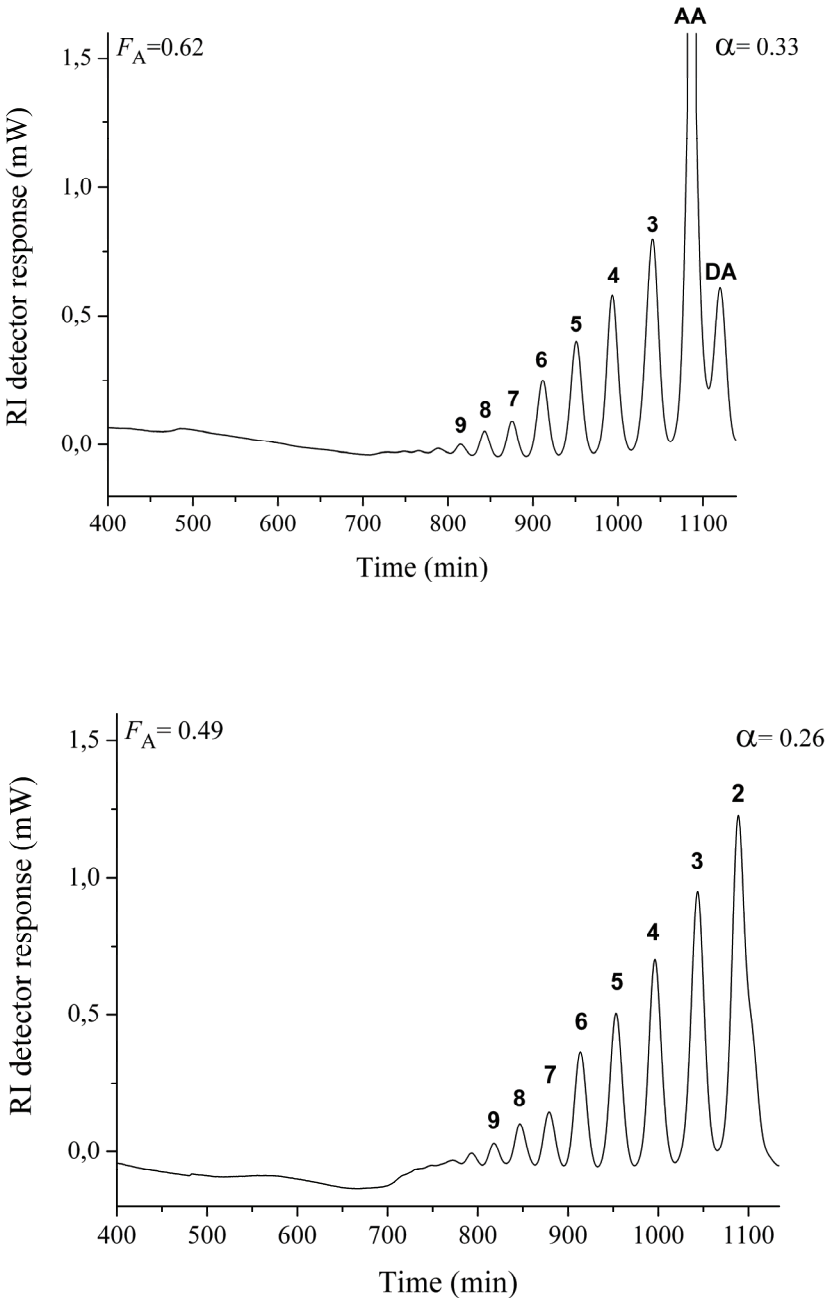
F_A=0.62
α= 0.33
AA
DA
3
4
5
6
7
8
9
RI detector response (mW)
Time (min)
F_A= 0.49
α= 0.26
2
3
4
5
6
7
8
9
RI detector response (mW)
Time (min)

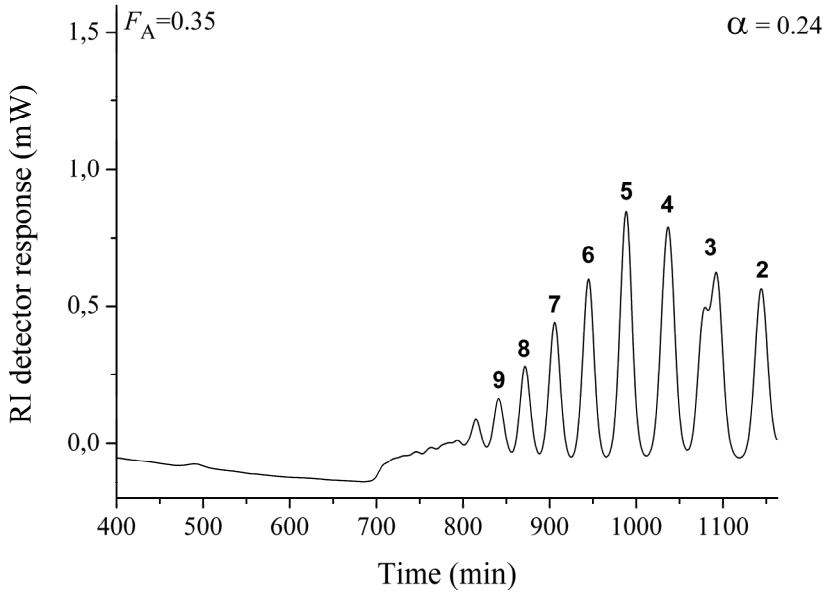
F_A=0.35
α = 0.24
RI detector response (mW)
1,5
1,0
0,5
0,0
9
8
7
6
5
4
3
2
400
500
600
700
800
900
1000
1100
Time (min)

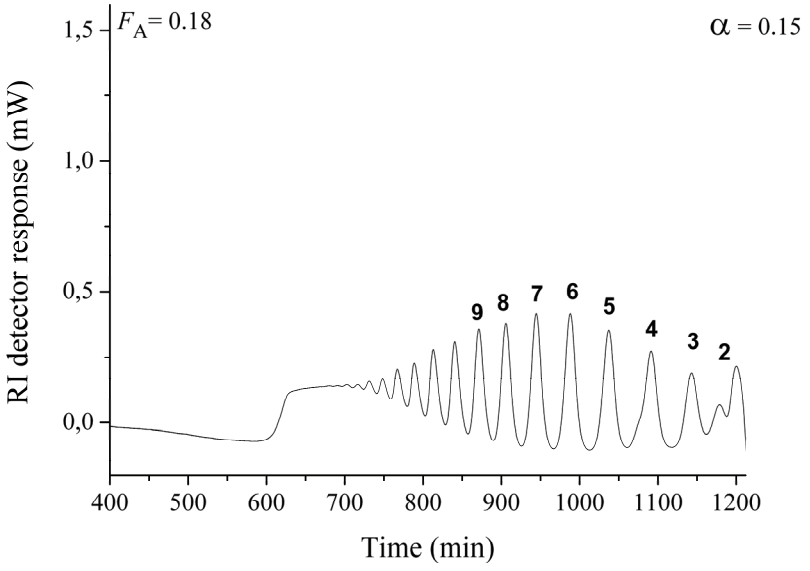
F_A= 0.18
α = 0.15
RI detector response (mW)
1,5
1,0
0,5
0,0
9
8
7
6
5
4
3
2
400
500
600
700
800
900
1000
1100
1200
Time (min)

Fig. 4. Degradation of chitosans with varying F_A to maximum degree of scission. To ensure reaching maximum α, samples were collected after it had been established that addition of enzyme to the reaction mixtures did not yield further increase in α.

Fig. 5.

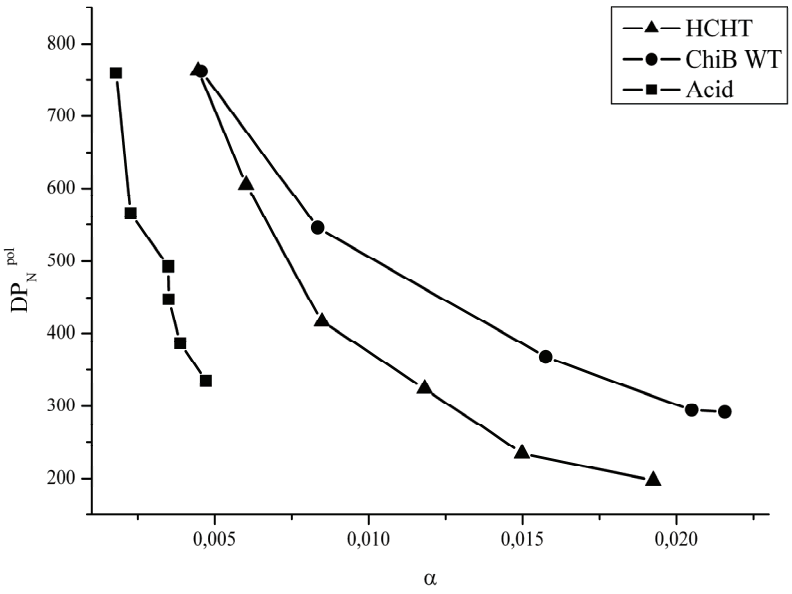

Fig. 5. Changes in the DP_n^{pol} as a function of the reaction extent α.

Fig. 6.

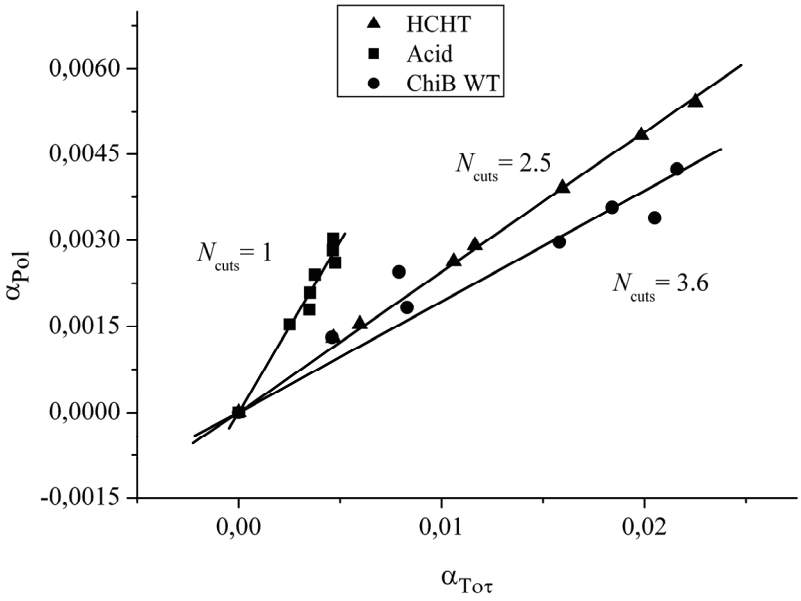

Fig. 6. Degree of scission of the polymer fraction (α_{Pol}) as a function of the total degree of scission (α_{tot}).

PAPER V

Analysis of productive binding modes reveals differences between human chitinases

Anne Line Norberg[1], Kristine Bistrup Eide[1], Anne Rita Lindbom[1], Vincent G.H. Eijsink[1] and Morten Sørlie[#1]

[1]*Department of Chemistry, Biotechnology and Food Science, Norwegian University of Life Sciences, PO 5003, N-1432 Ås, Norway*.

[#] To whom correspondence should be addressed. E-mail: morten.sorlie@umb.no. Telephone: +47 64965902. Fax: +47 64965901.

ABSTRACT

Human chitotriosidase (HCHT) and acidic mammalian chitinase (AMCase) are family 18 chitinases that are innate parts of the immune system. We have mapped preferred productive binding modes of oligosaccharide substrates to HCHT and compared the results with those of a similar study on AMCase. The data show that HCHT has an anomer-specific binding affinity in the +3 subsite that is much stronger than in AMCase, and that HCHT even may have affinity in a "+4" subsite. These observations are compatible with notable structural differences between these enzymes in the +3/+4 area. These features could endorse HCHT with higher endo-activity and a higher transglycosilation potential.

Keywords: Chitotriosidase; AMCase; human chitinases; transglycosilation

1. Introduction

Chitin, a crystalline polymer consisting of β-1-4 linked *N*-acetyl glucosamine units, is an abundant structural polysaccharide appearing in exoskeleton of arthropods, in the cell wall of fungi [1]. Humans do not possess chitin, but do have active chitinases referred to as Acidic Mammalian Chitinase (AMCase; [2]) and Human Chitotriosidase (HCHT; [3]), that are believed play roles in anti-parasite responses [4-6]. HCHT is synthesized and secreted as a 50-kDa two-domain protein in human macrophages. A considerable amount of produced enzyme is routed to lysosomes and processed into a 39-kDa isoform, lacking the C-terminal chitin binding domain.

The two human chitinases share considerable sequence and structural similarity, but current literature data indicate several (possible) functional differences. AMCase has a high acid tolerance which has been ascribed to the presence of His^{208}, His^{269}, and Arg^{145} near the catalytic residues, where HCHT has Asn^{208}, Arg^{269}, and Gln^{145} [7]. It has been suggested that HCHT is acting as an endo-enzyme, whereas AMCase probably primarily acts as an exo-enzyme [2,8,9]. Finally, there are indications that HCHT has a particularly high transglycosylation activity [10]. Endo-activity would benefit from an extended substrate binding cleft with more than two subsites on each site of the catalytic center where cleavage takes place. High oligosaccharide affinity in multiple aglycon subsites could be beneficial for transglycosilation [11] (Zakariassen et al submitted Biochemistry).

While the structures of AMCase [7,9] and HCHT [7,9] are known there are no structures of complexes with longer ligands that could provide comprehensive insight into the subsite structure of the enzymes. The presence of stretches of aromatic residues, including a conserved Trp-Tyr-Trp-Trp motif spanning an area corresponding to what could be subsites –6 to –1 and a Trp-Trp motif in the +1 and +2 subsites (Fig. 1) suggests extended substrate-

binding clefts in both enzymes. The situation beyond subsite +2 is less clear, but the structures do show that the two enzymes differ in this area (Fig. 1). For comparison, Fig. 1 also shows that structure of ChiA from *S. marcescens*, which has a similar long stretch of aromatic amino acids and for which structural data have shown that a chito-octamer binds from -6 to +2 [12].

To obtain insight into the differences between AMCase and HCHT, we have studied the interaction of HCHT with fully acetylated chito-oligosaccharides by analyzing hydrolysis patterns, and we have compared the results with results of a similar study on AMCase [8]. The results provide deeper insight into the binding properties of the aglycon subsites of HCHT and reveal differences with AMCase that could explain differences in functionality.

2. **Materials and methods**

2.1 Chemicals.

N-acetylated chito-oligosaccharides were purchased from Seikagaku (Tokyo, Japan). Purified Bovine Serum Albumin (BSA) were purchased from New England Biolabs (Ipswich, MA, USA). Dihydroxy benzoic acid (DHB), and all other chemicals were purchased from Sigma (St. Louis, MO, USA).

2.2 HCHT expression and purification.

The HCHT gene was expressed in *Pichia pastoris*. Cells were grown in 100 ml buffered glycerol-complex (BMGY) medium at 28 ºC for 24 hours and 10 ml of this culture was used to inoculate 500 ml fresh BMGY. After incubation for 48 hours at 30 ºC and 200

rpm, cells were harvested through centrifugation at 3500 rpm for 30 min at 20 ºC. Subsequently, pellets were resuspended in 500 ml fresh BMGY and incubated for additional 120 hours at 30 ºC and 200 rpm. Every 24 hours 5 ml of high quality methanol were added to the culture. After 4 additions of methanol, cells were harvested through centrifugation for 30 minutes at 3500 rpm and 20 ºC. HCHT is secreted into the culture medium and is present in the supernatant after centrifugation. The supernatant was filtered through a 0.22 µm filter and concentrated using a Vivaflow 200 PES with 10 000 MWCO, until a total volume of 30-50 ml. Concentrated supernatant was dialysed against 50 mM sodium acetate pH 4.2 at 4 ºC for 72 hours in order to get rid of components from the medium. HCHT was then purified using ion exchange chromatography with a HiTrap CM FF 5 ml column (GE Healthcare; Piscataway, NJ, USA), using 50 mM sodium acetate pH 4.2 as running buffer and a flow of 5 ml/min. Protein was eluted from the column by applying a linear gradient to 100% 50 mM sodium acetate pH 6.5 over 20 column volumes, and detected using UV-detection. The contents of the collected fractions were analyzed using SDS-PAGE (Fig. S1). Fractions containing only HCHT were pooled and concentrated to approximately 10 $mgml^{-1}$ using Amicon centrifuge tubes (10 000 MWCO), which were centrifuged at 4000 rpm for approximately 20 minutes. Enzyme purity was analyzed by SDS-PAGE and found to be over 95% in all cases. Protein concentrations were determined by using the Quant-It protein assay kit and a Qubit fluorometer (Invitrogen; CA, USA).

2.3 Degradation of N-acetylated-glucosamine oligomers.

$(GlcNAc)_4$ to $(GlcNAc)_6$ were dissolved to a concentration of 100µM in 50 mM sodium acetate buffer pH 4.2 containing 0.1 $mgml^{-1}$ BSA. HCHT was added to a concentration between 1 nM and 25 nM depending on the substrate. Hydrolysis reactions

were run in a shaking water bath at 37 ºC. Aliquots where withdrawn at several time points and enzyme activity was quenched by adding an equal volume of 100% acetonitrile.

2.4 High performance liquid chromatography (HPLC).

Immediately after quenching, the reaction products were analyzed by isocratic HPLC using an Amide-80 column (Tosoh Bioscience, Montgomeryville, PA, USA) coupled to a Gilson Unipoint HPLC system (Gilson; Middleton, WI, USA) as described earlier [13]. Chromatograms were collected and analyzed using the Chromeleon software (Dionex, Germiering, Germany).

2.5 Matrix Assisted Laser Desorption Ionization Time of Flight (MALDI TOF) Mass Spectrometry.

Immediately after quenching the reaction with acetonitril, 1µl of the resulting solution was mixed with 1 µl matrix solution (15 $mgml^{-1}$ DHB in 30% ethanol) and 1 µl of the resulting mixture was spotted on a target plate and dried at room temperature. MS experiments were conducted using a Ultraflex^{TM} TOF mass spectrometer (Bruker Daltonik GmbH, Bremen, Germany) with gridless optics under sontrol of Flexcontrol 4.1. Experiments were conducted using an accelerating potential of 20 kV in the reflector mode.

3. Results and discussion

Productive binding of $(GlcNAc)_6$, $(GlcNAc)_5$, and $(GlcNAc)_4$ to HCHT was analyzed using HPLC under conditions that permitted determination of both the concentrations and the

β/α-anomer ratios of substrates and products (Fig. 2). The α- and β-anomers of chito-oligosaccharides exist in an equilibrium ratio of about 60% α and 40% β, while newly formed reducing ends will have the β-anomeric configuration [14]. All α-anomeric oligomers must originate from the original reducing end of the substrate, although this is not absolute since a minor fraction of newly formed β-anomers will convert to α-anomers during the (minimized) time needed for sample handling and HPLC analysis.

Generally, the anomeric ratios of the products showed a strong dominance of β-anomers. This dominance, which is much stronger than previously observed for AMCase [14], cannot be explained by the retaining mechanism of family 18 chitinases alone, but must also reflect a preference for selectively cleaving β-anomers of the substrate; i.e. there must be preferences for β-anomeric reducing end configurations in the aglycon subsites.

Hydrolysis of $(GlcNAc)_6$ yielded $(GlcNAc)_3$ as the major product and equal amounts of $(GlcNAc)_4$ and $(GlcNAc)_2$ as minor products. The tetrameric and dimeric products are both predominantly in the β-anomer form that may be explained in two ways. Firstly,
there could be binding from –4 to +2 with a β-anomer preference in +2; such a preference has indeed been observed in ChiB from *S.marcescens* [15], an enzyme with at least three aglycon subsites [16], and may be due to an unfavorable interaction between the terminal hydroxyl group of the α-anomer with the NH group on the indole ring at a Trp in the +2 subsite [7]. This Trp (Trp218; Fig. 1) is also present in HCHT and AMCase; the latter enzyme also shows β-anomer preference in +2 [7] albeit not as pronounced as HCHT (see tetramer data, below). Secondly, one could envisage binding from –2 to +4 with some β-anomer preference in +4. Both binding modes were confirmed by MALDI-TOF-MS analysis were $(GlcNAc)_8$, transglycosylation product from combination of $(GlcNAc)_6$ and $(GlcNAc)_2$ after productive binding from –2 to +4, and $(GlcNAc)_{10}$, transglycosylation product from combination of $(GlcNAc)_6$ and $(GlcNAc)_4$ after productive binding from –4 to +2, were observed (Fig. 3).

Moreover, $(GlcNAc)_9$ is also observed that would be the transglycosylation product from combination of $(GlcNAc)_3$ after productive binding from –3 to +3 and $(GlcNAc)_6$.

The preferred productive binding of $(GlcNAc)_6$ to subsites –3 to +3 implies a clear difference with AMCase where cleavage into $(GlcNAc)_2$ and $(GlcNAc)_4$ occurs about twice as fast as conversion to two $(GlcNAc)_3$ [8]. This suggests strong affinity for binding of a GlcNAc molecule in what would be a +3 subsite in HCHT, an idea that is supported by the results obtained with $(GlcNAc)_5$. The pentamer is converted to dimers and trimers and the dimer occurs mainly as β-anomers. This indicates that productive binding predominantly involves subsites –2 to "+3". The trimer has a considerably lower dominance of β-anomers, a dominance that may result from both some productive binding from –3 to +2 and from substrate selection through a β-anomer preference in subsite +3. For ChiA, it has been shown that stacking of a sugar moiety with the Trp-residue in the –3 subsite (Trp167 in ChiA, Trp31 in HCHT) yields a considerable –1.8 kcal/mol in binding free energy [17]. Thus, the fact that the pentamer primarily binds from –2 to +3, despite the presence of Trp31 indicates that there must be considerable binding energy in the +3 subsite.

Hydrolysis of $(GlcNAc)_4$ yielded only $(GlcNAc)_2$ with a β/α-ratio of 87/13 indicating that only binding from –2 to +2 occurs with a β-anomer preference in +2 that seems somewhat stronger than the β-anomer preference in the +2 subsite of AMCase [8].

Interestingly, the GlcNAc-oligomer degradations tend to display biphasic kinetics. Estimation of rate constants for the slow kinetic phases of the degradation yield values in the order of $2 \cdot 10^{-4}$ s^{-1}, a value that is remarkably similar with the determined rate constant for the mutarotation of the α-GlcNAc to the β-anomer of $2.20 \cdot 10^{-4}$ s^{-1} [18]. This indicates that mutarotation becomes the rate determining step, supporting the idea that there are β-anomer preferences in subsites +3 and even +4.

An exact interpretation of the present HCHT and the previous AMCase [8] results is not straightforward because of the difficulty of discriminating between newly generate product β-anomeric ends and product β-anomeric ends resulting from a β-anomer preference in substrate binding. Nevertheless, the present data clearly reveal a few characteristic features that make HCHT special. Firstly, HCHT shows a remarkable and unprecedented dominance of β-anomers among in *all* products, indicating strong preferences for binding β-anomeric substrate reducing ends. Thus, HCHT seems to have highly specific interactions with the substrate, not only in +2 but also in +3 and presumably also in +4. The existence of strong binding interactions in the +3 subsite is confirmed by the high level of trimer production in the reaction with $(GlcNAc)_6$. All in all, these results indicate that HCHT has an extended substrate-binding groove, providing stronger aglycon binding than e.g. AMCase.

Previous studies have indicated that HCHT has high transglycosylation activity that may be observed without applying typical "transglycosylation conditions" (high substrate and enzyme concentrations) [10]. The high transglycosilation activity of HCHT further supports the idea that this enzyme has relatively strong binding affinities for the aglycon; high affinity for sugar acceptors is known to promote transglycosylation activity in family 18 chitinases [11] (Zakariassen et al, submitted biochem).

Comparison of the active site of HCHT with those of AMCase and chitinase A (ChiA) (Fig. 1), shows that the HCHT active site cleft is "tighter" in the area beyond subsite +2. There are two regions of HCHT that differs from AMCase and that would seem to be able to interact with +3 and/or +4 sugars, either directly or via a water molecule (Fig. 1). In the first region (marked as I in Fig. 1), there are three non-conserved amino acids on α-helix 5 in the TIM-barrel (Glu^{188}, Thr^{189}, and Tyr^{190}) and an amino acid on a loop (Gln^{145}) in HCHT that are Ile^{188}, Ser^{189}, and Asn^{190} (helix) and Arg^{145} (loop) in AMCase. Furthermore, at the start of α-

helix 6 in the TIM-barrel, from residue 232 to 239, there is a SGAAAS sequence in HCHT (region marked as II in Fig. 1) that corresponds to PTDTGSNAY (232 to 240) in AMCase.

It is interesting to compare HCHT with ChiA from *Serratia marcescens* (Fig 1), since this enzyme is quite well known. ChiA has a similar stretch of aromatic amino acids as HCHT on going from –6 to +2 (Phe-Tyr-Trp-Trp-Trp-Phe vs. Trp-Tyr-Trp-Trp-Trp-Trp). ChiA resembles HCHT in that studies of productive binding of oligomeric substrates indicate the existence of a "+3" subsite [15], but differs from HCHT in that it has a more open aglycon region (in the "+3" and "+4" area where region I corresponds to Lys^{367}, Asp^{368}, Lys^{369}, and Lys^{320} and region II to DTAY from 415 to 418) and a presumably weaker +2 subsite (Phe 396 replaces Trp218). The fact that ChiA shows low transglycosilation activity, even under "transglycosilation conditions" [19] (Zakariassen et al., submitted) correlates with its seemingly weaker aglycon subsites.

Substrate-association is the rate-limiting step in enzymatic degradation of chitin [20] and high affinity subsites clearly help in overcoming this barrier. It is quite conceivable that the most challenging binding mode of all, namely binding in an endo fashion, depends on the presence of binding affinities beyond both the –2 and the +2 subsites. ChiA has many glycon subsites (Fig. 1; [12]) and, as discussed above, at least three aglycon subsites. This extended substrate-binding cleft, extending "on both sides" of the catalytic center beyond subsites –2 and +2, correlates with the observation that this enzyme indeed exhibits endo-activity in addition to its ability to degrade chitin chains processively from the reducing end [21-23]. The substrate-binding cleft of HCHT has the openness that is generally thought to promote endo-binding [9] and has more extended and tighter-binding aglycon subsites than both ChiA and AMCase. This may confer considerable endo-activity on HCHT, an activity that indeed has been suggested [2,24]. It is interesting to note that endo-activity reduces the need for association to only chain ends for productive binding, thus increasing the number of binding

sites on chitin containing materials dramatically. This could promote the fungistatic effect observed for HCHT [25].

In conclusion, we have shown that HCHT differs from AMCase (and ChiA) by higher substrate-binding affinities in its aglycon subsites, especially beyond subsite +2. Structural comparisons provide possible explanations for this difference that may be a crucial determinant of the transglycosilation and the endo-binding potential of HCHT.

Acknowledgements

The *Pichia pastoris* cells producing the 39 kDa form of HCHT gene were a kind gift from Prof. Daan M.F. van Aalten, University of Dundee. This work was supported by Grants 164653/V40, 178428/V40, and 177542/V30 from the Norwegian Research Council.

Reference List

[1] Rinaudo, M. (2006). Chitin and chitosan: Properties and applications. Prog. Polym. Sci. 31, 603-632.

[2] Boot, R.G., Blommaart, E.F.C., Swart, E., Ghauharali-van der Vlugt, K., Bijl, N., Moe, C., Place, A. and Aerts, J. (2001). Identification of a novel acidic mammalian chitinase distinct from chitotriosidase. J. Biol. Chem. 276, 6770-6778.

[3] Renkema, G.H., Boot, R.G., Au, F.L., Donker-Koopman, W.E., Strijland, A., Muijsers, A.O., Hrebicek, M. and Aerts, J. (1998). Chitotriosidase, a chitinase, and the 39-kDa human cartilage glycoprotein, a chitin-binding lectin, are homologues of family 18 glycosyl hydrolases secreted by human macrophages. Eur. J. Biochem. 251, 504-509.

[4] Shibata, Y., Foster, L.A., Bradfield, J.F. and Myrvik, Q.N. (2000). Oral administration of chitin down-regulates serum IgE levels and lung eosinophilia in the allergic mouse. J. Immunol. 164, 1314-1321.

[5] van Eijk, M., Scheij, S.S., van Roomen, C.P.A.A., Speijer, D., Boot, R.G. and Aerts, J.M.F.G. (2007). TLR- and NOD2-dependent regulation of human phagocyte-specific chitotriosidase. FEBS Lett. 581, 5389-5395.

[6] Elias, J.A., Homer, R.J., Hamid, Q. and Lee, C.G. (2005). Chitinases and chitinase-like proteins in TH2 inflammation and asthma. J. Allergy Clin. Immun. 116, 497-500.

[7] Olland, A.M. et al. (2009). Triad of polar residues implicated in pH specificity of acidic mammalian chitinase. Protein Sci. 18, 569-578.

[8] Chou, Y.T. et al. (2006). Kinetic Characterization of Recombinant Human Acidic Mammalian Chitinase. Biochemistry 45, 4444-4454.

[9] Fusetti, F., von Moeller, H., Houston, D., Rozeboom, H.J., Dijkstra, B.W., Boot, R.G., Aerts, J. and van Aalten, D.M.F. (2002). Structure of human chitotriosidase - Implications for specific inhibitor design and function of mammalian chitinase-like lectins. J. Biol. Chem. 277, 25537-25544.

[10] Aguilera, B. et al. (2003). Transglycosidase activity of chitotriosidase - Improved enzymatic assay for the human macrophage chitinase. J. Biol. Chem. 278, 40911-40916.

[11] Taira, T. et al. (2010). Transglycosylation reaction catalyzed by a class V chitinase from cycad, Cycas revoluta: A study involving site-directed mutagenesis, HPLC, and real-time ESI-MS. BBA-Prot. Proteom. 1804, 668-675.

[12] Papanikolau, Y., Prag, G., Tavlas, G., Vorgias, C.E., Oppenheim, A.B. and Petratos, K. (2001). High resolution structural analyses of mutant chitinase A complexes with substrates provide new insight into the mechanism of catalysis. Biochemistry-US 40, 11338-11343.

[13] Krokeide, I.M., Synstad, B., Gåseidnes, S., Horn, S.J., Eijsink, V.G.H. and Sørlie, M. (2007). Natural substrate assay for chitinases using high-performance liquid chromatography: A comparison with existing assays. Anal. Biochem. 363, 128-134.

[14] Davies, G. and Henrissat, B. (1995). Structures and mechanisms of glycosyl hydrolases. Structure 3, 853-9.

[15] Horn, S.J., Sørlie, M., Vaaje-Kolstad, G., Norberg, A.L., Synstad, B., Vårum, K.M. and Eijsink, V.G.H. (2006). Comparative studies of chitinases A, B and C from Serratia marcescens Biocatal.Biotransfor. 24, 39-53.

[16] van Aalten, D.M.F., Komander, D., Synstad, B., Gåseidnes, S., Peter, M.G. and Eijsink, V.G.H. (2001). Structural insights into the catalytic mechanism of a family 18 exo-chitinase. Proc.Natl.Acad.Sci.U.S.A 98, 8979-8984.

[17] Baban, J., Fjeld, S., Sakuda, S., Eijsink, V.G.H. and Sørlie, M. (2010). The Roles of Three *Serratia marcescens* Chitinases in Chitin Conversion Are Reflected in Different Thermodynamic Signatures of Allosamidin Binding. J. Phys. Chem. B 114, 6144-6149.

[18] Yanase, Y., Fukamizo, T., Hayashi, K. and Goto, S. (1987). Retention of anomeric form in lysozyme-catalyzed reaction. Arch.Biochem.Biophys. 253, 168-175.

[19] Aronson, N.N., Halloran, B.A., Alexeyev, M.F., Zhou, X.E., Wang, Y.J., Meehan, E.J. and Chen, L.Q. (2006). Mutation of a conserved tryptophan in the chitin-binding cleft of *Serratia marcescens* Chitinase A enhances transglycosylation. Biosci. Biotech. Bioch. 70, 243-251.

[20] Zakariassen, H., Eijsink, V.G.H. and Sørlie, M. (2010). Signatures of activation parameters reveal substrate-dependent rate determining steps in polysaccharide turnover by a family 18 chitinase. Carbohyd.Polym. 81, 14-20.

[21] Brurberg, M.B., Nes, I.F. and Eijsink, V.G.H. (1996). Comparative studies of chitinases A and B from Serratia marcescens. Microbiology 142, 1581-1589.

[22] Hult, E.L., Katouno, F., Uchiyama, T., Watanabe, T. and Sugiyama, J. (2005). Molecular directionality in crystalline beta-chitin: hydrolysis by chitinases A and B from Serratia marcescens 2170. Biochem. J. 388, 851-856.

[23] Sikorski, P., Sørbotten, A., Horn, S.J., Eijsink, V.G.H. and Vårum, K.M. (2006). Serratia marcescens chitinases with tunnel-shaped substrate-binding grooves show endo activity and different degrees of processivity during enzymatic hydrolysis of chitosan. Biochemistry 45, 9566-9574.

[24] Renkema, G.H., Boot, R.G., Muijsers, A.O., Donker-Koopman, W.E. and Aerts, J.M.F.G. (1995). Purification and Characterization of Human Chitotriosidase, a Novel Member of the Chitinase Family of Proteins. J. Biol. Chem. 270, 2198-2202.

[25] van Eijk, M. et al. (2005). Characterization of human phagocyte-derived chitotriosidase, a component of innate immunity. Int. Immunol. 17, 1505-1512.

[26] Papanikolau, Y., Prag, G., Tavlas, G., Vorgias, C.E., Oppenheim, A.B. and Petratos, K. (2001). High resolution structural analyses of mutant chitinase A complexes with substrates provide new insight into the mechanism of catalysis. Biochemistry 40, 11338-11343.

[27] Zakariassen, H., Aam, B.B., Horn, S.J., Vårum, K.M., Sørlie, M. and Eijsink, V.G.H. (2009). Aromatic Residues in the Catalytic Center of Chitinase A from *Serratia marcescens* Affect Processivity, Enzyme Activity, and Biomass Converting Efficiency. J. Biol. Chem. 284, 10610-10617.

[28] Horn, S.J. et al. (2006). Costs and benefits of processivity in enzymatic degradation of recalcitrant polysaccharides. P. Natl. Acad. Sci. USA 103, 18089-18094.

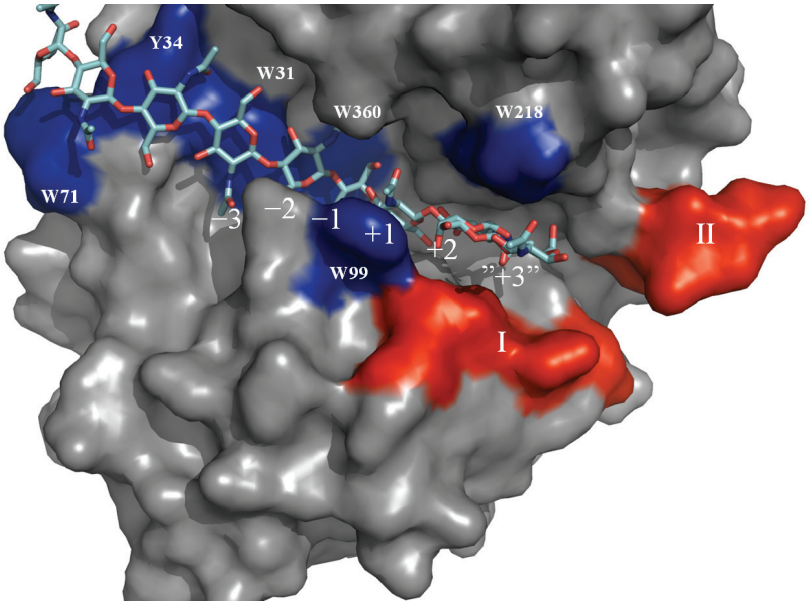
Y34
W31
W360
W218
W71
−3
−2
−1
+1
+2
"+3"
W99
II
I

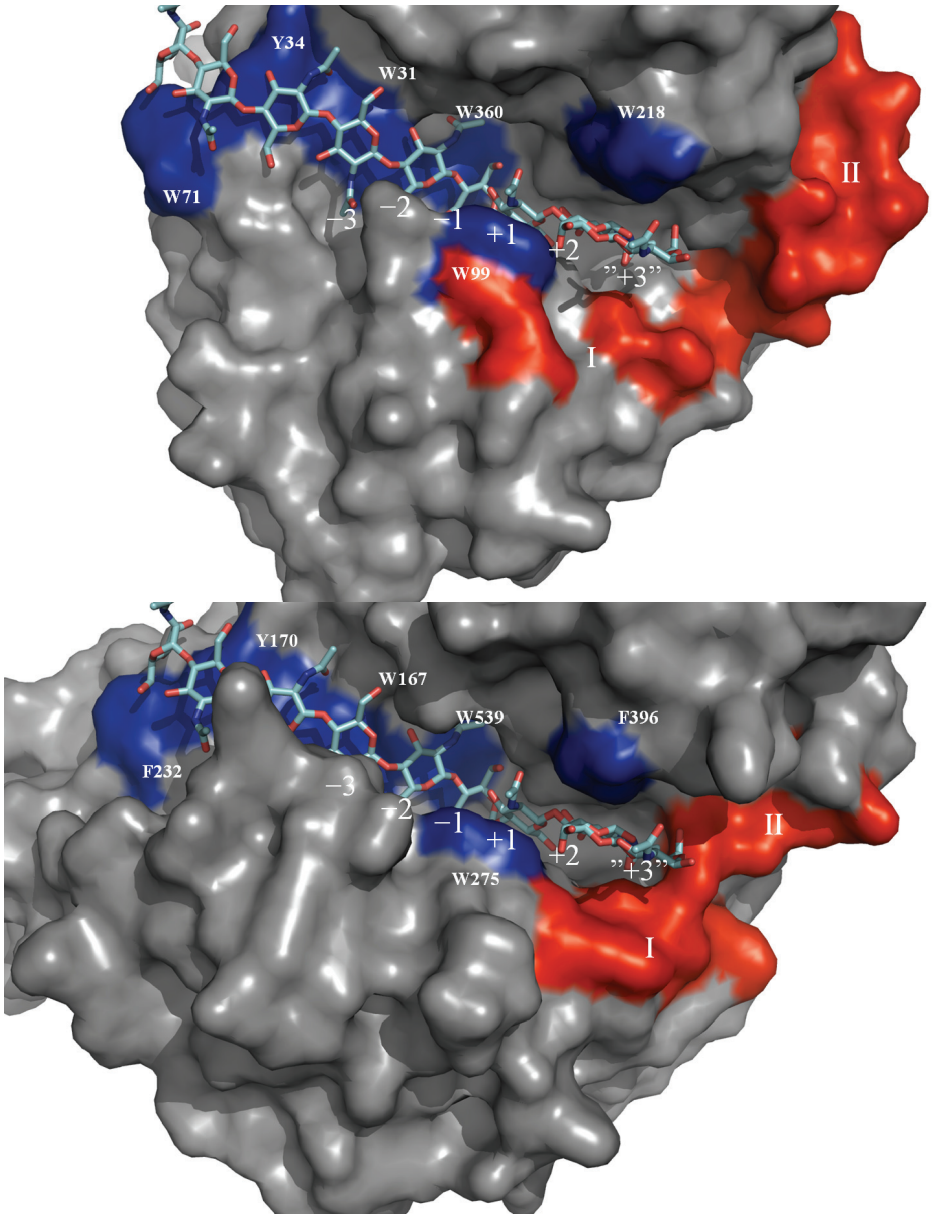

Fig. 1. Aligned crystal structures of HCHT, (top [9], 1guv) AMCase, (middle [7], 3fxy), and ChiA from *S. marcescens* (bottom [26], 1ehn) showing enzyme-ligand interactions. The structures contain a nonasaccharide that was constructed and positioned as described in [9] using enzyme-ligand complexes described in [26] and [16]. It is important to note that this is a

modeled substrate and that the position of the +3 sugar is the most uncertain. Aromatic amino acids lining the substrate-binding cleft and known to be important determinants of enzyme properties [27,28] are coloured blue. Regions that are different in HCHT compared to AMCase and that may interact with GlcNAc-units in “+3” and “+4” positions are highlighted in red and labeled with Roman numbers (see text for details). For comparison, corresponding regions are also colored red in AMCase and ChiA.

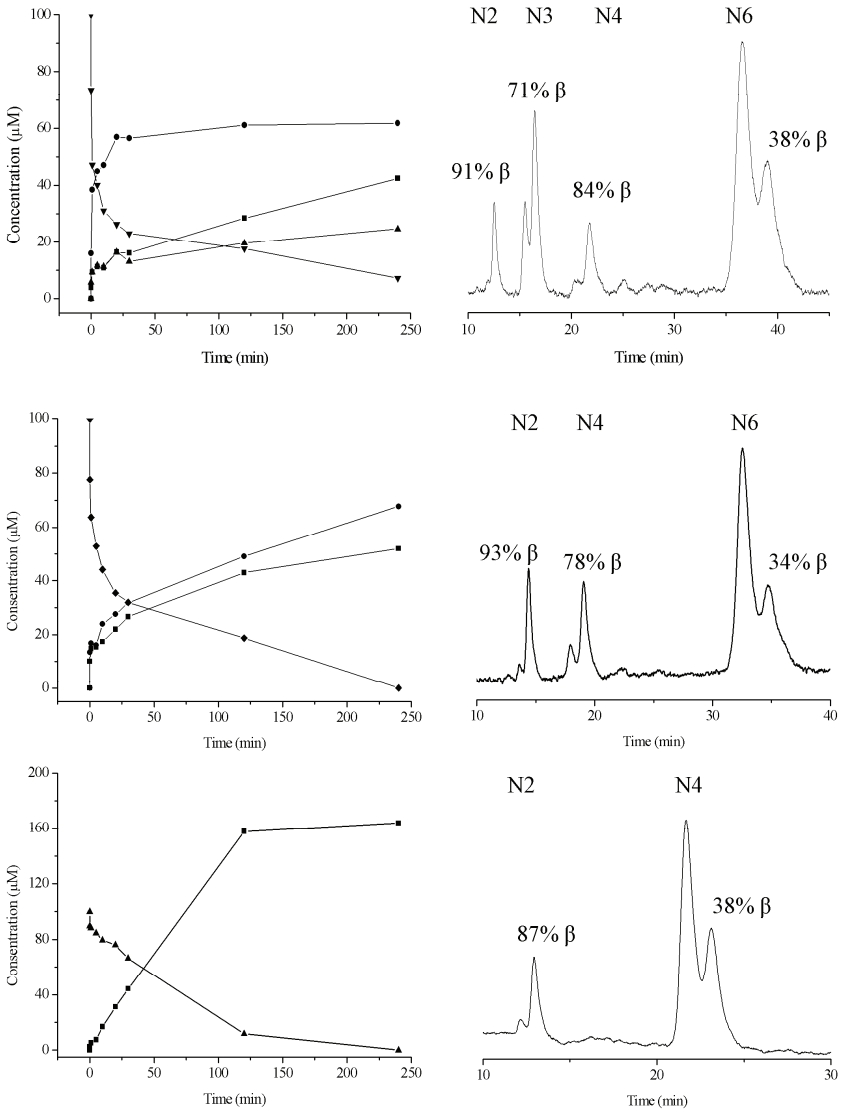

Fig 2. Hydrolysis of the different GlcNAc oligomers by HCHT. The left panels show HPLC-based time course plots for the degradation of 100 μM $(GlcNAc)_6$ (upper panel) $(GlcNAc)_5$ (middle panel) and $(GlcNAc)_4$ (lower panel). ▼ $(GlcNAc)_6$, ♦ $(GlcNAc)_5$, ▲ $(GlcNAc)_4$, ● $(GlcNAc)_3$, ■ $(GlcNAc)_2$. The relative higher abundance of $(GlcNAc)_3$ compared to $(GlcNAc)_2$ during $(GlcNAc)_5$ degradation likely reflects the dominance in (–2 to +3) binding

compared to (–3 to +2) resulting in more $(GlcNAc)_2$ compared to $(GlcNAc)_3$ serving as sugar donor to $(GlcNAc)_5$ in transglycosylation reactions. This is in accordance with the work of Aguilera *et al*. where $(GlcNAc)_7$ is the main transglycosylation product when $(GlcNAc)_5$ is the substrate [10]. The right panels show HPLC chromatograms for samples taken after 10 seconds (i.e. relatively early during the reaction, during the fast first phase) that reveal the α/β anomeric ratios of the products; these ratios are indicated in the figures. The equilibrium α/β ratio for the starting material is 60/40. The ratios visualized in the figures provide information on possible selective binding of one of the substrate anomers and on preferential productive binding modes (new reducing ends are β); see text for discussion.

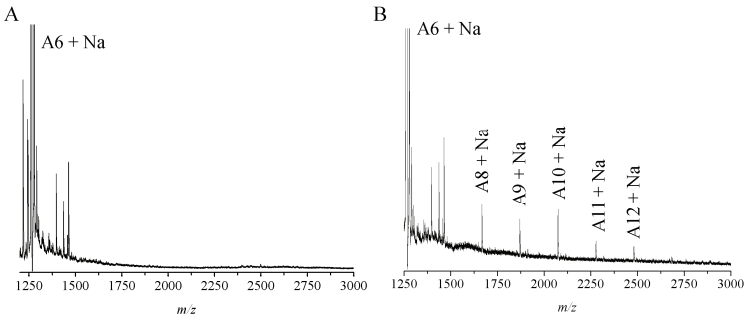

Fig. 3. MALDI-TOF-MS analysis of products obtained during the early phase of a reaction with HCHT and 100 μM $(GlcNAc)_6$. The presence of longer oligomeric products after incubation with HCHT (panel B; panel A is from a control reaction without enzyme) shows the occurrence of transglycosylation.

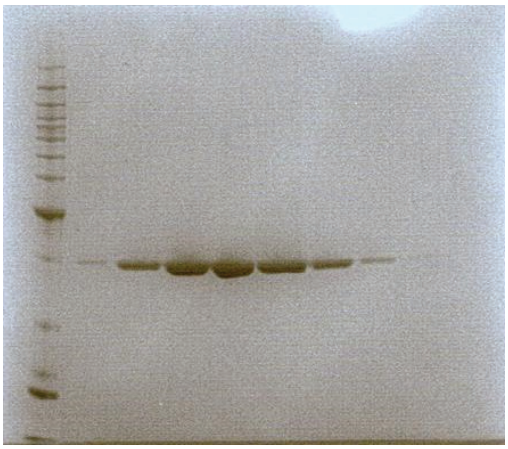

Fig S1. SDS-PAGE gel of collected fractions after ion exchange chromatography.

PAPER VI

analytical chemistry

ARTICLE

pubs.acs.org/ac

Analysis of Noncovalent Chitinase-Chito-Oligosaccharide Complexes by Infrared-Matrix Assisted Laser Desorption Ionization and Nanoelectrospray Ionization Mass Spectrometry

Anette I. Dybvik,[†] Anne Line Norberg,[‡] Veronika Schute,[§] Jens Soltwisch,[§] Jasna Peter-Katalinić,[§] Kjell M. Vårum,[†] Vincent G. H. Eijsink,[‡] Klaus Dreisewerd,[§] Michael Mormann,[§] and Morten Sørlie*[,‡]

[†]Department of Biotechnology, Norwegian University of Science and Technology, Sem Sælandsvei 6-8, N-7491 Trondheim, Norway

[‡]Department of Chemistry, Biotechnology and Food Science, Norwegian University for Life Sciences, PO 5003, N-1432 Ås, Norway

[§]Institute of Medical Physics and Biophysics, University of Münster, Robert-Koch-Str. 31, D-48149 Münster, Germany

Supporting Information

ABSTRACT: Transferring noncovalently bound complexes from the condensed phase into the gas phase represents a challenging task due to weak intermolecular bonds that have to be maintained during the phase transition. Currently, electrospray ionization (ESI) is the standard mass spectrometric (MS) technique to analyze noncovalent complexes. Although infrared matrix-assisted laser desorption ionization (IR-MALDI)-MS also provides particular soft desorption/ionization conditions, this method has so far hardly been applied for the analysis of noncovalent complexes. In this study, we employed IR-MALDI orthogonal time-of-flight (o-TOF)-MS in combination with the liquid matrix glycerol to characterize the specific complex formation of chito-oligosaccharide (CHOS) ligands with two variants of Chitinase A (ChiA) from *Serratia marcescens*, the inactive E315Q mutant and the active W167A mutant, respectively. The IR-MALDI-o-TOF-MS results were compared to those obtained using nano-ESI-quadrupole (q)-TOF-MS and ultraviolet (UV)-MALDI-o-TOF-MS. Using IR-MALDI-o-TOF-MS, specific noncovalent complexes between ChiA and CHOS were detected with distributions between enzymes with bound oligosaccharides vs free enzymes that were essentially identical to those obtained by nano-ESI-q-TOF-MS. Chitinase-CHOS complexes were not detected when UV-MALDI was employed for desorption/ionization. The results show that IR-MALDI-MS can be a valuable tool for fast and simple screening of noncovalent enzyme-ligand interactions.

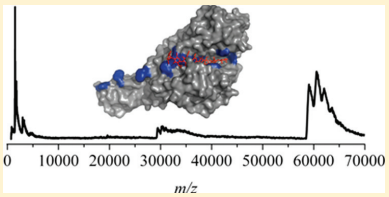

Chitin is an insoluble polymer composed of β-(1−4)-linked units of *N*-acetyl-D-glucosamine (GlcNAc). It is an essential structural component in crustaceans, insects, algae, fungi, mollusks, and yeast.[1] In nature, metabolism of chitin is controlled by enzymatic systems like chitin synthases and chitinases that produce and break down chitin, respectively.[2] Chitinases play a pivotal role in the development of organisms that need to degrade and reshape chitinous structures during their life cycles. As a consequence of the known and putative biological roles of family 18 chitinases, inhibition of these enzymes is a target for the development of plant protecting compounds[3] and medicines for allergic and inflammatory disorders.[4] Hetero-oligomers of GlcNAc and deacetylated GlcNAc, D-glucosamine (D), which are collectively referred to as chito-oligosaccharides (CHOS), have considerable potential as inhibitors. This is due to their specificity toward chitinases and the possibility of fine-tuning binding strength and specificity by manipulating oligomer length and acetylation pattern.[5−7]

Enzyme-ligand interactions are primarily of a noncovalent nature and are mediated by forces like electrostatic/ionic interaction, hydrogen bindings, and hydrophobic interactions, allowing rapid binding equilibria.[8] For mass spectrometric analysis of such interactions, particularly soft desorption and ionization conditions are required that enable the transfer of intact noncovalent complexes into the gas phase.[9] In the past two decades, several studies have shown that nano-electrospray ionization (ESI)-MS-based methods may allow for characterization of noncovalent protein-ligand complexes. Examples include studies of the interactions of different proteins with oligosaccharides or glycan-derived ligands, addressing issues such as binding specificity, binding strength, and dissociation kinetics.[8,10−17]

Ultraviolet matrix assisted laser desorption ionization (UV-MALDI-MS) has been employed as an alternative approach to ESI ionization of noncovalent complexes.[18−21] The UV-MALDI-MS approach has some limitations with respect to the choice of matrix and sample preparation. UV matrixes are often organic acids that tend to disrupt noncovalent interactions. The solid state of the matrix also contributes to complex dissociation. Using UV-MALDI-MS, noncovalent complexes are often detected only upon the first laser pulse(s) that hit a previously not

Received: November 29, 2010
Accepted: April 7, 2011
Published: April 07, 2011

exposed position. This is referred to as the "first-shot phenomenon"[18,22−24] and is the result of dissociation of complexes in the matrix crystals due to the thermal load that is generated by the previous laser exposure(s).

Infrared (IR)-MALDI provides softer desorption/ionization conditions than its UV-MALDI counterpart. This can be related to the different pathways of energy deposition into the matrix, where absorbed UV light leads to electronic excitation while absorption of IR photons results in excitation of vibrational modes, and to different material ejection characteristics.[25] Typically, erbium-doped yttrium aluminum garnet (Er:YAG) lasers (λ = 2.94 μm) and optical parametric oscillator (OPO) lasers emitting around 3 μm are utilized in IR-MALDI-MS. These emission wavelengths allow the use of the O−H and N−H stretch vibrations of suitable matrix compounds. Glycerol solutions are near physiological pH and provide a homogeneous sample preparation resulting in a higher shot-to-shot signal stability compared to crystalline matrixes. Glycerol has been applied for the IR-MALDI-MS analysis of bioactive compounds such as oligosaccharides,[26] lipids,[27,28] DNA (including double stranded),[29,30] peptide-carbohydrate interactions,[31] and proteins (including triple helixes of collagen).[32]

Here, we report the use of IR-MALDI-orthogonal time-of-flight (o-TOF)-MS to study the formation of noncovalent complexes between CHOS and two variants of Chitinase A (ChiA) from *Serratia marcescens* that are engineered such that (i) only binding of CHOS takes place with no hydrolysis (ChiA-E315Q) and (ii) the majority of CHOS is hydrolyzed leaving only a small fraction available for binding (ChiA-W167A). The results were validated by carrying out nano-ESI-quadrupole (q)-TOF-MS analyses using conditions that are known to allow detection of CHOS-Chitinase complexes.[11] For further method comparison, we also carried out experiments using UV-MALDI-o-TOF-MS.

EXPERIMENTAL SECTION

Materials. 2,5-Dihydroxybenzoic acid (DHB), 2-hydroxy-5-methoxybenzoic acid, 1-acetyl-2,4-dihydroxybenzene (DHAP), 2,4,6-trihydroxyacetophenone (THAP), dimethylsulfoxide (DMSO), glycerol, urea, succinic acid, trifluoroacetic acid (TFA), acetonitrile (AcN), ethanol (EtOH), and ammonium acetate (AmAc) were purchased from Sigma-Aldrich (Taufkirchen, Germany) and used without further purification. Bovine serum albumin (BSA, MW 66430 Da) was purchased from Gerbu Biotechnik (Gaiberg, Germany).

Chito-Oligosaccharide Preparation. Chitin was isolated from shrimp shells as previously described by Hackman.[33] Chitosan with a fraction of N-acetylated units (F_A) of 0.32, an intrinsic viscosity of 730 mL/g at pH 5.5, and an ionic strength of 0.1[34] corresponding to a (weight-average) M_r of 233 000[35] was prepared by homogeneous de-N-acetylation of chitin.[36] CHOS were prepared as follows: Chitosan (F_A = 0.32) was dissolved in H_2O to 20 mg/mL by gentle shaking overnight. An equivalent volume of 0.08 M sodium acetate buffer containing 0.2 M NaCl (pH 5.5) was added, together with 0.1 mg of BSA, at a final chitosan concentration of 10 mg/mL. The mixture was incubated in a shaking water bath at 37 °C, and the depolymerization reaction was started by adding 0.5 μg chitosanase Q9RJ88/mg chitosan.[37] The reaction was stopped after 52 h by immersing the test tube in boiling water for 5 min, giving a degree of scission (α) of 0.29 as determined by proton NMR spectroscopy.[38] After a centrifugation to remove protein precipitates, the enzymatically degraded chitosan was fractionated by degree of polymerization (DP) using three SuperdexTM 30 columns (Amersham Pharmacia Biotech, Uppsala, Sweden) connected in series as previously described.[38] CHOS of similar DP were collected in fractions (denoted DPn, where *n* indicates the number of sugar units) and analyzed by ^{1}H NMR spectroscopy to determine F_A and DP.[38] In this work, only CHOS with DP6 and DP8 were used.

Chitinase A from *Serratia marcescens*. The cloning and expression of the gene encoding Chitinase A has been described previously.[39] The mutant ChiA-W167A was produced, expressed, and purified using ion exchange chromatography and hydrophobic interaction chromatography, as described previously.[40] The ChiA-E315Q mutant, which is inactive due to a mutation of the catalytic acid, was prepared using the QuikChangeTM site-directed mutagenesis kit from Stratagene (La Jolla, CA), essentially as described by the manufacturer and using the following primers: 5′ GGATATCGACTGGCAGTTCCCGGGC 3′ (forward) and 5′ GCCCGGGAACTGCCAGTCGATATCC 3′ (reverse). The mutant was expressed and purified as described earlier.[40] Enzyme purity was verified by sodium dodecyl sulfate-polyacrylamide gel electrophoresis (SDS-PAGE) and estimated to be >95% in all cases. Protein concentrations were determined using the Quant-ItTM protein assay kit and QubitTM fluorometer from Invitrogen (Town, CA).

Preparation of Noncovalent ChiA-CHOS Complexes. Stock solutions, of ChiA-E315Q or ChiA-W167A, and CHOS were mixed and stirred at 450 rpm and 37 °C to give final concentrations of 10 pmol/μL of protein and 60 pmol/μL of CHOS in ammonium acetate buffer (10 mM, pH 5.0). Aliquots were collected and kept on ice prior to MS analysis.

MALDI-o-TOF Mass Spectrometry. MALDI-MS experiments were performed with a modified o-TOF instrument (MDS Sciex, Concord, ON, Canada), which has been described in detail previously.[28] Briefly, the MALDI-o-TOF system is equipped with two lasers: (a) a nitrogen laser (VSL 337 ND, Laser Science Inc. Newton, MA, USA) emitting pulses of 3 ns at a wavelength of 337 nm and a repetition rate of 30 Hz (used for UV MALDI) and (b) an electro-optically (Q-)switched Er:YAG laser (BiOptics Laser Systeme, Berlin, Germany) emitting ∼150 ns-long pulses at a wavelength of 2.94 μm and a repetition rate of 2 Hz (used for IR-MALDI). The beams of both lasers were focused onto the sample surface at 30° (relative to the ion optical axis) to produce spots with diameters of approximately 200 μm. Gas-phase ions were generated in an elevated pressure ion source filled with nitrogen of adjustable pressure. For the analysis of the noncovalent complexes, the pressure was typically set to $p \sim 1.8-2.2$ mbar of N_2, which is about a factor of 3 higher than standard settings used for the analysis of peptides.[41] The elevated buffer gas pressure increases the collisional cooling efficiency and thus stabilizes weakly bound complexes. The extraction voltage between sample plate and skimmer was set to 50 V. The transfer quadrupole of the instrument was filled with N_2 at $p \sim 10^{-2}$ mbar. For the obtainment of a mass spectrum, ∼50 laser shots at slightly elevated laser fluences of $5.3 \cdot 10^3$ J/m^2 were employed. The TOF analyzer was operated in the positive ion mode with an accelerating voltage of 10 kV. External calibration was achieved using singly and doubly charged BSA. Mass spectra were acquired and processed with the software Tofma (Ens and Spicer, University of Manitoba, Winnipeg, Canada), extracted as ASCII data files, and plotted using Origin software (version 5.5, OriginLab, Northampton, MA).

Sample Preparation for MALDI-MS. Glycerol was used as liquid matrix for IR-MALDI, and the following solid state matrix

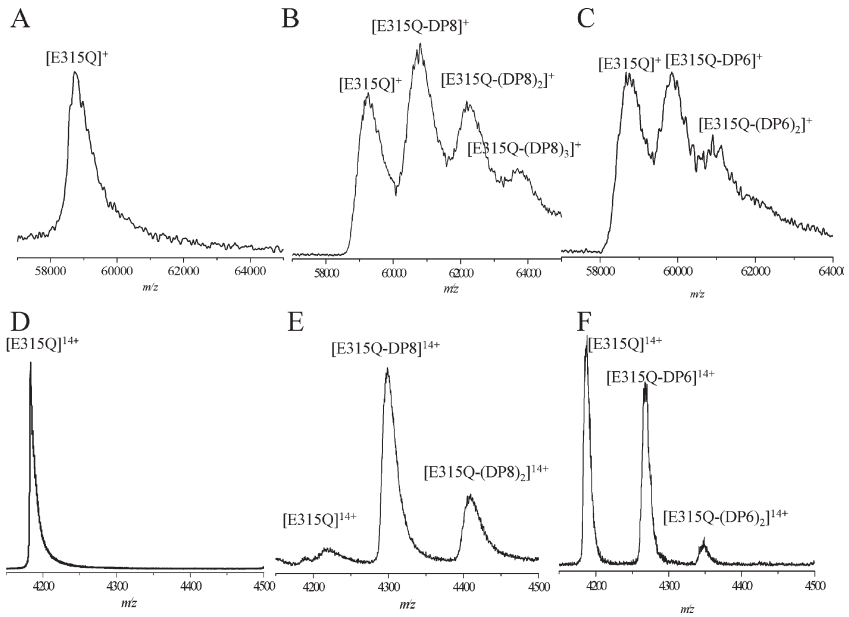

Figure 1. IR-MALDI mass spectra of ChiA-E315Q (A), ChiA-E315Q incubated with CHOS-DP8 for 5 min (B), and ChiA-E315Q incubated with CHOS-DP6 for 5 min (C). Samples were analyzed after mixing with glycerol and proton exchange beads. The spectrum of the incubation mixture shows that both the free enzyme and CHOS-DP8 are detected in one single spectrum in addition to the noncovalent complexes [ChiA-E315Q-DP8], [ChiA-E315Q-$(DP8)_2$], and [ChiA-E315Q-$(DP8)_3$]. Moreover, it is clear that when ChiA-E315Q is incubated with the weaker binding CHOS-DP6, the intensity of enzyme-ligand complex decreases compared to that of CHOS-DP8. Nano-ESI-q-TOF mass spectra of ChiA-E315Q (D), ChiA-E315Q with CHOS-DP86 (E), and ChiA-E315Q with CHOS-DP6 (F) at the same concentrations and incubation times as for the uptake of the IR-MALDI mass spectra are also shown.

compositions were investigated using both UV- and IR-MALDI: (1) 10 mg/mL DHB in 40% acetonitrile containing 0.01% TFA; (2) 40 mg/mL DHAP in H_2O; (3) 40 mg/mL THAP in H_2O; (4) 40 mg/mL succinic acid in H_2O; (5) 40 mg/mL urea in water, and (6) 50% sinapic acid in water. Sample preparations using solid matrixes were prepared by the "dried droplet" method, mixing 1 μL of each analyte with 1 μL of matrix solution on a stainless steel sample plate followed by drying in a stream of air at room temperature. Samples with glycerol as matrix were prepared by thorough mixing with the aqueous analyte solution in a 1:1 volume ratio, on the sample plate. Proton-loaded cation exchange polymer beads (Dowex 50W X88 (Dow Chemical Co, Midland, Michigan) activated with water or ammonia) were added to the sample to reduce the formation of adducts as previously reported.[42] Before insertion of the samples into the vacuum of the sample chamber, excessive water was evaporated in a prevacuum chamber at a pressure of $\sim 10^{-2}$ mbar for 30 min.

Nano-ESI-q-TOF Mass Spectrometry. Nanoelectrospray ionization mass spectra were acquired with an orthogonal hybrid TOF mass spectrometer (q-TOF, Micromass, Manchester, UK) equipped with a Z-spray nano-ESI ion source. The instrument was operated in the positive-ion mode. The MassLynx software (Waters Micromass, Manchester, UK) was used to acquire, process, and deconvolute the mass spectra. For all experiments, the following parameters were used: the ion-source temperature was set to 80 °C, desolvation gas was used at a flow rate of 100 L/h, a potential of 900 V was applied to the capillary tip, and the sampling cone voltage was set to 80 V. For collision-induced dissociation (CID)-analysis, the parent ions were selected by the first quadrupole and the ion acceleration voltage was set initially to 4 V. The parent ions were subsequently fragmented in the collision cell using argon as collision gas at a nominal pressure of 2 mbar and initial ion acceleration voltage of 10 V that was increased stepwise during continuous signal acquisition until sufficient fragmentation was achieved. The MS and MS/MS signals were acquired over a range of m/z 100−5000 at a scan rate of 2.0 s/scan. All scans were displayed in a single spectrum.

RESULTS AND DISCUSSION

IR-MALDI-MS analysis of ChiA-E315Q yielded intense signals of the free enzyme at $m/z \sim 59\,000$, being in good agreement with the calculated theoretical average molecular mass of 58 549 Da (Figure 1A). When ChiA-E315Q was incubated with CHOS of DP8, intact noncovalent complexes were detected (Figure 1B) in addition to both free enzyme and unbound oligosaccharides of DP8. The free oligosaccharides show variation in m/z values because the CHOS sample contains a variety of octamers that differ in terms of the degree of acetylation and acetylation patterns (Supplementary Figure S1, Supporting Information).[37,43] The difference between observed and theoretical masses is due to adduct formations. When proton exchange beads were not used, the peaks exhibited considerably more tailing due to massive formation of matrix and salt adducts

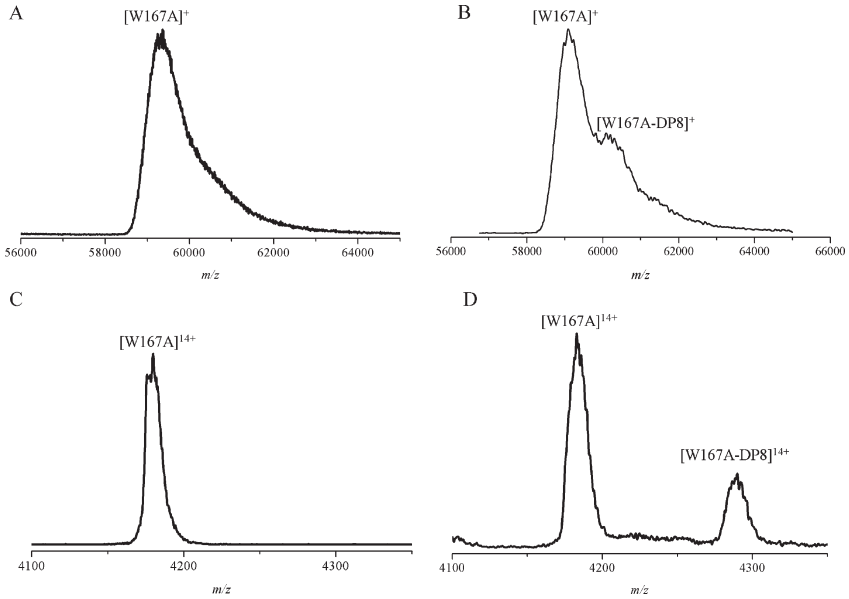

Figure 2. IR-MALDI mass spectra of ChiA-W167A (A) and ChiA-W167A incubated with CHOS-DP8 for 5 min (B). Samples were prepared by mixing with a glycerol matrix containing proton exchange beads. The spectrum of the mixture shows the presence of both the free enzyme and a seemingly minor amount of the noncovalent [ChiA-W167A-DP8] complex. Note that there is much less complex formation than in Figure 1. Nano-ESI-q-TOF mass spectra of ChiA-W167A (C) and ChiA-W167A with CHOS-DP8 (D) at the same concentrations and incubation times as for the uptake of the IR-MALDI mass spectra are also shown.

(results not shown). Extensive adduct formation is common for IR-MALDI-MS of proteins with a glycerol matrix.[44] This results in an increase of the apparent mass of the protein and reduced mass resolution. We found that the use of proton exchange beads also improved the signal-to-noise ratio, whereas no negative influence on the desorption process could be observed. One important experimental factor influencing the successful desorption/ionization of intact gaseous complex species is sufficient collisional cooling to stabilize the noncovalent complexes, mediated by the buffer gas used in the ion source of the o-TOF instrument. We found that values between 1.8 and 2.2 mbar provided optimal conditions. Lower pressures, more typical for standard MALDI MS analyses (~0.6 mbar)[41] resulted in partial cleavage of the complexes, notable in reduced signal intensities and tailing of the ion signals to lower m/z values (data not shown). However, a disadvantage of the elevated pressure is that adduct formation is enhanced.

The spectrum for the samples with the DP8 CHOS showed additional ionic species at m/z 60 500 and m/z 62 000, as well as a minor peak at m/z 63 500 (Figure 1B). CHOS of DP8 and a degree of acetylation in the order of 50% (Supplementary Figure S1 (Supporting Information) shows D_3A_5, D_4A_4, and D_5A_3, where D is short for a deacetylated unit, glucosamine, and A is short for an acetylated unit, *N*-acetylglucosamine) have masses in the order of 1 500 Da. The peak at m/z 60 500 corresponds well to the noncovalent [ChiA-E315Q-DP8] complex. The peaks at m/z 62 000 and 63 500 represent complexes containing two and three CHOS of DP8, respectively. The crystal structure of ChiA shows a large number of exposed aromatic amino acids both near and further away from the active site.[45] It is thus conceivable that the enzyme simultaneously binds more than one oligomer, as indeed has been observed for shorter oligomers in a recent study.[5] The complexes with multiple CHOS may also originate from specific binding of one octamer and association of other octamers to the bound ligand through formation of Schiff bases, a common associative process in chitosans.[46] Although somewhat puzzling, the observation of complexes with multiple CHOS underpins the gentleness of the IR-MALDI process since additional oligomers must be expected to bind weakly. Moreover, ChiA-E315Q was also incubated with DP6 CHOS (Figure 1C) that binds weaker than DP8 CHOS since the binding strength of CHOS increases with increasing DP.[7] It is clearly seen that the enzyme-ligand signal intensity in the mass spectrum is reduced and that Schiff base formation is virtually nonexistent due to the relatively weaker binding. For nonspecific, noncovalent gas-phase aggregates produced under MALDI conditions, signal intensities are typically accompanied by an exponential decrease.[16] This is not observed in our experiments, suggesting that only specific binding is observed.

To verify that the detected complexes reflect the nature of the chemistry in the condensed phase and are not the result of unspecific gas-phase interactions, the same experiments were repeated using another mutant, ChiA-W167A, with octameric sugars (DP8; Figure 2). ChiA-W167A is highly active toward soluble substrates such as CHOS, even in cases where a considerable fraction of the sugars is deacetylated.[40] Formation of stable complexes occurs when a glucosamine is situated in the −1 subsite since the *N*-acetyl group of the −1 sugar is essential for

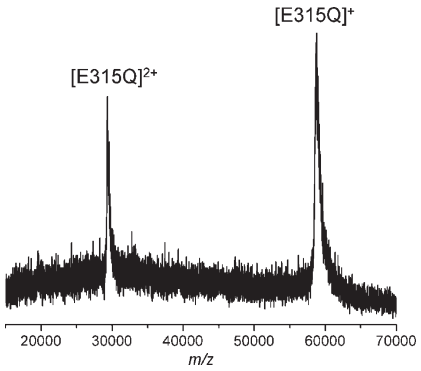

Figure 3. UV-MALDI mass spectrum of ChiA-E315Q incubated with CHOS-DP8 for 5 min; DHB was used as matrix. The spectrum shows only the free enzyme as singly and doubly charged ions, detected at m/z 58 500 and m/z 29 250, respectively. Note that a DHB matrix yields less adduct formation than glycerol.

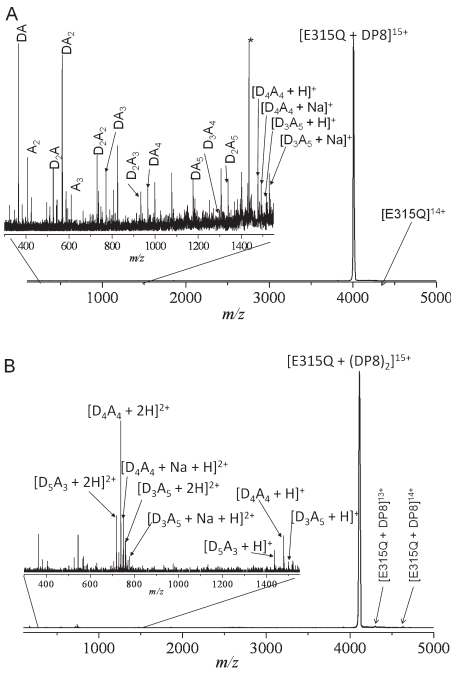

Figure 4. Nano-ESI-q-TOF MS tandem analysis of [ChiA-E315Q-DP8]$^{15+}$ (A) and [ChiA-E315Q-$(DP8)_2$]$^{15+}$ (B). The parent ions have m/z values of 4 006 and 4 101, respectively, and were subjected to collision-induced dissociation. The spectra demonstrate that one and two DP8 oligomer(s), respectively, were bound to the enzyme. The asterisk denotes a broad unresolved peak arising from the fragmentation of the protein backbone.

catalysis to take place.[6,47] The majority of the DP8 CHOS is degraded to CHOS of shorter DP, resulting in a lowering of the concentration (Supplementary Figure S1, Supporting Information), and only minor amounts of ChiA-W167A complexes with DP8 were detected with IR-MALDI-MS, as expected (Figure 2). This clearly demonstrates that reduced concentration of CHOS yields lower signal intensity in the mass spectrum. Furthermore, this confirms that the gas-phase molecular complex detected in the IR-MALDI mass spectra reflect the chemistry in the condensed phase. If the interaction would be nonspecific and gas phase induced, the results for the ChiA-E315Q and ChiA-W167A mutants should be similar, since the exchange of a single amino acid would not significantly alter the nonspecific binding properties of the enzyme. Thus, the observed interactions are specific and not an artifact from the MALDI process.

Using a variety of solid MALDI matrixes (see Experimental Section) both for UV- and IR-ionization did not lead to detection of the noncovalent complexes in any case. For all conditions, only free enzymes were detected. A representative example, in this case a UV-MALDI-o-TOF mass spectrum of ChiA-E315Q and CHOS of DP8 acquired with the solid matrix DHB, is displayed in Figure 3. We did not observe the "first-shot phenomenon"[23] when solid matrixes were used, neither with the UV nor IR laser. This indicates that the solid matrix itself is a key factor promoting dissociation of noncovalent assemblies initially formed in the incubation mixture. Probably, the acidic conditions and crystalline morphology of the matrixes promote dissociation.

As further control experiments, nano-ESI-q-TOF mass spectra of ChiA-E315Q incubated with CHOS-DP8 and CHOS-DP6 and ChiA-W167A with CHOS DP8 were obtained. The spectra show four different charge states from +13 to +16, where only the +14 charge state is shown (Figure 1D), that, after deconvolution, yielded a molecular weight of 58 546 Da (theoretical average MW 58 549 Da). Similar to what was observed in the IR-MALDI mass spectra for ChiA-E315Q in the presence of CHOS-DP8, additional ionic species corresponding after deconvolution to masses of 60 012 Da and 61 494 Da were observed (Figure 1E), representing [ChiA-E315Q-DP8] and [ChiA-E315Q-$(DP8)_2$] complexes, respectively. The [ChiA-E315Q-$(DP8)_3$] complex was not visible but may be obscured by a lower charge state of the free enzyme. The [ChiA-E315Q-(DP6)] and [ChiA-E315Q-$(DP6)_2$] complexes are observed as well using nano-ESI-q-TOF-MS (Figure 1F). Similar analyses of ChiA-W167A incubated with CHOS-DP8 showed a much lower degree of complex formation (Figure 2), in accordance with the results obtained with IR-MALDI-MS. Moreover, distributions between enzymes with bound oligosaccharides vs free enzymes were essentially identical using IR-MALDI compared to that observed for nano-ESI (Supplementary Table S1, Supporting Information).

To further analyze whether the detected complexes with 1:1 and 1:2 stoichiometry reflect the chemistry in the condensed phase and are not due to an unspecific gas-phase interaction, top-down sequencing of both ionic species were performed by collision-induced dissociation (CID) MS/MS.[11] Precursor ions with m/z 4 005 and m/z 4 101 corresponding to [ChiA-E315Q-DP8]$^{15+}$ and [ChiA-E315Q-$(DP8)_2$]$^{15+}$, respectively, were isolated in the first quadrupole, and intact CHOS ions and fragment ions arising from cleavage of the glycosidic bonds of DP8 were detected in MS/MS spectra after the collision-induced dissociation (Figure 4). High laboratory-frame energies, E_{lab} of 375 to 450 eV, were required for the dissociation of the [ChiA-E315Q-DP8] complex, in accordance with previous studies.[48] Mainly, B-type ions were formed, and also, minor fragmentation of the

dx.doi.org/10.1021/ac1031308 |*Anal. Chem.* 2011, 83, 4030–4036

protein backbone was observed. For the dissociation of an octamer from the [ChiA-E315Q-$(DP8)_2$] precursor ions in a CID analysis, significantly less energy (E_{lab} of 195 to 225 eV corresponding to a center-of-mass energy of $E_{c.o.m.}$ = 0.13−0.15 eV) was required (Figure 4B). In this case, the dissociated ions mainly represented the intact octameric oligosaccharides occurring as singly and doubly charged ions. The fact that dissociation from the complex with 1:2 stoichiometry required much less energy suggests that the dissociated CHOS bound outside the active site, i.e., with lower affinity.

CONCLUSIONS

We have shown that IR-MALDI mass spectrometry can be used to study noncovalent enzyme-ligand interactions. While this method offers lower resolution than ESI-based methods, it offers several advantages that make it a valuable tool, e.g., for fast and simple screening in inhibitor development work. The IR-MALDI approach takes advantage of a liquid glycerol matrix that resembles native physiological conditions for the formation of enzyme-ligand complexes. The advantages of the IR-MALDI method compared to ESI methods include (i) a well-controllable ion formation time, as samples are only depleted if the laser is switched on, (ii) possibilities for automation through multiple samples on a single sample stage as ESI capillary needles do not need to be changed, (iii) less sample consumption, and (iv) as a potentially especially important feature, a higher tolerance toward detergents and salts. The latter could allow adjusting pH values necessary to detect weakly bound complexes by adding suitable buffers. In contrast, already low concentrations of salts in the ESI solution typically deteriorate the MS performance. While the more commonly used UV-MALDI-MS technology, with crystalline matrixes, so far does not offer the possibility of easy and reproducible detection of noncovalent complexes, the IR-MALDI-MS technology does. A particular advantage of the utilized o-TOF instrument is the provision of efficient collisional cooling that is readily stabilizing desorbed complexes in the gas phase.

ASSOCIATED CONTENT

Supporting Information. Additional information as noted in text. This material is available free of charge via the Internet at http://pubs.acs.org.

AUTHOR INFORMATION

Corresponding Author

*E-mail: morten.sorlie@umb.no. Telephone: +47 64965902. Fax: +47 64965901.

ACKNOWLEDGMENT

A.L.N. and A.I.D. contributed equally to this work. This work was supported by Grant 177542/V30 from the Norwegian Research Council. Financial support by the Deutsche Forschungsgemeinschaft (Sonderforschungsbereich 492, Project Z2 to M.M.) and the funds "Innovative Medical Research" of the University of Münster Medical School (Grant DR520805 to K.D.) is also gratefully acknowledged. We wish to thank Stefan Berkenkamp and Sequenom GmbH for use of the o-TOF instrument.

REFERENCES

(1) Tharanathan, R. N.; Kittur, F. S. *Crit. Rev. Food Sci.* **2003**, *43*, 61.
(2) Cohen, E. *Arch. Insect Biochem.* **1993**, *22*, 245.
(3) Saguez, J.; Dubois, F.; Vincent, C.; Laberche, J. C.; Sangwan-Norreel, B. S.; Giordanengo, P. *Pest Manage. Sci.* **2006**, *62*, 1150.
(4) Donnelly, L. E.; Barnes, P. J. *Trends Pharmacol. Sci.* **2004**, *25*, 509.
(5) Macdonald, J. M.; Tarling, C. A.; Taylor, E. J.; Dennis, R. J.; Myers, D. S.; Knapp, S.; Davies, G. J.; Withers, S. G. *Angew. Chem., Int. Ed.* **2010**, *49*, 2599.
(6) Cederkvist, F. H.; Parmer, M. P.; Vårum, K. M.; Eijsink, V. G. H.; Sørlie, M. *Carbohydr. Polym.* **2008**, *74*, 41.
(7) Norberg, A. L.; Karlsen, V.; Hoell, I. A.; Bakke, I.; Eijsink, V. G. H.; Sørlie, M. *FEBS Lett.* **2010**, *584*, 4581.
(8) Kitova, E. N.; Bundle, D. R.; Klassen, J. S. *J. Am. Chem. Soc.* **2002**, *124*, 5902.
(9) Hillenkamp, F., Peter-Katalinić, J., Eds. *MALDI MS A Practical Guide to Instrumentation, Methods and Applications*; WILEY-VCH: Weinheim, 2007.
(10) Cederkvist, F. H.; Mormann, M.; Froesch, M.; Eijsink, V. G. H.; Sørlie, M.; Peter-Katalinić, J. *Int. J. Mass Spectrom.* **2010**, DOI:10.1016/j.ijms.2010.10.031.
(11) Cederkvist, F.; Zamfir, A. D.; Bahrke, S.; Eijsink, V. G. H.; Sørlie, M.; Peter-Katalinic, J.; Peter, M. G. *Angew. Chem., Int. Ed.* **2006**, *45*, 2429.
(12) Kitova, E. N.; Bundle, D. R.; Klassen, J. S. *J. Am. Chem. Soc.* **2002**, *124*, 9340.
(13) Kitova, E. N.; Kitov, P. I.; Paszkiewicz, E.; Kim, J.; Mulvey, G. L.; Armstrong, G. D.; Bundle, D. R.; Klassen, J. S. *Glycobiology* **2007**, *17*, 1127.
(14) Kitova, E. N.; Wang, W. J.; Bundle, D. R.; Klassen, J. S. *J. Am. Chem. Soc.* **2002**, *124*, 13980.
(15) Soya, N.; Shoemaker, G. K.; Palcic, M. M.; Klassen, J. S. *Glycobiology* **2009**, *19*, 1224.
(16) Song, F. *J. Am. Soc. Mass Spectrom.* **2007**, *18*, 1286.
(17) König, S.; Kollas, O.; Dreisewerd, K. *Anal. Chem.* **2007**, *79*, 5484.
(18) Bolbach, G. *Curr. Pharm. Design* **2005**, *11*, 2535.
(19) Harvey, D. J. *Mass Spectrom. Rev.* **1999**, *18*, 349.
(20) Kiselar, J. G.; Downard, K. M. *J. Am. Soc. Mass Spectrom.* **2000**, *11*, 746.
(21) Bich, C.; Zenobi, R. *Curr. Opin. Struct. Biol.* **2009**, *19*, 632.
(22) Cohen, L. R. H.; Strupat, K.; Hillenkamp, F. *J. Am. Soc. Mass Spectrom.* **1997**, *8*, 1046.
(23) Yanes, O.; Aviles, F. X.; Roepstorff, P.; Jorgensen, T. J. D. *J. Am. Soc. Mass Spectrom.* **2007**, *18*, 359.
(24) Rosinke, B.; Strupat, K.; Hillenkamp, F.; Rosenbusch, J.; Dencher, N.; Krüger, U.; Galla, H.-J. *J. Mass Spectrom.* **1995**, *30*, 1462.
(25) Von Seggern, C. E.; Cotter, R. J. *J. Am. Soc. Mass Spectrom.* **2003**, *14*, 1158.
(26) Dreisewerd, K.; Kölbl, S.; Peter-Katalinic, J.; Berkenkamp, S.; Pohlentz, G. *J. Am. Soc. Mass Spectrom.* **2006**, *17*, 139.
(27) Müsken, A.; Souady, J.; Dreisewerd, K.; Zhang, W. L.; Distler, U.; Peter-Katalinic, J.; Miller-Podraza, H.; Karch, H.; Müthing, J. *Rapid Commun. Mass Spectrom.* **2010**, *24*, 1032.
(28) Dreisewerd, K.; Müthing, J.; Rohlfing, A.; Meisen, I.; Vukelic, Z.; Peter-Katalinic, J.; Hillenkamp, F.; Berkenkamp, S. *Anal. Chem.* **2005**, *77*, 4098.
(29) Kirpekar, F.; Berkenkamp, S.; Hillenkamp, F. *Anal. Chem.* **1999**, *71*, 2334.
(30) Berkenkamp, S.; Kirpekar, F.; Hillenkamp, F. *Science* **1998**, *281*, 260.
(31) Von Seggern, C. E.; Cotter, R. J. *J. Mass Spectrom.* **2004**, *39*, 736.
(32) Woods, A. S.; Ugarov, M.; Jackson, S. N.; Egan, T.; Wang, H. Y. J.; Murray, K. K.; Schultz, J. A. *J. Proteome Res.* **2006**, *5*, 1484.
(33) Hackman, R. H. *Aust. J. Biol. Sci.* **1954**, *7*, 168.
(34) Draget, K. I.; Vårum, K. M.; Moen, E.; Gynnild, H.; Smidsrød, O. *Biomaterials* **1992**, *13*, 635.

(35) Berth, G.; Dautzenberg, H. *Carbohydr. Polym.* **2002**, *47*, 39.
(36) Sannan, T.; Kurita, K.; Iwakura, Y. *Makromol. Chem.* **1976**, *177*, 3589.
(37) Heggset, E. B.; Dybvik, A. I.; Hoell, I. A.; Norberg, A. L.; Sørlie, M.; Eijsink, V. G. H.; Vårum, K. M. *Biomacromolecules* **2010**, *11*, 2487.
(38) Sørbotten, A.; Horn, S. J.; Eijsink, V. G. H.; Vårum, K. M. *FEBS J.* **2005**, *272*, 538.
(39) Brurberg, M. B.; Eijsink, V. G. H.; Nes, I. F. *FEMS Microbiol. Lett.* **1994**, *124*, 399.
(40) Zakariassen, H.; Aam, B. B.; Horn, S. J.; Vårum, K. M.; Sørlie, M.; Eijsink, V. G. H. *J. Biol. Chem.* **2009**, *284*, 10610.
(41) Soltwisch, J.; Souady, J.; Berkenkamp, S.; Dreisewerd, K. *Anal. Chem.* **2009**, *81*, 2921.
(42) Nordhoff, E.; Cramer, R.; Karas, M.; Hillenkamp, F.; Kirpekar, F.; Kristiansen, K.; Roepstorff, P. *Nucleic Acids Res.* **1993**, *21*, 3347.
(43) Aam, B. B.; Heggset, E. B.; Norberg, A. L.; Sørlie, M.; Vårum, K. M.; Eijsink, V. G. H. *Marine Drugs* **2010**, *8*, 1482.
(44) Dreisewerd, K.; Rohlfing, A.; Spottke, B.; Urbanke, C.; Henkel, W. *Anal. Chem.* **2004**, *76*, 3482.
(45) Perrakis, A.; Tews, I.; Dauter, Z.; Oppenheim, A. B.; Chet, I.; Wilson, K. S.; Vorgias, C. E. *Structure* **1994**, *2*, 1169.
(46) Tømmeraas, K.; Vårum, K. M.; Christensen, B. E.; Smidsrød, O. *Carbohydr. Res.* **2001**, *333*, 137.
(47) Tews, I.; van Scheltinga, A. C. T.; Perrakis, A.; Wilson, K. S.; Dijkstra, B. W. *J. Am. Chem. Soc.* **1997**, *119*, 7954.
(48) Lane, L. A.; Ruotolo, B. T.; Robinson, C. V.; Favrin, G.; Benesch, J. L. P. *Int. J. Mass Spectrom.* **2009**, *283*, 169.